



**HAL**  
open science

# Towards a novel approach for the calculation of many-body Green's functions

Giovanna Lani

► **To cite this version:**

Giovanna Lani. Towards a novel approach for the calculation of many-body Green's functions. Strongly Correlated Electrons [cond-mat.str-el]. Ecole Polytechnique X, 2011. English. NNT: . pastel-00667923

**HAL Id: pastel-00667923**

**<https://pastel.hal.science/pastel-00667923>**

Submitted on 8 Feb 2012

**HAL** is a multi-disciplinary open access archive for the deposit and dissemination of scientific research documents, whether they are published or not. The documents may come from teaching and research institutions in France or abroad, or from public or private research centers.

L'archive ouverte pluridisciplinaire **HAL**, est destinée au dépôt et à la diffusion de documents scientifiques de niveau recherche, publiés ou non, émanant des établissements d'enseignement et de recherche français ou étrangers, des laboratoires publics ou privés.

Thèse présentée pour obtenir le grade de  
DOCTEUR DE L'ÉCOLE POLYTECHNIQUE

par

Giovanna LANI

---

**Towards a Novel Approach for the Calculation  
of Many-Body Green's Functions**

---

Soutenue le 14 Novembre 2011 devant le jury composé de :

Dr	Christian BROUDER	Rapporteur
Prof	Eberhard K. U. GROSS	Rapporteur
Prof	Silke BIERMANN	Examinatrice
Prof	Rex W. GODBY	Examineur
Dr	Lucia REINING	Directrice
Dr	Pina ROMANIELLO	Co-Directrice



<b>1</b>	<b>Preface</b>	<b>1</b>
1.1	Introduction . . . . .	1
1.2	Review of model calculations for elementary excitations . . . . .	4
1.3	Probing excitations through spectroscopies . . . . .	6
1.3.1	Photo-emission spectroscopy . . . . .	6
<b>2</b>	<b>Description of one-particle excitations</b>	<b>9</b>
2.1	A brief introduction to second quantization . . . . .	9
2.1.1	Pictures . . . . .	9
2.1.2	Field operators . . . . .	12
2.2	The Green's function . . . . .	13
2.3	The Green's function in Many-body physics . . . . .	14
2.3.1	The spectral representation for the Green's function . . . . .	17
2.4	From the definition of the one-body Green's function to its calculation . . . . .	18
2.4.1	Straightforward diagrammatic expansion . . . . .	21
2.4.2	<i>Self-energy</i> based methods . . . . .	25
2.4.3	Cumulant expansion approximation . . . . .	29
2.5	Green's function from the solution of a functional differential equation . . . . .	34
<b>3</b>	<b>Exact Green's function in a simplified framework</b>	<b>37</b>
3.1	Tackling the functional equation I: linearization . . . . .	37
3.2	Tackling the functional equation II: 1-point model . . . . .	40
3.2.1	Limits and validity of the model . . . . .	41
3.2.2	Exact general solution . . . . .	42
3.2.3	Exact particular solution: alternative solution of the initial value problem	43
3.2.4	Exact particular solution: traditional solution of the initial value problem	44
3.2.5	DE's solution by iteration . . . . .	47
3.3	A singular perturbation problem . . . . .	48

3.3.1	An approximate solution from asymptotic expansions . . . . .	48
3.3.2	Other famous examples of divergences . . . . .	50
<b>4</b>	<b>Insights from the 1-point model</b>	<b>53</b>
4.1	Established approximations . . . . .	53
4.1.1	$G_0W_0$ and fully self-consistent GW . . . . .	54
4.1.2	Vertex corrections . . . . .	57
4.2	Alternative approximations . . . . .	58
4.2.1	An alternative vertex correction . . . . .	58
4.2.2	Continued fraction approximations . . . . .	62
4.2.3	Large electron-electron interaction expansions . . . . .	66
4.3	Self-consistent calculations of the Hartree Green's function . . . . .	68
<b>5</b>	<b>Beyond the 1-point model</b>	<b>71</b>
5.1	Restoring the time dependence of the Green's function . . . . .	71
5.1.1	Iterative solution for the N-times DE . . . . .	72
5.1.2	Connection with the cumulant expansion formula for the Green's function	75
5.1.3	The cumulant expansion $W$ explained through Feynman diagrams . . . .	77
5.2	The decoupling approximation for real materials calculations . . . . .	79
<b>6</b>	<b>The full functional differential equation</b>	<b>81</b>
6.1	An ansatz for the one-body Green's function . . . . .	81
6.2	The quest for $q([\varphi])$ and $\mathcal{J}(5, 2; [\varphi])$ . . . . .	85
6.2.1	$q([\varphi])$ from limiting cases . . . . .	85
6.2.2	Finding $\mathcal{J}(5, 2; [\varphi])$ . . . . .	86
<b>7</b>	<b>Conclusions and Outlook</b>	<b>89</b>
<b>A</b>	<b>Useful manipulations for <math>G</math></b>	<b>93</b>
A.1	Defintion of $G_0$ . . . . .	93
A.2	Defintion of the inverse of $G$ . . . . .	93
A.3	Expressing $\frac{\delta G([\varphi])}{\delta \varphi}$ through $\frac{\delta G^{-1}([\varphi])}{\delta \varphi}$ . . . . .	94
A.4	Inverting the Dyson equation . . . . .	94
A.5	Splitting a Dyson-like equation in two parts . . . . .	95
<b>B</b>	<b>Solving the DE</b>	<b>97</b>
<b>C</b>	<b>Some relations between special functions</b>	<b>99</b>
<b>D</b>	<b>N-points limited order differential equation</b>	<b>101</b>
<b>E</b>	<b>Self-consistent calculations of <math>y_H^0</math> and <math>u</math></b>	<b>105</b>
<b>F</b>	<b>Solving the integral equation for the auxiliary <math>G_{\bar{\varphi}}</math></b>	<b>107</b>

<b>G Algebra for solving the full functional DE</b>	<b>109</b>
G.1 Verifying the ansatz for $f$ and $a$ . . . . .	109
G.2 Formula for the integration of $\frac{\delta\mathcal{J}([\varphi])}{\delta\varphi}$ . . . . .	111
G.2.1 A simple functional to which the integration formula applies . . . . .	112
G.2.2 A simple functional to which the integration formula <i>does not</i> apply . . . . .	113
G.3 Insights from the N-times framework . . . . .	113
G.4 An alternative ansatz . . . . .	115
<b>Bibliography</b>	<b>121</b>



# CHAPTER 1

---

Preface

## 1.1 Introduction

Mean field theories such as the Hartree-Fock method [1, 2] or the density functional theory (DFT) [3], the different flavors of the Quantum Monte Carlo approach [4, 5], coupled cluster [6], configuration interaction (CI) [7, 8], dynamical mean field theory (DMFT) [9, 10], many-body perturbation theory [11, 12, 13, 14]... this is just a very brief list of the favorite tools that theorists in physics, chemistry and material science, have been devising and employing along the years to tackle with the many-body-problem. Not so surprisingly, without ever solving it *exactly*. Already starting from the '50s and the '60s, much progress has been done towards the understanding of the way particles in a solid can interact and behave quite differently from how they would if isolated from one another. The great majority of these insights have been gained thanks to the interplay of theory and experiments, the latter being a precious tool to validate more or less sophisticated theoretical approaches.

There are many circumstances under which a many-body system can be described, fairly well, through its *elementary excitations*: specifically one wants to single out the different type of excitations and analyze or model their mutual interaction. Two are the classes of well defined (which means long-lived) elementary excitations which are interesting for the condensed matter physicist, the first are the so-called *quasi-particle* excitation, which are nothing else than modified single-particle excitations, while the second kind are *density fluctuation* excitations, typically *collective modes* of the system. The concept of quasi-particle is fairly intuitive. If we think realistically about the propagation of a particle inside a solid, it is easy to imagine that its motion has to be greatly affected by the interaction with all the other particles: either pulling them apart or dragging them closer. This modified or *dressed* particle is what is labeled quasi-particle. Regarding the second type of elementary excitations in a system, perhaps the simplest

example can be given by *phonons*: an elementary unit of lattice excitation, where each atom vibrates around its equilibrium point. Another renowned type of collective mode are *plasmons*: quanta of charge oscillation in the electron gas, which correspond to the oscillations observed in classical plasma. Other examples are *polarons*, formed by the coupling of electrons and phonons or *excitons*, electron-hole bound pairs.

As we have hinted above the pool of approaches dealing with the many-body problem is quite large, since the problem is tremendously challenging. Later in this Preface we will detail a bit, for historical reasons, the very first methodologies employed, which were mainly based on model calculations. However in the last decades they yielded the way to computational approaches, in particular in their *ab-initio* (meaning without employing externally given parameters or data) implementation. Nowadays accurate calculations of quasi-particle band-gaps and spectral functions from core and valence photoemission or from electron energy loss experiments or optical absorption (just to mention a few type of experiments), can be carried out on a variety of solids and molecules.

This work aims mainly at finding a better description of the coupling between quasi-particles and plasmons in systems probed by means of photoemission experiments. The notion of quasi-particle can be put on a more mathematical and rigorous theoretical ground by introducing the so called *one-particle propagator* or *one particle Green's function*. The state-of-the-art approach for Green's functions calculations, and through them, quasi-particles band-gaps [15] and (core and valence) photoemission spectra [16, 17], is the so called *GW* approximation [14]. Lars Hedin can be considered the progenitor of the approach: building on earlier works, in the middle of the '60s, he devised a theoretical and practical way to access the one-body Green's function, the main ingredients being a simple approximation to an effective potential -the self-energy- and a closed set five integral equations, to be solved, in principle, self-consistently. Since then the approach has been blooming and now it is implemented in the majority of *ab-initio* computer codes. Its success has been exceeding expectations for band gaps of weak and moderately correlated systems, but started to exhibit shortcomings or even failures on more correlated electron solids. In addition to that its description of spectral functions is overall satisfactory, as far as the quasi-particle peak and sometimes a first plasmon satellite are concerned, but in a few cases turned out to be unable to describe additional features, more or less well defined.

In order to remedy these shortcomings many paths have been beaten, particularly the one of self-consistency and the one of vertex corrections beyond *GW*, however difficulties and open questions remain. In this thesis an alternative route has been pursued: following earlier works of Kadanoff, Baym and Schwinger, we reformulate the problem in terms of a set of non-linear, differential, functional equations for the calculation of  $G$  and attempt to solve *directly*.

This thesis is structured as follows.

In Chapter (2) we provide an extended background on the one-body Green's function: what is its mathematical formulation, the physical significance and which quantity it can give access to. We will then detail different approaches employed nowadays for Green's function calculations: starting with a straightforward Feynman-Dyson diagrammatic expansion, moving to self-energy based methods, in particular we will analyze the different *GW* flavors to conclude with the so called cumulant expansion approximation. We will also begin to detail more the approach we will pursue throughout the rest of the work.

In Chapter (3) we will introduce a linearization approximation to the set of functional differential equations. We will show that it contains a great deal of physics, well beyond what is provided by state-of-the-art approaches, and starting there, we will only focus on the linearized version of the equations. We will then introduce a simple framework, so called 1-point model, where the set of -linearized- equations reduces to a single algebraic differential equation, which we will solve exactly. Plenty of room will be given to the discussion about solving the initial value problem for the differential equation, in order to access a physical particular solution. Such discussion is not a simple technicality: being this issue one of the drawbacks of our alternative approach, we felt it was worth clarification and some extra elaboration. We finally elucidate the divergent behaviour of the iterative solution for the DE and we discuss the mathematical nature of the DE as a prototypical singular perturbation problem.

In Chapter (4) we compare the exact solution for the 1-point DE with established approximations, gaining greater insight into various *GW* flavors for a wide range of electron-electron interactions strengths. We also devise some new approximations, namely an alternative vertex correction, a continued fraction based approximation and a large electron-electron interaction expansion. We test all of them against the exact result and generalize the most promising one to their full function form (where possible).

In Chapter (5) we will go beyond the 1-point model results, by restoring the time dependence (and consequently the frequency dependence) of the Green's function in the differential equations. The resulting N-times differential equation will be solved analytically by re-summing *exactly* its iterative solution and the propagator thus obtained will have an exponential form which we show to be analogous to the so-called cumulant expansion approximation for  $G$ . Later on we will discuss how the newly derived Green's function has been employed by Matteo Guzzo *et al.* for the calculation of a valence photoemission spectrum in Silicon, yielding an unprecedented agreement with experimental data. We will finally provide an outlook on how to go beyond the cumulant expansion approximation.

In the last chapter we will go back to the problem of solving the full functional set of (linearized) differential equations for the one-body Green's function. We will discuss all the hurdles encountered on the way to the solution, which we tried to devise with an *ansatz*, mainly based on insights obtained from the 1-point framework. We will show how, within the chosen *ansatz*, composed of three terms which are solutions to three simpler (than the original) differential equations, it is still very challenging even to obtain the general solution for the full DE. We will focus on the main difficulty encountered within our approach, namely the functional integration of one piece of the *ansatz*. In this context we show how the integration can be performed upon the introduction of a new functional quantity that has to be chosen so that **i)** it obeys a sum rule and **ii)** some symmetry requirements. Once a proper choice for this new functional quantity is made, one can access a formal (general) solution for the differential equation. Finally we present our conclusions and perspective for future work.

## 1.2 Review of model calculations for elementary excitations

The first investigations of elementary excitations and their interactions were carried out mainly by means of model calculations and/or straightforward application of perturbation expansions; we will detail in the following two of them, which both provided a great deal of insights during the '60s.

The first model studied was the so-called *high density electron gas*. Its analysis revealed how a series expansion in  $r_s$ , reading:

$$E_0 = \frac{2.21}{r_s^2} - \frac{0.916}{r_s} + 0.062 \ln(r_s) + 0.096 + \epsilon r_s \ln(r_s) + \phi R_s + \dots \quad (1.1)$$

can provide the ground state total energy [11] in terms of the average inter-electron spacing  $r_s^a$ ; and such expansion is valid for  $r_s < 1$  [12]. The elementary excitations in this system were found to be quasi-particles and plasmons and the energy *versus* momentum curves were given respectively, in the works of Gell-Mann [11], Quinn and Ferrell [18] (for quasi-particles) and Bohm and Pines [19], Nozières and Pines [12] (for plasmons). In both cases one has expansions in  $r_s$  and  $p^2/p_f^2$ , where  $p_f$  is the momentum of the electron at the Fermi surface. One of the main physical effects ongoing in the high density electron gas is the *polarization* of the medium: it consists of the screening of the effective interactions between two electrons due to the movements and readjustments of all the other particles in the medium. Pictorially the screening can be seen as the "cloud" following the propagation of a single-particle and can be described by the longitudinal component of the dielectric function. A description of this system can be obtained through the so-called random phase approximation (RPA), where each momentum transfer between couples of electron can be treated separately; it was shown by Hubbard [20] that the RPA corresponds to summing only the lowest order polarization diagrams (so-called bubble diagrams) of the perturbation expansion for the screened interaction  $W$ . In the figure below we show the expansion in terms of diagrams. The results for the electron gas was employed

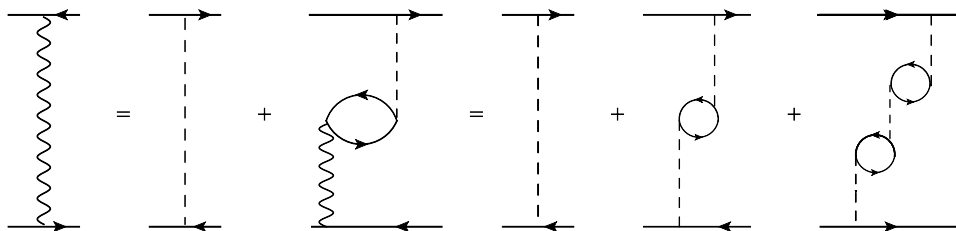


**Figure 1.1:** Here we show the diagrammatic expansion which was found by Hubbard [20] to be equivalent to the RPA approximation. The screened interaction (wiggly line) is first recast in terms of a Dyson-like equation containing the bare Coulomb potential (dashed lines) and then expanded in terms of it, together with pairs of Green's functions (so called bubbles in the diagrams language).

as a guideline for describing the behavior of the electrons in a simple metal (where instead of

---

<sup>a</sup>Measured in units of the Bohr radius  $a_0$

a uniform background of positive charge one has a lattice of positive ions), although keeping in mind that, in this case, since  $1.9 < r_s < 5.5$ , the perturbation expansion associated with the RPA approximation cannot be that accurate. However, with the use of interpolation schemes [20, 21], it has been shown that the application of the theory presented above to metals may lead to an accuracy of 10% in the calculation of the ground state total energy.

The other limit that has been treated from the dawn of the many-body era is the *low density electron solid*. In this limit it's the Coloumb interaction dominating the behaviour of the electrons in the solid: the resulting effect (due also to their very reduced kinetic energy with respect to the potential one) will be their localization, up to forming a stable lattice (so called Wigner crystal). An expansion [22, 23] going as  $\sqrt{r_s}$  was found to describe the ground state energy:

$$E_0 = \frac{1.79}{r_s} + \frac{2.66}{r_s \sqrt{r_s}} + \frac{\alpha}{r_s^2} + \frac{\beta}{r_s^2 \sqrt{r_s}} + \dots \quad (1.2)$$

where the first term is the potential energy of a localized electron, the second represents zero point oscillations around each electronic site and higher terms in  $r_s^{-1/2}$  describes the anharmonic effects. When  $r_s$  reaches the critical value of 20 [24], the solid will melt: this is clearly a limiting case of the low density regime.

We will now examine a low density (dilute) electron gas, which one can obtain, for instance, from the melting of a Wigner crystal. Once again the ground state total energy can be calculated through perturbation theory (see e.g. Refs [25], [26]) and one finds two types of elementary excitations: quasi-particles and zero sound vibrations. In both cases, in the energy *versus* momentum curve one finds that the expansion parameter is  $\frac{a}{r_0}$ <sup>b</sup>, this shows how, the ruling physical mechanism taking place in this regime, is the repeated scattering of pair of isolated particles. They propagate independently, coming together several times and interacting only weakly with the other particles.

One of the best approximations for the description of this multiple scattering landscape is obtained through the summation of *ladder diagrams* [26, 27]: here the vertex term which should account for the correlated motion of particle pairs is substituted by a *scattering matrix* (also known as t-matrix), which describes precisely their repeated coming together and apart (see figure below)

One may wonder if the main results of these model calculations are only valuable in the specific

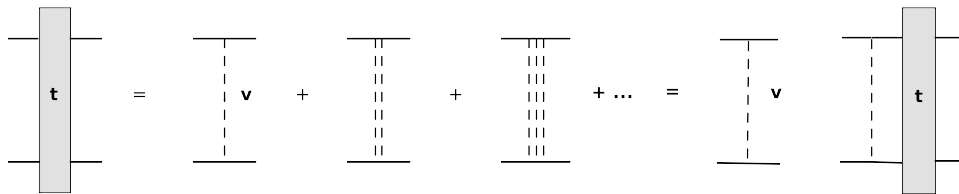


**Figure 1.2:** Diagrams for the t-matrix: the expansion is in the bare coulomb interaction. In the last diagram the t-matrix resums the multiple scattering processes.

limit for which they were conceived for. The answer is no: often they have been straightforwardly extended and their range of accuracy and applicability has considerably increased. When

<sup>b</sup> $a$  is a coefficient of the expansion appearing in all terms and  $r_0$  is the average interparticle spacing.

extensions were either not possible or not so convenient, novel theories -some of which are now applicable to real system calculations- were formulated and, as we will see all throughout this thesis, many of them were (are) heavily relying on these early models: this is clearly a signature that, despite some overall roughness, the early works I have just described contained already all the important physics of many-body systems.

## 1.3 Probing excitations through spectroscopies

### 1.3.1 Photo-emission spectroscopy

The electronic structure of solids can be probed by different types of spectroscopies. In this thesis preface, we will center our discussions around *photoemission spectroscopy*. This choice is not accidental, rather it stems from the fact that *the* ingredient to calculate a photoemission spectral function is the one-body Green's function. As photoemission of this work is to improve on the state-of-the-art approaches for Green's function calculations, it's worth providing some details on *which* improvements a better method would yield and *where*.

Through photoemission one can investigate the bulk structure of atoms, molecules or solids by analyzing how a beam of monochromatic light, with varying intensities (depending on the light source employed), interacts with the sample. By simply analyzing the photoemitted electrons, one can aim at reconstructing the occupied density of states of any material.

The physical mechanism behind photoemission is the *photoelectric effect*, observed already by Hertz [28] and Hallwachs [29] in 1887, but explained in terms of a quantum mechanical process only later by Einstein [30]. Since then, the typical photoemission experience and experimental setup hasn't changed much, schematically we can describe the process in three steps. **i)** Monochromatic photons with energy  $\hbar\nu$  and a given polarization impinge, with a given angle  $\alpha$ , on the sample, **ii)** photoelectrons are excited from either core or valence levels of the sample and start traveling towards its surface, **iii)** the emitted photoelectrons (with energy  $E_{kin}(\alpha, \beta) > \hbar\nu + E_\phi$ , where  $E_\phi$  is the work function and  $\beta$  is the emission angle) are analysed by an electrostatic analyzer.

Different light sources can be employed, but in general one distinguishes mainly between ultraviolet photoemission (UPS), employed for angle resolved investigations of valence bands and x-ray photoemission (XPS), where one rather probes core levels and hence higher binding energies.

Let's now see more in detail how one can theoretically describe this physical process. The description we will employ is a single-particle one, which gives a first idea when interested in quasi-particle energies (hence contains a moderate degree of many-body correlation). The observable we are interested in is the so called *photocurrent*  $J_k$  (with  $k$  representing the momentum); by using Fermi's golden rule, within a first order perturbation theory it can be expressed as [31]:

$$J_k = \frac{2\pi}{\hbar} \sum_s |\langle \Psi_{k,s} | H_1 | \Psi_i \rangle|^2 \delta(\epsilon_k - \epsilon_s - \hbar\nu) \quad (1.3)$$

where  $|\Psi_i\rangle$  and  $\langle \Psi_{k,s}|$  are respectively the initial (ground state) and the final state of the system and  $s$  runs over all the possible excited (final) states,  $\epsilon_k$  is the photoelectron energy and where

$\hat{H}_1$ <sup>c</sup> is the perturbation added to the unperturbed Hamiltonian  $\hat{H}_0$ .

To proceed further one has to adopt the so-called *sudden approximation*, which is to say the photoemitted electron is instantaneously removed from the solid, without undergoing any loss in the trajectory to the vacuum: all the *extrinsic* effects are hence neglected. Such an approximation is justified when high energy photons are employed<sup>d</sup>; assuming we are in such regime we can write:

$$\begin{cases} |\Psi_{k,s}\rangle = |k; N-1, s\rangle \rightarrow c_{k,s}^\dagger |N-1, s\rangle \\ J_k = \frac{2\pi}{\hbar} \sum_{sk} |\langle \Psi_k | H_1 | \Psi_j \rangle|^2 |\langle N-1, s | c_j | N \rangle|^2 = \sum_s |\Delta_{kj}|^2 A_j(\epsilon_k - \hbar\nu) \end{cases} \quad (1.4)$$

where  $\Delta_{kj}$  is the photoemission matrix element and  $A_j$  is the spectral function<sup>e</sup>, which can be related to the one particle Green's function as:  $A_j(\omega) = -\frac{1}{\pi} |\mathcal{I}mG_j(\omega)|$ .<sup>f</sup>

How can  $A_j(\omega)$  look like?

For a non-interacting system it will have only a sharp quasi-particle peak:  $A_j(\omega) = \delta(\omega - \epsilon_j)$ . In the more realistic case of an interacting spectrum the peaks will broaden and additional structure will appear. The following constraints will apply [35]:

$$\begin{cases} \int_{-\infty}^{\infty} A_j(\omega) d\omega = 1 \\ \int_{-\infty}^{\mu} A_j(\omega) d\omega = \langle c_j^\dagger c_j \rangle = n_j \\ \int_{-\infty}^{\infty} \omega A_j(\omega) d\omega = \epsilon_j^F \end{cases} \quad (1.5)$$

Using the sum rules, and knowing  $n_j, \epsilon_j^F$  and the quasi particle energy  $E_k$  one can guess that **i)** some of the spectral weight has to be in the satellite region, **ii)** the sharpness of the QP will be maximum at the Fermi surface, while away from it the peak will be broader, **iii)** electron-hole pairs and plasmons are important excitations and the peak that they induce in  $A_j(\omega)$  will probably lie just a bit below (few plasmon energies) the QP peak.

All of the above observations are very valuable to give a qualitative idea of the shape of a typical spectral function, however, in particular in the satellite region, little is known, in particular about the number and shape of the possible peaks. We will come back to the calculation of satellites in a photoemission spectra several times in this manuscript, in particular in Chap. (2) and more in depth in Chap. (5).

<sup>c</sup>The perturbing Hamiltonian employed here reads:  $H_1 = \frac{e}{m_e c} \mathbf{A} \cdot \mathbf{p}$ . This form is obtained neglecting the second order term in the perturbation and neglecting surface photoemission.

<sup>d</sup>Suggestions to go beyond the sudden approximation came for example from Berglund and Spicer [32], with their three-step-process or, later, from Schaich and Ashcroft [33] or Mahan [34], which opted for a one-step though quantum mechanical process.

<sup>e</sup>Note the presence of one index only: it is due to considering only the diagonal of the transition matrix element.

<sup>f</sup>We will see later on how this identity can be established.



# CHAPTER 2

---

## Description of one-particle excitations

*In this chapter we will introduce the definition of Green's function. We will first touch on its origins, as it was devised in the context of mathematics, to later move to its utility and significance in the field of many-body physics. After discussing some of its properties, a review of the different methodologies to access it will be presented. More space will be devoted to the self-energy based methods and in particular to the GW approximation: this choice is mainly due to the blossoming interest in this methodology in the last twenty years. Finally we will introduce the basic constituents of the alternative route which we want to pursue to calculate the one-body Green's function; while details about the methodology will occupy all the remaining chapters of this thesis.*

### 2.1 A brief introduction to second quantization

Before going into a detailed discussion of Green's function in many-body physics, let's very briefly introduce the so-called *second quantization* formalism, which is particularly convenient when treating systems with a variable number of particles due to the creation or destruction of elementary excitations.

We will first introduce the three main quantum mechanical pictures found in second quantization and later on field operators and Fock space.

#### 2.1.1 Pictures

Let's now discuss the three pictures, namely the Schrödinger, Heisenberg, and interaction one (for a more detailed coverage see textbooks such as [36, 37]).

### Evolution operator

Let  $|\Psi(t)\rangle$  be a solution of the time-dependent Schrödinger equation (TDSE). The time evolution operator  $\hat{U}(t, t')$  is defined by the relation

$$|\Psi(t)\rangle = \hat{U}(t, t_0)|\Psi(t_0)\rangle, \quad (2.1)$$

i.e. it maps a wave function at time  $t_0$  into a wave function at time  $t$ . Inserting (2.1) in the TDSE yields

$$i \frac{\partial \hat{U}(t, t_0)}{\partial t} |\Psi(t_0)\rangle = \hat{H}(t) \hat{U}(t, t_0) |\Psi(t_0)\rangle. \quad (2.2)$$

Since  $|\Psi(t_0)\rangle$  is arbitrary we find that

$$i \frac{\partial \hat{U}(t, t_0)}{\partial t} = \hat{H}(t) \hat{U}(t, t_0), \quad (2.3)$$

with the initial condition  $\hat{U}(t_0, t_0) = 1$ . Furthermore, one can show that the evolution operator  $\hat{U}(t, t_0)$  has the following properties

$$\begin{aligned} \hat{U}^\dagger(t, t') &= \hat{U}^\dagger(t, t_1) \hat{U}^\dagger(t_1, t') && \text{(group property)} \\ \hat{U}^\dagger(t, t') &= \hat{U}^{-1}(t, t') = \hat{U}(t', t). && \text{(unitary operator)} \end{aligned}$$

### The Schrödinger picture

In the Schrödinger picture operators and wave functions have their natural time-dependence. Therefore if the Hamiltonian is explicitly time-independent in the Schrödinger picture, then one can readily solve the operator differential equation (2.80), the solution being

$$\hat{U}_S(t, t_0) = e^{-i\hat{H}_S(t-t_0)}, \quad (2.4)$$

where the subscript "S" indicates that the Schrödinger picture is used.

### The Heisenberg picture

In the Heisenberg picture the wave functions are constant in time

$$|\Psi_H(t)\rangle = |\Psi_S(t_0)\rangle = \text{constant}, \quad (2.5)$$

and the operators are given by

$$\hat{O}_H(t) = \hat{U}_S^\dagger(t, t_0) \hat{O}_S(t) \hat{U}_S(t, t_0). \quad (2.6)$$

If  $\hat{H}_S$  is explicitly time-independent then

$$\hat{O}_H(t) = e^{i\hat{H}_S t} \hat{O}_S(t) e^{-i\hat{H}_S t}, \quad (2.7)$$

where we used  $t_0 = 0$ . One can show that operators in the Heisenberg picture evolve according to the following equation of motion

$$i \frac{d\hat{O}_H(t)}{dt} = i \left[ \frac{\partial \hat{O}}{\partial t} \right]_H + [\hat{O}_H, \hat{H}_H]. \quad (2.8)$$

### The interaction picture

Let us consider the Hamiltonian

$$\hat{H}(t) = H_0 + \hat{H}'(t), \quad (2.9)$$

where  $\hat{H}_0$  is well understood and exactly solvable, and  $\hat{H}'(t)$  contains some perturbation to this system. The wave function in the interaction picture is given by

$$|\Psi_I(t)\rangle = e^{i\hat{H}_0 st} |\Psi_S(t)\rangle, \quad (2.10)$$

and the operators by

$$\hat{O}_I(t) = e^{i\hat{H}_0 st} \hat{O}_S(t) e^{-i\hat{H}_0 st}. \quad (2.11)$$

In particular the operator  $\hat{H}_0$  is the same in the Schrödinger and interaction picture. Therefore, transforming the Schrödinger equation into the interaction picture gives

$$i \frac{\partial}{\partial t} |\Psi_I(t)\rangle = \hat{H}'_I(t) |\Psi_I(t)\rangle, \quad (2.12)$$

whereas the evolution of the operators follows the same equation of motion as in the Heisenberg picture, with  $\hat{H} = \hat{H}_0$ ,

$$i \frac{d\hat{O}_I(t)}{dt} = i \left[ \frac{\partial \hat{O}}{\partial t} \right]_I + [\hat{O}_I, \hat{H}_0]. \quad (2.13)$$

Since the Hamiltonian in the interaction picture is time-dependent, then the solution of the differential equation (2.80) for the evolution operator is more complicated than in the Schrödinger picture. Integrated between  $t$  and  $t_0$  (2.80) gives

$$\hat{U}_I(t, t_0) = 1 - i \int_{t_0}^t (t') \hat{U}_I(t', t_0) dt', \quad (2.14)$$

where we have used that  $\hat{U}(t_0, t_0)_I = 1$ . One can attempt to solve the integral in Eq. (2.14) by iteration, always keeping the proper ordering of the operators. The solution thus takes the form:

$$\hat{U}_I(t, t_0) = \mathcal{T} \sum_{n=0}^{\infty} \frac{(-1)^n}{n!} \left( \int_{t_0}^t dt' H'_I(t') \right)^n. \quad (2.15)$$

Note that since

$$|\Psi_I(t)\rangle = e^{i\hat{H}_0 st} |\Psi_S(t)\rangle = e^{i\hat{H}_0 st} \hat{U}_S(t, t_0) |\Psi_S(t_0)\rangle = e^{i\hat{H}_0 st} \hat{U}_S(t, t_0) |e^{-i\hat{H}_0 st_0} \Psi_I(t_0)\rangle \quad (2.16)$$

then

$$\hat{U}_I(t, t_0) = e^{i\hat{H}_0 st} \hat{U}_S(t, t_0) e^{-i\hat{H}_0 st_0}. \quad (2.17)$$

Equation (2.77), together with (2.7) and (2.11), allows us to derive the following transformation between the Heisenberg and interaction picture for an operator  $\hat{O}$ ,

$$\hat{O}_H(t) = e^{i\hat{H}st} \hat{O}_S(t) e^{-i\hat{H}st} = e^{i\hat{H}st} e^{-i\hat{H}_0 st} \hat{O}_I(t) e^{i\hat{H}_0 st} e^{-i\hat{H}st} = \hat{U}_I(0, t) \hat{O}_I(t) \hat{U}_I(t, 0), \quad (2.18)$$

where in the last step we use the fact that  $\hat{U}_I^\dagger(t, 0) = \hat{U}_I(0, t)$ .

### 2.1.2 Field operators

The occupation number vectors are basis vectors in an abstract linear vector space, the Fock space  $\mathcal{F}$ . This latter consists of the direct sum of all  $N$ -particle Hilbert spaces  $\mathcal{H}_a^{(N)}$ , with  $N = 0, 1, 2, \dots$

$$\mathcal{F} = \mathcal{H}^{(0)} \oplus \mathcal{H}^{(1)} \oplus \mathcal{H}_a^{(2)} \oplus \dots \quad (2.19)$$

The Fock space contains states for unlimited and variable number of particles. We can now define the creation and annihilation operators in the Fock space. The operator of annihilation  $a_i$  and creation  $a_i^\dagger$  change a  $N$ -particle state in a  $N - 1$ - and  $N + 1$ -particle state, respectively:

$$a_i |n_1, \dots, n_i, \dots\rangle = n_i \cdot (-1)^{\sum_{j < i} n_j} |n_1, \dots, n_i - 1, \dots\rangle \quad (2.20)$$

$$a_i^\dagger |n_1, \dots, n_i, \dots\rangle = (1 - n_i) \cdot (-1)^{\sum_{j < i} n_j} |n_1, \dots, n_i + 1, \dots\rangle. \quad (2.21)$$

In a simplified and clearer way this means:

$$a_i |n_1, \dots, 1_i, \dots\rangle = \pm |n_1, \dots, 0_i, \dots\rangle \quad a_i^\dagger |n_1, \dots, 1_i, \dots\rangle = 0 \quad (2.22)$$

$$a_i |n_1, \dots, 0_i, \dots\rangle = 0 \quad a_i^\dagger |n_1, \dots, 0_k, \dots\rangle = \pm |n_1, \dots, 1_i, \dots\rangle. \quad (2.23)$$

The operator  $a_i$  destroys hence a particle in the state  $\varphi_i$  and the number of particle decreases by one, if  $\varphi_i$  is occupied, otherwise the result is zero. The operator  $a_i^\dagger$  creates a particle in the state  $\varphi_i$ , provided that it is empty (otherwise the result is zero), and hence the number of particle increases by 1.

Applying the creation operator to the vacuum  $|0, 0, \dots\rangle$ , all possible  $N$ -particle states can be created:

$$|n_1, n_2, \dots, n_N\rangle = a_1^\dagger a_2^\dagger \dots a_N^\dagger |0, 0, \dots\rangle. \quad (2.24)$$

We now arrive at the most important property of the creation and annihilation operators for fermions: their anti commutation relations,

$$\{a_i, a_j\} = 0 \quad \{a_i^\dagger, a_j^\dagger\} = 0 \quad \{a_i^\dagger, a_j\} = \delta_{ij}. \quad (2.25)$$

If  $\{\phi_i(x)\}$  is an orthonormal basis set ( $\int dx \phi_i^*(x) \phi_j(x) = \delta_{ij}$ ) then one can define new annihilation and creation operators as:

$$\psi(x) = \sum_i \phi_i(x) a_i \quad (2.26)$$

$$\psi^\dagger(x) = \sum_i \phi_i^*(x) a_i^\dagger. \quad (2.27)$$

The operators  $\psi(x)$  et  $\psi^\dagger(x)$  are traditionally called field operators. These operators satisfy the same anti commutation relations as the operators  $a_i$  and  $a_i^\dagger$ , i.e.,

$$\{\psi(x), \psi(x')\} = 0 \quad \{\psi^\dagger(x), \psi^\dagger(x')\} = 0 \quad \{\psi^\dagger(x), \psi(x')\} = \delta(x - x'). \quad (2.28)$$

Using the field operators one can express each one-body and two-body operator  $\hat{O}_1$  and  $\hat{O}_2$ , respectively as

$$\hat{O}_1 = \int dx \hat{\psi}^\dagger(x) o(x) \hat{\psi}(x) \quad (2.29)$$

$$\hat{O}_2 = \int dx dx' o(x, x') \hat{\psi}^\dagger(x) \hat{\psi}^\dagger(x') \hat{\psi}(x') \hat{\psi}(x). \quad (2.30)$$

Therefore, a general Hamiltonian

$$\hat{H}(t) = \sum_i^N h(x_i, t) + \frac{1}{2} \sum_{i \neq j}^N \frac{1}{|r_i - r_j|} \quad (2.31)$$

can be written, in terms of the field operators, as

$$\hat{H} = \int dx \psi^\dagger(x) h(x, t) \psi(x) + \frac{1}{2} \int dx dx' \psi^\dagger(x) \psi^\dagger(x') \frac{1}{|r - r'|} \psi(x') \psi(x). \quad (2.32)$$

We will use this framework to define the Green's function in many-body physics. Let's now spend a few words on the mathematical meaning of a Green's function.

## 2.2 The Green's function

Suppose we have a first order homogeneous or inhomogeneous partial differential equation reading:

$$\left[ \frac{i}{c} \frac{\partial}{\partial t} - \mathcal{L}(r) \right] \phi(r, t) = 0, \quad (2.33a)$$

$$\left[ \frac{i}{c} \frac{\partial}{\partial t} - \mathcal{L}(r) \right] \hat{\psi}(r, t) = f(r, t), \quad (2.33b)$$

where  $\mathcal{L}(r)$  is a time-independent, hermitian, linear differential operator and the same boundary condition as for  $\phi(r, t)$  and  $\hat{\psi}(r, t)$  apply and  $c$  is just some positive constant.

The Green's function  $G(r, r', t, t')$  is defined as solution of:

$$\left[ \frac{i}{c} \frac{\partial}{\partial t} - \mathcal{L}(r) \right] G(r, r', t, t') = \delta(r - r') \delta(t - t'), \quad (2.34)$$

Since  $\mathcal{L}(r)$  is time-independent one can express the Green's function as a function of the time difference  $t - t' = \tau$ , so that its Fourier transform reads:

$$G(r, r', \tau) = \frac{1}{2\pi} \int_{-\infty}^{\infty} d\omega' g(r, r', \omega') e^{-i\omega' \tau}. \quad (2.35)$$

Substitution of the  $\mathcal{F}$ -transform into (2.34) yields:

$$\left[ \frac{\omega}{c} - \mathcal{L}(r) \right] G(r, r', \omega) = \delta(r - r'). \quad (2.36)$$

The above expression somehow suggests to see  $G$  as the *inverse* of the operator  $\mathcal{L}(r)$ . If we replace  $\mathcal{L}$  with a well known operator:  $\mathcal{L}(r) \rightarrow -i \frac{\partial}{\partial t} + \hat{H}_0(x)$  we can recast Eq. (2.36) as:

$$\left[ -\frac{i}{c} \frac{\partial}{\partial t} + \hat{H}_0(r) \right] G(r, r', \omega) = -\delta(r - r'). \quad (2.37)$$

We will see now, throughout the rest of the chapter, how physicists define, use and calculate the one-body Green's function.

## 2.3 The Green's function in Many-body physics

The definition of the zero-temperature, equilibrium, time-ordered, one-body Green's function for a fermion reads:

$$G(1, 2) = -i \langle \Psi_0^N | \mathcal{T} [\hat{\psi}_H(1) \hat{\psi}_H^\dagger(2)] | \Psi_0^N \rangle, \quad (2.38)$$

here and throughout the manuscript atomic units ( $\hbar = e^2 = m_e = 1$ ) are used. In (2.38) the index (1), for the sake of compactness, includes the space, spin and time variables:  $(1) = (x_1, t_1) = (r_1, \sigma_1, t_1)$ .  $\Psi_0^N$  is the N-body ground state wave function of the system,  $\hat{\psi}_H(1)$ ,  $\hat{\psi}_H^\dagger(2)$  are field operators in the Heisenberg representation:

$$\begin{cases} \hat{\psi}_H(1) = e^{iHt_1} \hat{\psi}_S(r_1, \sigma_1) e^{-iHt_1} \\ \hat{\psi}_H^\dagger(2) = e^{iHt_2} \hat{\psi}_S^\dagger(r_2, \sigma_2) e^{-iHt_2} \end{cases} \quad (2.39)$$

( $\hat{\psi}_S^\dagger$  is the corresponding Schrödinger representation) and  $\mathcal{T}$  is the so called Wick operator, which accounts for the *time ordering* of the field operators. Eq. (2.38) can be equivalently recast as:

$$\begin{aligned} G(1, 2) &= -i \left[ \theta(t_1 - t_2) \langle \Psi_0 | [\hat{\psi}_H(1) \hat{\psi}_H^\dagger(2)] | \Psi_0 \rangle - \theta(t_2 - t_1) \langle \Psi_0 | [\hat{\psi}_H^\dagger(2) \hat{\psi}_H(1)] | \Psi_0 \rangle \right] \\ &= G^>(1, 2) \theta(t_1 - t_2) + G^<(1, 2) \theta(t_2 - t_1) \end{aligned} \quad (2.41)$$

where  $G^>(1, 2)$  and  $G^<(1, 2)$  are the so-called *greater and lesser* Green's functions and are defined as follows:

$$\begin{cases} G^>(1, 2) = -i \langle \Psi_0 | [\hat{\psi}_H(1) \hat{\psi}_H^\dagger(2)] | \Psi_0 \rangle \\ G^<(1, 2) = i \langle \Psi_0 | [\hat{\psi}_H^\dagger(2) \hat{\psi}_H(1)] | \Psi_0 \rangle \end{cases} \quad (2.42)$$

This latter notation turns out to be practical when dealing extensively and analytically with the different time-orderings.

The one-particle Green's function expresses the probability amplitude for an *electron* (a *hole*) which at time  $t_1$  ( $t_2$ ) is added to the system (in its ground-state) in  $r_1$  ( $r_2$ ) with spin  $\sigma_1$  ( $\sigma_2$ ) to be found at  $r_2$  ( $r_1$ ) with spin  $\sigma_2$  ( $\sigma_1$ ) at a time  $t_2 > t_1$  ( $t_1 > t_2$ ). For this reason sometimes in literature the greater Green's function is called *electron* Green's function and the lesser Green's function *hole* Green's function. *Which kind of information the one-body Green's function can provide us with?* There are mainly three types [36], all of them very useful for condensed matter physicists, namely: **i)** the expectation value of any single-particle operator in the ground state of the system, **ii)** the total ground state energy, **iii)** the excitation spectrum.

Let's proceed with order. We have seen that with a time-independent Hamiltonian any one-body operator  $\hat{O}$  can be expressed in the second quantization formalism as in Eq. (2.29); a comparison with the definition of the *GF*, Eq. (2.40), shows that the expectation value  $\langle \Psi_0 | \hat{O} | \Psi_0 \rangle$  can be expressed in terms of the one-particle Green's function as:

$$\langle \hat{O} \rangle = -i \lim_{x_2 \rightarrow x_1} \lim_{t_2 \rightarrow t_1^+} \int dx_1 o(x_1) G(x_1, t_1; x_2, t_2) \quad (2.43)$$

where the limit  $t_1^+ = t_1 + \delta$ , with  $\delta$  a small positive quantity. For example, the expectation value of the electronic density is the diagonal in space, spin, and time of the GF:

$$\langle \hat{n}(x_1) \rangle = -iG(x_1, t_1, x_1, t_1^+). \quad (2.44)$$

The Green's function can, maybe surprisingly at first sight, be employed also for calculating a quantity which in principle contains two-body operators (for the evaluation of which the two-body Green's function is needed, rather than the one body-one), namely the ground state *total energy*. Galitskii and Migdal [26, 36] first, realized that this was possible starting from the equation of motion for the field operator (see Eq. (2.8)). Some algebra leads to:

$$E = \langle \hat{T} \rangle + \langle \hat{V} \rangle = -\frac{i}{2} \int dx_1 \lim_{x_2 \rightarrow x_1} \lim_{t_2 \rightarrow t_1^+} \left[ i \frac{\partial}{\partial t_1} - \frac{1}{2} \nabla_{x_1}^2 \right] G(x_1, x_2; t_1 - t_2). \quad (2.45)$$

We will now deal with the third type of observable obtainable from the one-body Green's function, that is the spectral function.

However, before proceeding further with the discussion, we will move to the representation of the one-body GF in the frequency domain: this is an undoubtedly useful transformation in the case of an Hamiltonian which does not depend explicitly on time <sup>a</sup>. We report below the main algebraic steps needed to switch from the time to the frequency domain. We will treat only the so-called *greater* Green's function, since the *lesser* can be treated in an analogous way. Writing down the field operators in the Heisenberg picture explicitly yields:

$$G^>(x_1, t_1, x_2, t_2) = -i\theta(t_1 - t_2) \langle \Psi_0^N | e^{i\hat{H}t_1} \hat{\psi}_S(x_1) e^{-i\hat{H}t_1} e^{i\hat{H}t_2} \hat{\psi}_S^\dagger(x_2) e^{-i\hat{H}t_2} | \Psi_0^N \rangle. \quad (2.46)$$

Inserting the completeness relation in Fock space between couples of field operators combined with the action of the exponential operators on the ground state and the  $(N+1)$  particle states yields:

$$G^>(x_1, t_1, x_2, t_2) = -i \sum_s \theta(t_1 - t_2) e^{-i(E_s^{N+1} - E_0^N)(t_1 - t_2)} \langle N | \hat{\psi}(x_1) | \Psi_s^{N+1} \rangle \langle \Psi_s^{N+1} | \hat{\psi}^\dagger(x_2) | N \rangle \quad (2.47)$$

We want now to exploit the fact that the GF only depends on the difference between  $t_1$  and  $t_2$ . To this purpose we define the so-called *Feynman-Dyson* amplitudes:

$$f_s(x_1) = \langle \Psi_0^N | \hat{\psi}_S(x_1) | \Psi_s^{N+1} \rangle \quad (2.48a)$$

$$f_s^*(x_2) = \langle \Psi_s^{N+1} | \hat{\psi}_S^\dagger(x_2) | \Psi_0^N \rangle. \quad (2.48b)$$

Eq. (2.47) becomes:

$$G^>(x_1, x_2, \tau) = -i \sum_s \theta(\tau) e^{-i(E_s^{N+1} - E_0^N)\tau} f_s(x_1) f_s^*(x_2) \quad (2.49)$$

where  $\tau = t_1 - t_2$ . Manipulating  $G^<$  in an analogous way and upon introducing a second set of amplitudes which reads:

$$g_p(x_1) = \langle \Psi_p^{N-1} | \hat{\psi}_S(x_1) | \Psi_0^N \rangle \quad (2.50a)$$

---

<sup>a</sup>This has the important implication that the one-body  $G$  depends only on the difference of the times  $\tau_{12} = t_1 - t_2$

$$g_p^*(x_2) = \langle \Psi_0^N | \hat{\psi}_S^\dagger(x_2) | \Psi_p^{N-1} \rangle. \quad (2.50b)$$

one ends up with full time-ordered Green's function reading:

$$G(x_1, x_2; \tau) = - \left[ i \left[ \theta(\tau) \sum_s e^{-i(E_s^{N+1} - E_0^N)\tau} f_s(x_1) f_s^*(x_2) \right. \right. \\ \left. \left. - \theta(-\tau) \sum_p e^{i(E_p^{N-1} - E_0^N)\tau} g_p(x_1) g_p^*(x_2) \right] \right]. \quad (2.51)$$

We can now Fourier-transform ( $\mathcal{F}$ -T) the above expression<sup>b</sup> Using the following expression for the Heaviside step function  $\theta(\tau)$ ,

$$\theta(\tau) = -\frac{1}{2i\pi} \lim_{\eta \rightarrow 0^+} \int_{-\infty}^{\infty} d\omega \frac{1}{\omega + i\eta} e^{-i\omega\tau}. \quad (2.54)$$

Eq. (2.51) becomes:

$$G(x_1, x_2; \omega) = \lim_{\eta \rightarrow +0} \left[ \sum_s \frac{f_s(x_1) f_s^*(x_2)}{\omega - (E_s^{N+1} - E_0^N) + i\eta} + \sum_p \frac{g_p(x_1) g_p^*(x_2)}{\omega - (E_0^N - E_p^{N-1}) - i\eta} \right] \quad (2.55)$$

In Eq. (2.55) the quantities of interest are sitting in the denominator: the energy differences  $(E_s^{N+1} - E_0^N)$  and  $(E_0^N - E_p^{N-1})$  are the *true electron addition and removal energies* of the system. The first set of energies represents the energies gained when an electron is added to the system (*addition energies*); the largest electron addition energy is the electronic affinity  $\mathcal{A}$  of the system. The second set represents the energies for the removal of an electron from the system (*removal energies*); the smallest electron removal energy is the ionization potential  $\mathcal{I}$ . If the system under consideration is a metal, the energy  $\mathcal{I} = \mathcal{A}$  is the chemical potential  $\mu$ ; instead, if the system is insulating, the band gap  $E_g$  is defined as the energy difference between ionization potential and electron affinity, i.e.  $E_g = \mathcal{I} - \mathcal{A}$ , and the Fermi level lies somewhere inside the gap. Note how the greater Green's function is analytic in the upper half of the complex plane, whereas the lesser Green's function is analytic in the lower half of the complex plane, since their poles lie in the corresponding opposite half of the complex plane, as shown in Fig. 2.3

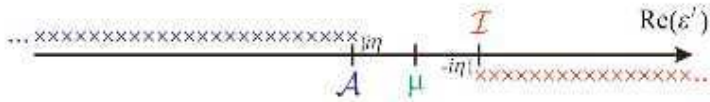


**Figure 2.1:** Figure from [38]. Poles of the time ordered Green's function in the complex  $\omega$ -plane. The poles (crosses) are located above the real axis for frequencies lower than the chemical potential  $\mu$  (lesser GF), and below for frequencies greater than  $\mu$  (greater GF).

<sup>b</sup>We use the following definition of Fourier transform of a general function  $f$ :

$$\tilde{f}(\omega) = \int dt f(t) e^{i\omega t}; \quad (2.52)$$

and for the reverse Fourier transform

$$f(t) = \frac{1}{2\pi} \int d\omega \tilde{f}(\omega) e^{-i\omega t}; \quad (2.53)$$

### 2.3.1 The spectral representation for the Green's function

The Lehmann representation for the Green's function will be the starting point to discuss its *spectral representation*. One can recast the *GF* as:

$$G(x_1, x_2; \omega) = \int_{-\infty}^{\mu} d\omega' \frac{A^h(x_1, x_2; \omega')}{\omega - \omega' - i\eta} + \int_{\mu}^{\infty} d\omega' \frac{A^e(x_1, x_2; \omega')}{\omega - \omega' + i\eta} \quad (2.56)$$

where  $A^e$  ( $A^h$ ) is called electron (hole) *spectral function* and is a *real valued function* for an Hamiltonian independent of magnetic fields. Using the relation

$$\lim_{\eta \rightarrow 0^+} \frac{g(x)}{x \pm i\eta} = \mathcal{P} \frac{g(x)}{x} \mp i\pi g(x) \delta(x) \quad (2.57)$$

where  $\mathcal{P}$  is the Cauchy principal value, one can reformulate Eq. (2.56) as:

$$\begin{aligned} G(x_1, x_2; \omega) &= i\pi \int_{-\infty}^{\mu} d\omega' A^h(x_1, x_2; \omega') \delta(\omega - \omega') + \int_{-\infty}^{\mu} d\omega' \frac{A^h(x_1, x_2; \omega')}{\omega - \omega'} \\ &\quad - i\pi \int_{\mu}^{\infty} d\omega' A^e(x_1, x_2; \omega') \delta(\omega - \omega') + \int_{\mu}^{\infty} d\omega' \frac{A^e(x_1, x_2; \omega')}{\omega - \omega'} \end{aligned} \quad (2.58)$$

Since both  $A^h$  and  $A^e$  are real valued, by comparing the above expressions, one can write the identity:

$$\begin{aligned} A^h(x_1, x_2; \omega) &= \frac{1}{\pi} \mathcal{I}m G(x_1, x_2; \omega) & \omega < \mu \\ A^e(x_1, x_2; \omega) &= -\frac{1}{\pi} \mathcal{I}m G(x_1, x_2; \omega) & \omega > \mu \end{aligned} \quad (2.59)$$

The prototypical spectral function may resemble the one in Fig. 2.5. The advantage of working with spectral functions over Green's function is at least twofold. Firstly, as we have just demonstrated the two quantities are related in a very straightforward manner and if we have access to one, obtaining the other is relatively simple, however, while spectral functions are real, Green's function are not. Secondly spectral functions are directly related to quantities measurable in direct and inverse photo emission experiments: this fact makes them very attractive since they are some observable that both theorists and experimentalists can access at the same time.

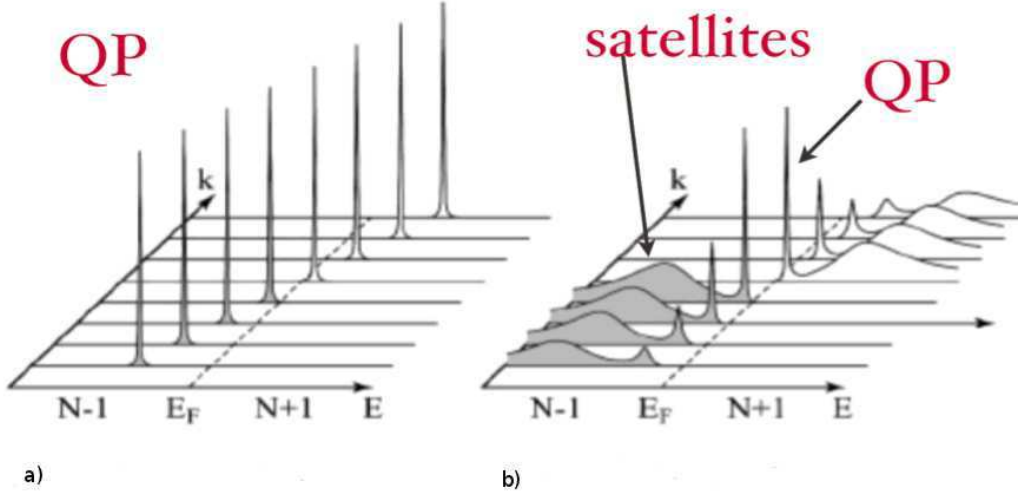


**Figure 2.2:** From in [39] (Fig. 3). Typical spectral functions of an extended system resolved in  $k$ -space. In Figure **a)** we can observe the spectral function of a system of non-interacting electrons: it is simply a delta-peak function, which indicates that the life-time of the excitations in such system is infinite. In Figure **b)** the spectral function of a fully interacting system is shown. The main peak, so-called quasi-particle (QP) peak appears together with additional structures. Close to the Fermi level the QP peak is very sharp and well defined, the renormalization effects on the single-particle peak is fairly small. The secondary structure (broader peak), is called satellite and it accounts for some other type of many-particle excitation. Often it's a plasmonic one (collective charge density oscillations), but not only: it could be also a mixing of different excitations, making almost impossible to associate each peak to a particular excitation. An accurate description of QP peaks is, nowadays, achieved routinely, while the description of satellite peaks is already more challenging, in particular when *satellite replicas* are to be reproduced. Ideally, however, one wishes to have such an accurate Green's function to be able to obtain a spectral function accounting for all many-body effects in a given material.

## 2.4 From the definition of the one-body Green's function to its calculation

Suppose we are dealing with a many-body system, described using the following Hamiltonian [36] (in the second quantization formalism):

$$\hat{H} = \int dx_1 \hat{\psi}^\dagger(x_1) h(r_1) \hat{\psi}(x_1) + \frac{1}{2} \int dx_1 dx_2 \hat{\psi}^\dagger(x_1) \hat{\psi}^\dagger(x_2) v(r_1, r_2) \hat{\psi}(x_2) \hat{\psi}(x_1) \quad (2.60)$$

being  $h(r_1) = -\frac{1}{2}\nabla^2 + V_{ext}(r_1)$  and  $v(r_1, r_2)$  respectively the kinetic energy operator and the instantaneous Coulomb potential. Obviously the definition in Eq. (2.38) cannot provide the value of the Green's function because it assumes the ground state wave function of the system to be known, and in general this is not the case. So in practice one *propagates* in time the one-body  $G$ , that is:

$$i \frac{\partial}{\partial t_1} G(x_1, t_1, x_2, t_2) \quad \text{or equivalently} \quad i \frac{\partial}{\partial t_2} G(x_1, t_1, x_2, t_2). \quad (2.61)$$

From now on we will work only with the first of the two expressions (the derivative with respect to  $t_2$  can be treated in the same way). Furthermore we work in the Heisenberg picture; for simplicity we will drop the subscript "H" indicating this picture in the following. Differentiating Eq. (2.40) with respect to  $t_1$  we obtain:

$$\begin{aligned} \frac{\partial}{\partial t_1} G(x_1, t_1, x_2, t_2) &= -i \left[ \langle \Psi_0^N | \frac{\partial}{\partial t_1} \theta(t_1 - t_2) \hat{\psi}(x_1, t_1) \hat{\psi}^\dagger(x_2, t_2) \right. \\ &+ \theta(t_1 - t_2) \frac{\partial}{\partial t_1} \hat{\psi}(x_1, t_1) \hat{\psi}^\dagger(x_2, t_2) \\ &- \frac{\partial}{\partial t_1} \theta(t_2 - t_1) \hat{\psi}^\dagger(x_2, t_2) \hat{\psi}(x_1, t_1) \\ &\left. - \theta(t_2 - t_1) \hat{\psi}^\dagger(x_2, t_2) \frac{\partial}{\partial t_1} \hat{\psi}(x_1, t_1) | \Psi_0^N \rangle \right], \end{aligned} \quad (2.62)$$

Using  $\frac{\partial}{\partial t_1} \hat{\psi}(x_1, t_1) = -i [\hat{\psi}(x_1, t_1), \hat{H}]$ , with some algebra Eq. (2.62) becomes:

$$\begin{aligned} \frac{\partial}{\partial t_1} G(x_1, t_1, x_2, t_2) &= -i \delta(x_1, x_2) \delta(t_1, t_2) - i h_0(x_1) \langle \Psi_0^N | \mathcal{T} [\hat{\psi}(x_1, t_1) \hat{\psi}^\dagger(x_2, t_2)] | \Psi_0^N \rangle \\ &- \int dx_3 dt_3 v(x_1, t_1, x_3, t_3) [\theta(t_1, t_2) \langle \Psi_0^N | \hat{\psi}^\dagger(x_3, t_3) \hat{\psi}(x_3, t_3) \hat{\psi}(x_1, t_1) \hat{\psi}^\dagger(x_2, t_2) | \Psi_0^N \rangle \\ &- \theta(t_2 - t_1) \langle \Psi_0^N | \hat{\psi}^\dagger(x_2, t_2) \hat{\psi}^\dagger(x_3, t_3) \hat{\psi}(x_3, t_3) \hat{\psi}(x_1, t_1) | \Psi_0^N \rangle]. \end{aligned} \quad (2.63)$$

In the last two lines of Eq. (2.63) the pair of operators  $\hat{\psi}_H^\dagger(3) \hat{\psi}_H(3)$  is actually evaluated at  $t_3 = t_1$ , due to the  $\delta(t_1, t_3)$  coming from the Coulomb potential  $v(1, 3)$ .

We have finally obtained an expression containing two different combination of field operators, namely the well known one for the one-body Green's function ( $G(1, 2)$ ) and a new, more complicated one, which we recognize being a two-body Green's function:

$$G(1, 3; 4, 2) = -i^2 \langle \Psi_0^N | \mathcal{T} [\hat{\psi}_H(1) \hat{\psi}_H(3) \hat{\psi}_H^\dagger(2) \hat{\psi}_H^\dagger(4)] | \Psi_0^N \rangle. \quad (2.64)$$

Eq. (2.63) can then be recast as:

$$\left[ i \frac{\partial}{\partial t_1} - h(r_1) \right] G(1, 2) + i \int d^3 v(1^+, 3) G_2(1, 3; 2, 3^+) = \delta(1, 2), \quad (2.65)$$

where we have replaced  $v(1, 3)$  with  $v(1^+, 3)$  to take into account the correct ordering of field operators. Eq. (Eqn:eom4) is the so-called *equation of motion* (EOM) for the one-body G. The differential form  $\left[ i \frac{\partial}{\partial t_1} - h(r_1) \right]$  is not an easy one to deal with. We can employ the following definition:

$$\left[ i \frac{\partial}{\partial t_1} - h(r_1) \right] G_0(1, 2) = \delta(1, 2), \quad (2.66)$$

to recast Eq. (2.65) in a more handy form:

$$G(1, 2) = G_0(1, 2) - i \int d^3 d^4 G_0(1, 3) v(3^+, 4) G_2(3, 4; 2, 4^+). \quad (2.67)$$

Here  $G_0$ , the non-interacting Green's function, determines the appropriate *initial condition in time*<sup>c</sup>, note in fact that the solutions to (2.65) and (2.66) are not unique.

If we turn to the expression in (2.67) it is obvious that no advantage has been gained over the initial EOM for  $G$ : to calculate the one-body Green's function the knowledge of the two-body one is now required. The EOM for the  $G_2$  would in turn depend on the knowledge of the three-body Green's function, which, if propagated in time too would depend on a four-body one and so on and so forth. Definitely we do not want to express the one-body  $G$  through a complicated hierarchy of higher order Green's functions [41].

One way to obtain a *closed expression* for  $G$  was first devised by Schwinger [42] in the '50s.

Roughly speaking, the physical intuition behind Schwinger functional machinery is that if a system is probed at a given time, through an external, time dependent, fictitious potential and which is then let vanish at some other time, one can observe the polarization of the system and the propagation of  $G$ . Let's now present the actual mathematical framework.

The one-body Green's function is first *generalized*, which is to say it is defined for a -now time dependent- many-body Hamiltonian, to which a term containing an external, time-dependent potential  $\varphi(t)$  has been added, namely  $\hat{H}'(t) = \int dx \psi_S^\dagger(x) \varphi(x, t) \psi_S(x)$ . The *GF* now reads:

$$G(1, 2; [\varphi]) = -i \frac{\langle \Psi_0 | \mathcal{T} \left[ \hat{S} \hat{\psi}_H(1) \hat{\psi}_H^\dagger(2) \right] | \Psi_0 \rangle}{\langle \Psi_0 | \mathcal{T} [\hat{S}] | \Psi_0 \rangle} \quad (2.68)$$

where the operator  $\hat{S}$  is formally defined as

$$\hat{S} = e^{-i \int_{-\infty}^{\infty} dt \hat{H}'_I(t)}. \quad (2.69)$$

with  $\hat{H}'_I(t) = e^{i\hat{H}t} \hat{H}'(t) e^{-i\hat{H}t}$  in the interaction picture. Eq. (2.68) can be differentiated within a very similar procedure to the one illustrated for the equilibrium ( $\varphi = 0$ ) Green's function yielding an expression equivalent to that of Eq. (2.67), where all the Green's function appearing are generalized to non-equilibrium<sup>d</sup>. Within this generalized writing for the GF one can show that the two-body Green's function can be recast in an *exact* way as<sup>e</sup>

$$G_2(3, 4; 2, 4^+; [\varphi]) = G(3, 2; [\varphi]) G(4, 4^+; [\varphi]) - \frac{\delta G(3, 2; [\varphi])}{\delta \varphi(4)}. \quad (2.70)$$

Finally inserting (2.70) into the generalized version of (2.67) yields a set of functional differential

<sup>c</sup>For an extensive discussion on this issue see i.e. [40], Chap.1, pagg. 4-8. Briefly: it is convenient to discuss this issue for finite temperatures and *imaginary* times ( $t = i\beta$ , where  $\beta = \frac{1}{k_b T}$ ) and one first finds an important conditions on the times for the lesser and the greater Green's function, namely  $G^<(1, 1')|_{t_1=0} = \pm e^{\beta\mu} G^>(1, 1')|_{t_1=-i\beta}$ . Further considerations on the boundaries for  $t_1$  yield an analogous conditions for the full Green's function:  $G(1, 1')|_{t_1=0} = \pm e^{\beta\mu} G(1, 1')|_{t_1=-i\beta}$ . Hence introducing a given  $G_0$  implicitly means to take care of the boundary condition implied by the time-derivative

<sup>d</sup>To do so it is sufficient to recast the one-body term of the Hamiltonian as  $h(r_1, t_1) = -\frac{1}{2}\nabla^2 + V_{ext}(r_1) + \varphi(r_1, t_1)$  embedding also the external potential  $\varphi$ .

<sup>e</sup>Note that Eq. (2.70) refers to the three-point  $G_2$ , which is needed in Eq. (2.67). A relation similar to (2.70) exists for the more general four-point  $G_2$ , where a non local external potential  $\varphi(1, 2)$  appears.

equations [40] for the unknown  $G$ :

$$\begin{aligned}
G(1, 2; [\varphi]) = G_0(1, 2) &+ \int d^3G_0(1, 3)V_H(3; [\varphi])G(3, 2; [\varphi]) \\
&+ \int d^3G_0(1, 3)\varphi(3)G(3, 2; [\varphi]) \\
&+ i \int d^4d^3G_0(1, 3)v(3^+, 4)\frac{\delta G(3, 2; [\varphi])}{\delta\varphi(4)}, \tag{2.71}
\end{aligned}$$

where  $V_H(3) = -i \int d^4v(3, 4)G(4, 4^+; [\varphi])$  is the Hartree potential. Notice that since the Hartree potential contains the Green's function, the above equations are *non-linear*. Once (2.71) is solved, the equilibrium  $G$  can be obtained by taking the limit of vanishing potential  $\varphi = 0$ . The calculation of  $G$  starting from (2.71) requires the solution of a set of coupled, non-linear, first-order differential equations (DEs), which is clearly a non trivial task.

Furthermore one would need an *initial condition* concerning  $G$  as a function of the potential  $\varphi$ , to completely define the desired solution of this DE, since the derivative  $\frac{\delta G([\varphi])}{\delta\varphi}$  has been introduced. This second initial value problem<sup>f</sup> is a really complicated one: to be solved the knowledge of the Green's function for a given external potential  $\varphi$  is required and unfortunately, there is no value of  $\varphi$  for which a full Green's function is already known *a-priori*.

The above arguments elucidate how the calculation of the one-body Green's function is a very challenging task. This is the reason why, along the years, many different routes were pursued. Among them the most ancient approach is the so-called *straightforward diagrammatic expansion*, which looks for an expression for the Green's function in terms of an infinite series, which is truncated at some order and has to be resummed. A second type is constituted by the so-called *self-energy based* methods: it presupposes the reformulation of Eq. (2.71) into an integral form, in which an effective potential, called most often self-energy ( $\Sigma$ ), is introduced. Approximations for  $\Sigma$  are sought and inserted in the integral equation for  $G$ , which is then solved within iterative schemes. The third class encompasses approaches which aim at calculating the  $GF$  in a *direct way* and are neither relying on approximations for  $\Sigma$  nor on finite order diagrammatic expansions. An eminent approach belonging to this group is the so called *cumulant expansion* approximation, which originally was derived as an exact solution to a model problem.

Another direct way to calculate the one-body Green's function could be to solve, at least approximately, the set of differential equations in (2.71): it is the approach that will be explored in this work.

### 2.4.1 Straightforward diagrammatic expansion

We will sketch here an approach to calculate the one-body Green's function which is, perhaps, the oldest ever conceived, and it is deeply rooted in quantum field theory. More detailed presentation of the approach can be found in a number of textbooks, e.g. [36], [43], [37] and others. The main idea is to express the full Green's function within a perturbation expansion in terms of

---

<sup>f</sup>The first initial value problem, or better boundary problem, was instead set by the differentiation with respect to the time of the  $GF$

the *non-interacting* GF ( $G_0$ ) and the bare Coulomb potential  $v$ . The main ingredients needed for the expansion will be the so called *interaction* or *mixed picture* for the representation of the field operators and the *evolution operator* defined accordingly to this new framework. We will then employ the *Gell-Mann and Low theorem* [44] and finally the *Wick's theorem* first and *Feynman diagrams* afterwards will be precious to write down the various terms of the expansion.

Let's begin with the many-body Hamiltonian  $\hat{H}$  which we will now split into two parts:  $\hat{H}_0$ , which represents a soluble problem and  $\hat{H}'$ , which instead contains all those effects which can be difficult to describe (i.e. the two-body Coulomb potential):

$$\hat{H} = \hat{H}_0 + e^{-\epsilon|t|}\hat{H}', \quad (2.72)$$

where  $\epsilon$  is a small positive quantity which allows for an *adiabatic* switching on (and off) [45] of the perturbation; this is an essential requisite for all the considerations we are about to make. At very large times ( $t = \pm\infty$ ) the Hamiltonian (2.72) reduces to  $\hat{H}_0$ , which we can solve, whereas at  $t = 0$  it becomes the dull Hamiltonian of the interacting system.

The interaction picture is a very handy representation of state vectors and operators when one has an Hamiltonian in the form (2.72). In this framework  $\hat{H}'$  fully determines the evolution of the state vectors, while  $\hat{H}_0$  governs the evolution of the operators<sup>§</sup>, specifically:

$$i\frac{\partial}{\partial t}|\hat{\Psi}_\epsilon(t)\rangle_I = e^{-\epsilon|t|}\hat{H}'_I(t)|\hat{\Psi}_\epsilon(t)\rangle_I = e^{-\epsilon|t|}e^{i\hat{H}_0t}\hat{H}'e^{-i\hat{H}_0t}|\hat{\Psi}_\epsilon(t)\rangle_I \quad (2.73)$$

and

$$i\frac{\partial}{\partial t}\hat{O}_I(t) = [\hat{O}_I(t), \hat{H}_0]. \quad (2.74)$$

Any state vector in the interaction picture evolves from the time instant  $t_0$  to the instant  $t$  according to:

$$|\Psi_\epsilon(t)\rangle_I = \hat{U}_\epsilon(t, t_0)|\Psi_\epsilon(t_0)\rangle_I \quad (2.75)$$

where  $U_\epsilon(t, t_0)$  is the so called *evolution operator*. Note that since

$$|\Psi_\epsilon(t)\rangle_I = e^{i\hat{H}_0t}|\Psi_\epsilon(t)\rangle_S = e^{i\hat{H}_0t}\hat{U}_\epsilon(t, t')|_S\Psi_\epsilon(t')\rangle_S = e^{i\hat{H}_0t}\hat{U}_\epsilon(t, t')|_S e^{-i\hat{H}_0t'}\Psi_\epsilon(t')\rangle_I \quad (2.76)$$

then

$$\hat{U}_\epsilon(t, t')_I = e^{i\hat{H}_0t}\hat{U}_\epsilon(t, t')_S e^{-i\hat{H}_0t'}. \quad (2.77)$$

Furthermore,

$$\hat{U}_\epsilon^\dagger(t, t') = U_\epsilon^{-1}(t, t') \quad (2.78a)$$

$$\hat{U}_\epsilon^\dagger(t, t_1)\hat{U}_\epsilon^\dagger(t_1, t') = \hat{U}_\epsilon^\dagger(t, t') \quad (2.78b)$$

$$\hat{U}_\epsilon^\dagger(t, t_1)\hat{U}_\epsilon^\dagger(t_1, t) = 1 \implies \hat{U}_\epsilon^\dagger(t, t_1) = \hat{U}_\epsilon^\dagger(t_1, t). \quad (2.78c)$$

Using (2.73) (2.75) it is easy to see that  $\hat{U}_\epsilon$  satisfies the following differential equation:

$$i\frac{\partial}{\partial t}U_\epsilon(t, t_0)_I = e^{-\epsilon|t|}\hat{H}'_I(t)U_\epsilon(t, t_0)_I, \quad (2.79)$$

---

<sup>§</sup>It may be clear after this explanation why the name "mixed", because it is the analogous of the Schrödinger picture on one hand and of the Heisenberg one on the other

which integrated between  $t$  and  $t_0$  gives

$$\hat{U}_\epsilon(t, t_0)_I = 1 - i \int_{t_0}^t e^{-i\epsilon|t|} \hat{H}'_I(t') \hat{U}_\epsilon(t', t_0)_I dt', \quad (2.80)$$

where we have used that  $\hat{U}_\epsilon(t_0, t_0)_I = 1$ . One can attempt to solve the integral in Eq. (2.80) by iteration, always keeping the proper ordering of the operators. The solution thus takes the form:

$$\hat{U}_\epsilon(t, t_0)_I = \mathcal{T} \sum_{n=0}^{\infty} \frac{(-1)^n}{n!} \int_{t_0}^t dt' e^{-i\epsilon|t'|} H'_I(t'). \quad (2.81)$$

Let's now go back to the definition of the one-particle GF and express the field operators in the newly defined interaction picture (rather than in the Heisenberg one). We simply need the following identities for the operators:

$$\hat{\psi}_H(t_1) = e^{i\hat{H}t_1} e^{-i\hat{H}_0 t_1} \hat{\psi}_I(t_1) e^{i\hat{H}_0 t_1} e^{-i\hat{H}t_1} = \hat{U}_\epsilon(0, t_1) \hat{\psi}_I(t_1) \hat{U}_\epsilon(t_1, 0) \quad (2.82)$$

where in the last step we have used Eq. (2.77), and the state vectors

$$|\Psi_\epsilon(t=0)\rangle_H = |\Psi_\epsilon(0)\rangle_I = U_\epsilon(0, \pm\infty) |\Phi_0\rangle. \quad (2.83)$$

In this last equation we relate a fully interacting many-body state of  $\hat{H}$  to the non-interacting ground state of  $\hat{H}_0$ <sup>h</sup>. Clearly  $|\Psi_\epsilon(t=0)\rangle$  depends on the magnitude of  $\epsilon$ , i.e. on how fast the perturbation  $\hat{H}'$  is turned on. If this is done adiabatically we can hope that at each time the ground state adjusts to the potential strength at that time; in this case  $|\Psi_0\rangle = \lim_{\epsilon \rightarrow 0} |\Psi_\epsilon(t=0)\rangle$ . The validity of this relation is guaranteed, for any non-degenerate  $|\Phi_0\rangle$ <sup>i</sup> by the Gell-Mann and Low theorem which states that<sup>j</sup>:

$$|\hat{\Psi}_0\rangle = \lim_{\epsilon \rightarrow 0} \frac{U_\epsilon(0, \pm\infty) |\phi_0^N\rangle}{\langle \phi_0^N | U_\epsilon(0, \pm\infty) | \phi_0^N \rangle}. \quad (2.84)$$

Hence the one-body Green's function can be written as:

$$G(x_1, x_2; t_1, t_2) = -i \lim_{\epsilon \rightarrow 0} \frac{\langle \Phi_0 | U_\epsilon(\infty, t_1) \hat{\psi}_I(x_1, t_1) U_\epsilon(t_1, t_2) \hat{\psi}_I^\dagger(x_2, t_2) U_\epsilon(t_2, -\infty) | \Phi_0 \rangle}{\langle \Phi_0 | U_\epsilon(\infty, -\infty) | \Phi_0 \rangle} \quad (2.85)$$

Using (2.81) one can rewrite (2.85) as

$$\begin{aligned} G(x, x'; t, t') &= -i \lim_{\epsilon \rightarrow 0} \left[ \frac{1}{\langle \Phi_0 | U_\epsilon(\infty, -\infty) | \Phi_0 \rangle} \sum_{n=0}^{\infty} \frac{-i^n}{n!} \int_{-\infty}^{\infty} dt_1 \cdots \int_{-\infty}^{\infty} dt_n \right. \\ &\quad \times \left. e^{-i\epsilon(|t_1| + \cdots + |t_n|)} \langle \Phi_0 | v(t_1)_I \cdots v(t_n)_I \hat{\psi}(x, t)_I \hat{\psi}^\dagger(x', t')_I | \Phi_0 \rangle \right] \quad (2.86) \end{aligned}$$

<sup>h</sup>Note that do to so we have used the fact that all kets are the same at  $t=0$  in *all* pictures and where  $|\Phi_0\rangle$  is the ground state for  $H_0$ , or the non-interacting part of our system

<sup>i</sup>Otherwise care has to be taken in choosing the initial states between the degenerate ones, for a complete discussion of this issue see e.g. [46]

<sup>j</sup>A proof of the theorem can be found in the original paper by Gell-Mann and Low [44] and also in textbooks, e.g. in [36]. Just a gloss about a few technicalities of the GL theorem. **i** Note the denominator appearing in the theorem: it is indispensable to cancel out divergences coming out from an expansion of the numerator - a pedagogical example of this issue can be found in [46]-. **ii**) The theorem holds both for  $t = \pm\infty$ : it means that the initial and final state of the system must be the same. This may be not so obvious, however it is mathematically sound. Also note that switching on and off a particle particle interaction may look trickier than doing the same operation on an external potential. **iii**) The state  $|\hat{\psi}_0^N\rangle$  is not guaranteed to be the ground state of the interacting system, but just *a* state, however in general it really is.

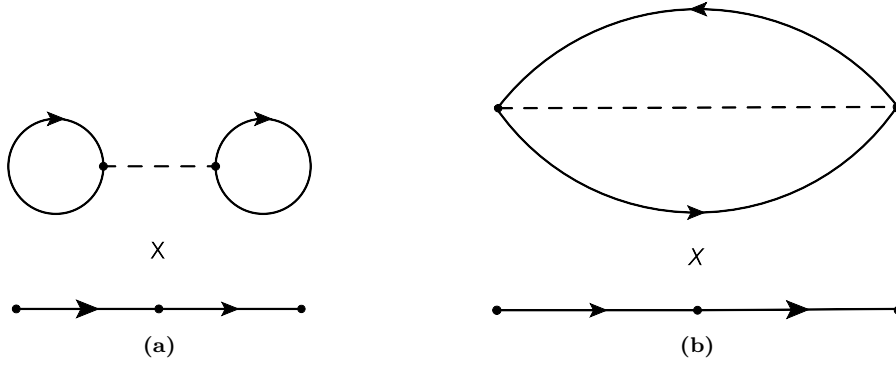


**Figure 2.3:** Fig 4.5a shows a diagram which appears both in the numerator and the denominator of Eq. (2.86). It is the product of a non-interacting Green's function (depicted with a fermion straight line) and two pairs of hole-electron Green's function interacting with each other. In Fig 4.5b another type of disconnected diagram is depicted: it is the product of a non interacting Green's function with a particle interacting with itself.

Considering  $\hat{H}'$  as the Coulomb potential in the second quantization, one ends up with a Green's function with the following schematic structure:

$$\frac{(-i)^n}{n!2^n} \int dx_1 dx_{1'} \dots \int d^n t \cdot e^{-\epsilon(|t_1| \dots)} \sum (\pm) \underbrace{\langle v \rangle \langle v \rangle}_{n \text{ factors}} \underbrace{(iG^{(0)}) \dots (iG^{(0)})}_{2n+1 \text{ factors for } G} \quad (2.87)$$

Note how, within this approach, the full Green's function is just a series expansion in terms of the non-interacting Green's function and the bare Coulomb interaction. For more details about its formulation and application, we suggest to refer to [36, 37].

The above expansion is a highly non trivial result: we can expect some pattern in the type of terms arising from higher orders and indeed it leaves hope for the possibility of *partially resumming* the series, keeping from time to time only the "most important" integrals.

In particular, for the above expression, a number of terms in the numerator *cancel out exactly* all the terms in the denominator. In the language of Feynman diagrams, one would say that the denominator cancels all of the *disconnected*<sup>k</sup> diagrams in the numerator. The Green's function is hence composed by *connected* diagrams only, such as those shown in Figs.2.4a and 2.4b. The caveat of the diagrammatic expansion is that summing up a finite number of terms may, in some cases, yield poor results. Ideally one would like to resum an infinite number of terms and this can be done recasting the differential equation into an integral one, so called Dyson-equation and then solve it (within a given approximation). We will discuss the importance of the Dyson equation in many-body perturbation theory in the next section.

<sup>k</sup>Disconnected diagrams contain subunits that are not connected to the rest of the diagram by any line (see Figs. 4.5a and 4.5b)

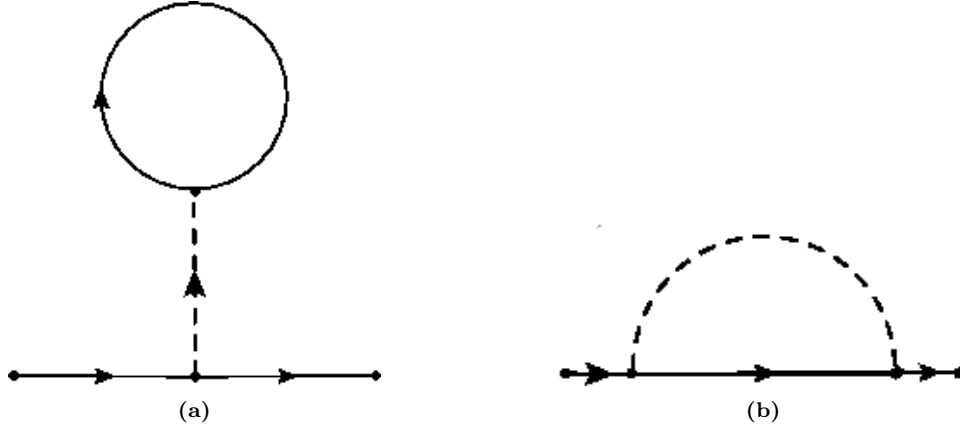


**Figure 2.4:** Fig 2.4a contains a *connected* diagram. It means it cannot be factorized, since the fermionic line is *interacting* with the remaining part of the diagram and not simply multiplying it (as we have instead observed in the *disconnected* diagrams). The first order of the perturbation expansions provides us with two of such diagrams. Higher order will yield more complicated diagrams of this type. Fig 2.4b show a different *connected* diagram. As the diagram in Fig. 2.4a it does not get canceled out from the expansion for the denominator.

## 2.4.2 Self-energy based methods

In the following we will briefly present methodologies to calculate the one-body Green's function based on approximations to the self-energy kernel. We will mainly focus on the so called *GW approximation*, which Hedin [14], derived building on earlier works [47]. It was then probably starting from the late '80s, with the works of Hanke [48], Hybertsen and Louie [49],[50] and Godby, Schlüter and Sham [51], [?] that the approach gained more and more popularity, to the point that it is nowadays the tool of choice for ab-initio band-structure [15] and photo emission spectra calculations [16, 17].

### Hedins' equations and the GW approximation

As previously discussed solving Eq. (2.71) is a fairly complicated task. In particular the one-body Green's function is still expressed in terms of an unknown quantity, the functional derivative  $\frac{\delta G(3, 2; [\varphi])}{\delta \varphi(4)}$ . It was found, that including such quantity (and hence all the many-body effect in the system beyond the Hartree term) in the definition of a *self-energy* kernel  $\Sigma$ , namely:

$$\Sigma(1, 3) = i \int d4d2 v(1^+, 4) \frac{\delta G(1, 2; [\varphi])}{\delta \varphi(4)} \Big|_{\varphi=0} G^{-1}(2, 3), \quad (2.88)$$

might be a promising route to calculate  $G$ . Reinserting (2.88) into the DE (for  $\varphi = 0$ ) one obtains:

$$\begin{aligned} G(1, 2) &= G_0(1, 2) + \int d3 G_0(1, 3) V_H(3) G(3, 2) \\ &+ \int d4d3 G_0(1, 3) \Sigma(3, 4) G(4, 2), \end{aligned} \quad (2.89)$$

which is the so-called integral form of the Dyson equation for  $G$ . In Chapter 4 we will see in a simplified framework how powerful this resummation is.

To obtain the one-body Green's function from the above expression the self-energy needs to be somewhat approximated. In many cases, approximating  $\Sigma$  -even in a simple way- and then solving Eq. (2.89) yields overall a better result than approximations performed directly on the  $GF$  itself. Starting here I will partially follow the discussion by Strinati [52] on how to obtain a closed set of equations (Hedin's equations), which coupled to Eq. (2.89) allow for the calculation of the GF.

Let's first introduce a useful quantity, the *total* classical potential:

$$V(1) := \varphi(1) - i \int d3v(1, 3)G(3, 3^+) \quad (2.90)$$

which is the sum of the external potential  $\varphi$  and the Hartree potential. Using a chain rule (and a basic identity derived in App. (A)), let's recast  $\Sigma$  in such a way that the total potential enters its definition:

$$\Sigma(1, 3) = -i \int d4d v(1^+, 4)G(1, 2; [\varphi]) \frac{\delta G^{-1}(2, 3; [\varphi])}{\delta V(5)} \frac{\delta V(5)}{\delta \varphi(4)} \Big|_{\varphi=0}, \quad (2.91)$$

a new quantity, accounting for the variation of the inverse of the Green's function with respect to the total potential, can now be defined<sup>1</sup>:

$$\tilde{\Gamma}(23; 5) := -\frac{\delta G^{-1}(2, 3; [\varphi])}{\delta V(5)}. \quad (2.92)$$

Such complicated 3-point quantity takes the name of *irreducible vertex*, in the following we will label as *irreducible* all the quantities defined with respect to the *total* potential, and *reducible* when defined with respect with the *external* potential  $\varphi$ .  $\tilde{\Gamma}$  can be related to the self-energy in the following way:

$$\tilde{\Gamma}(23; 5) = \delta(2, 5)\delta(3, 5) + \frac{\delta \Sigma(2, 3)}{\delta V(5)}, \quad (2.93)$$

employing a chain rule in Eq. (2.93) and inserting the resulting expression in Eq. (2.92) one obtains an integral equation for the vertex, namely:

$$\begin{aligned} \tilde{\Gamma}(23; 5) &= \delta(2, 5)\delta(3, 5) + \int d4d6 \frac{\delta \Sigma(2, 3)}{\delta G(4, 6)} \frac{\delta G(4, 6)}{\delta V(5)} \\ &= \delta(2, 5)\delta(3, 5) + \int d4d6d7d8 \frac{\delta \Sigma(2, 3)}{\delta G(4, 6)} G(4, 7)G(8, 6)\tilde{\Gamma}(7, 8; 5), \end{aligned} \quad (2.94)$$

where we have used  $\frac{\delta G}{\delta V} = -\frac{\delta G^{-1}}{\delta V}G$ . Eq. (2.94) is also the so-called Bethe-Salpeter equation for  $\tilde{\Gamma}$ .

We can further introduce the inverse of the (longitudinal) *dielectric matrix*:

$$\epsilon^{-1}(5, 4) := \frac{\delta V(5)}{\delta \varphi(4)} = \delta(5, 4) + \int d1v(5, 3) \frac{\delta \langle \hat{\rho}(1) \rangle}{\delta \varphi(4)} \quad (2.95)$$

---

<sup>1</sup>Note that the self-energy has here been taken at vanishing potential. Even the other observables which will be defined in the next are understood to be taken, in their final expression, at  $\varphi = 0$ .

where the reducible *polarizability* of the system can be defined as:

$$\chi(1, 4) := \frac{\delta \langle \overbrace{\hat{\rho}(1)}^{\text{density}} \rangle}{\delta \varphi(4)} \quad (2.96)$$

and can be related to the *irreducible* one<sup>m</sup> through the following Dyson-like equation:

$$\chi(1, 4) = \tilde{\chi}(1, 4) + \int d2d3 \tilde{\chi}(1, 2)v(2, 3)\chi(3, 4) \quad (2.97)$$

where  $\tilde{\chi}$ , because of the relation between *rho* and *G* can also be expressed as:

$$\tilde{\chi}(1, 4) = - \int d2d3 G(4, 2)G(3, 4)\tilde{\Gamma}(2, 3; 1). \quad (2.98)$$

On these cornerstones, Hedin grafted a theory which at first sight may look like a slight modification of what was already existing but is instead truly new and contains a great deal of physical insight.

He opted for a description of an extended solid as a collection of *dressed particles*, rather than bare electrons, interacting through a *screened* Coulomb potential, called *W*, rather than through the long-range bare Coulomb potential *v*. *W* can be defined equivalently through  $\epsilon^{-1}$  or through the polarizability  $\chi$ :

$$\begin{aligned} W(1, 2) &:= \int d3 \epsilon^{-1}(1, 3)v(3, 2) \\ &= v(1, 2) + \int d3d4 v(1, 3)\chi(3, 4)v(4, 2) \end{aligned} \quad (2.99)$$

and using the above expression and the integral one for  $\tilde{\Gamma}$ , Hedin recast the self-energy in one of its most well-known forms, namely:

$$\Sigma(1, 2) = i \int d3d4 W(1^+, 3)G(1, 4)\tilde{\Gamma}(4, 2; 3) \quad (2.100)$$

Eqs. (2.98), (2.100), (2.99), (2.94) and (2.89) constitute a set of closed, exact, equations (Hedin's equations) which has to be solved -in principle self-consistently- to obtain an expression for the one-body Green's function.

Some approximation for the unknown self-energy is however needed. The most well known one is again due to Hedin (although already suggested, under the name of shielded interaction approach, in [47]) and consists in completely neglecting the correlated motion of pairs of dressed particles. From a purely mathematical point of view this means that the vertex function takes the simple form:

$$\tilde{\Gamma}(2, 3; 5) = \delta(2, 5)\delta(3, 5). \quad (2.101)$$

Let's see if what is the effect of the above approximation for instance on a two-body Green's function. Taking the expression for the  $G_2$  as a function of  $\Gamma$  and inserting this definition into

---

<sup>m</sup>Defined as  $\bar{\chi}(1, 4) := \frac{\delta \langle \hat{\rho}(1) \rangle}{\delta V(4)}$

(2.101) we have:

$$\begin{aligned} G_2(3, 4; 2, 4^+; [\varphi]) &= G(3, 2; [\varphi])G(4, 4^+; [\varphi]) + \int d1d5 G(3, 1; [\varphi])\tilde{\Gamma}(1, 5; 4)G(5, 2; [\varphi]) \\ &= G(3, 2; [\varphi])G(4, 4^+; [\varphi]) + G(3, 4; [\varphi])G(4, 2; [\varphi]) \end{aligned} \quad (2.103)$$

the two body Green's function is now simply the sum of products of single-particle  $GF$ s. Turning back to the self-energy, setting the vertex function equal to unity yields:

$$\Sigma(1, 2) = iW(1^+, 2)G(1, 2) \quad (2.104)$$

from where the name  $GW$  approximation becomes obvious. Note that substituting in Eq. (2.104) the bare Coulomb potential  $v(1^+, 2)$  in place of  $W(1^+2)$  yields the Fock exchange operator. In the  $GWA$  the polarizability becomes:

$$\tilde{\chi}(1, 2) = \chi_0(1, 2) = -iG(1, 2)G(2, 1) \quad (2.105)$$

which has now the form of the random-phase approximation(RPA) [21], [20]. A pictorial idea of Hedin's  $GW$  is given in Fig 2.5.  $GW$ -based calculations of quasi-particles band structures [53, 54] of many materials and direct and inverse photo emission spectra (see e.g. Refs. [16, 17, 55, 56])

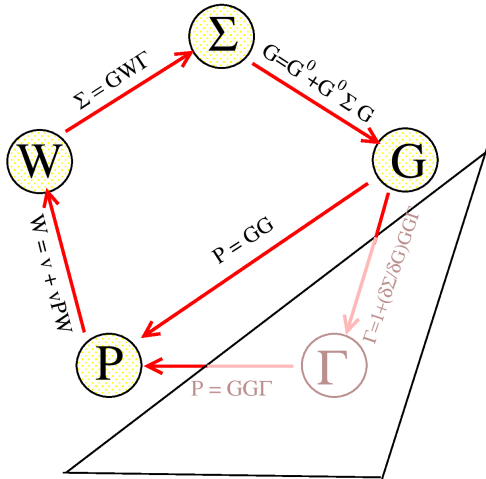


**Figure 2.5:** Hedin's pentagon. The result of the  $GW$  approximation yields, instead, a trapezium: in fact the equation for the vertex would be solved once, leaving only four other equations to solve once or more, if a self-consistency procedure is needed. The five equations are all expressed in the *irreducible* form (even if they don't display a *tilde* symbol on top of them. The polarizability is here indicated with the letter  $P$  rather than the Greek letter  $\chi$ .)

are abundant in the literature and they show to improve substantially over the results provided by static mean-field electronic structure methods; for example the screening reduces the large bandgap of Hartree-Fock.

Having said this, let's point out some shortcomings of the approximation, certain of which quite fundamental. First of all the  $GW$  approximation is not size consistent [57, 58], this problem often appears when a system is studied in the atomic limit (i.e. its atoms are pulled apart up to the point there is little or no overlap between their wave functions). An illustration of this issue can be observed by calculating the total energy of a system in this limit: it would turn out to be different from the sum of the total energies of the atoms. Therefore  $GW$  is not reliable in describing dissociation processes.

A second shortcoming is given by the so-called *self-screening error* and has been studied, for instance in [59, 60, 61, 62] and more recently in [63]. Its effect is to make the  $GW$  approach non-symmetric for the removal and addition of particle from a system and

stems from the fact that exchange interactions are not properly dealt with. Ways to overcome this type of shortcomings range from using non-local vertex functions [64] to spin dependent Coulomb potential [65, 66], hence treating the Hartree and the exchange term on the same foot-

ing.

Moreover, also strongly correlated materials constitute a challenge for the approximation: sometimes with some degree of self-consistency, e.g. performing a perturbative  $GW$  calculation, starting from a self consistent one based on a static (COHSEX [67])  $GW$  self-energy, can yield good agreement with experiments, but this is not always the case. A profound reason for this failure is illustrated by the fact that  $GW$  cannot treat correctly the atomic limit: calculations performed on model systems, such as the Hubbard molecule, at  $\frac{1}{4}$  filling, yield a single QP-peak in the electron addition spectral function: the exact one should exhibit two peaks, perfectly symmetric [63]. In this case the very poor result is due to the interpretation of the density in a classical way, rather than accounting for its quantum nature. In fact  $GW$  only includes correlation effects through the induced Hartree potential leading to a too delocalized description of the electrons. As a consequence the additional electron sees both atoms occupied with half an electron even in the atomic limit. This poor description of the atomic limit might be observed also in real systems that have localized electrons such as transition metal-oxides with very localized and partially filled d-bands. Other less dramatic shortcomings are encountered when  $G_0W_0$  provides a good (in terms of position and intensity) quasi-particle peak and a single plasmon satellite, but is unable to reproduce correctly additional features of the spectrum [68, 69, 70, 71]. For example, in core and valence photoemission spectroscopy of a number of materials, one should not observe only a broad satellite peak, rather a series of plasmon satellites; however to calculate these more complicated and realistic spectral features, one has to go beyond  $GW$ .

One could for example add higher orders in  $W$  by iterating the equations, but first of all it is a technically difficult route and furthermore there is no guarantee that results would quickly improve. Another possibility would be to formulate vertex corrections to be added to the self-energy. Examples are exchange-correlation kernels borrowed from (TD)DFT, such as in [64, 72]. Or also are the T-matrix [40, 73], which, unlike  $GW$ , correctly describes the atomic limit in simple models, or the cumulant expansion [74], from which spectral function containing multiple plasmon satellites -absent in  $GW$ - are ordained.

Knowing the approximations needed to obtain the T-matrix or the cumulant expansion from *exact equations* should allow one to reformulate their physical content into a vertex correction. In the following we will discuss more in detail the cumulant expansion approach, since it is a direct approximation to the GF and hence closer to the methodology we will be exploring through this thesis.

### 2.4.3 Cumulant expansion approximation

As briefly discussed in the previous section the  $G_0W_0$  has been quite successful as long as band-gaps and quasi-particles energy calculations are concerned, whereas in terms of spectral function calculations more shortcomings have appeared.

One may then build hopes that a fully self-consistent scheme might remedy those shortcomings. In calculations performed by Holm and Von Barth [75] and Schöne and Eguiluz [76], the satellite region had little agreement with experiments, even worse than the already poor  $G_0W_0$  result. In this particular case the failure of the self-consistent approach was attributed to the expression for  $W$ , which turned out to be very different from the correct one, resulting in a complete smoothing

of the spectral function satellites. Partially self-consistent calculations [77, 78], where only  $G$  was calculated in a self-consistent fashion, gave reasonable results and a slight improvement over  $G_0W_0$  was also obtained. However neither self-consistency nor vertex corrections have, so far, proved to be systematically better than the "one-shot"  $GW$  on top of a reasonable (for a given system) starting point.

In this section we will discuss the performances of an alternative approximation for Green's function calculation, which is *not* based on approximations to  $\Sigma$ , rather to the Green's function itself and has the aim of improving, above all, on the shortcomings of  $G_0W_0$  for spectral function calculations, particularly on the satellite part of the spectrum. The approximation, called *cumulant expansion* (we will see later why), has a fairly long story. We will first detail its origins, tied to model Hamiltonian's for X-ray emission and absorption spectroscopies and then we will discuss more recent implementations for the calculation of spectral function of valence levels in simple metals and semiconductors.

In Chap. (5) of this thesis we will come back to the approximation and show **i)** how it can be derived in a completely general and rigorous way, **ii)** briefly describe an application to valence photo emission spectroscopy in silicon.

### Origins and developments of the approximation

Langreth building up on earlier works of Lundqvist [79, 80], where in the context of X-ray absorption the coupling between the deep hole and plasmon excitations in the electron gas was discussed, showed how Lundqvist's model Hamiltonian could be solved exactly and used as a benchmark both for the  $GW$  approximation and for straightforward perturbation expansions. The expression for such Hamiltonian reads:

$$H = \epsilon c^\dagger c + cc^\dagger \sum_q g_q (a_q + a_q^\dagger) + \sum_q \omega_q a_q^\dagger a_q \quad (2.106)$$

where  $c^\dagger$  ( $c$ ) creates (annihilates) *core* electrons with energy  $\epsilon$  and  $a_q^\dagger$  ( $a$ ) creates (annihilates) a plasmon with energies  $\epsilon_c$  and  $\omega_q$  respectively and  $g_q$  is the coupling coefficient. In [81] an *exact* expression for the core (hole) one-body Green's function (and hence for the spectral function) is derived: such expression has an *exponential form* and yields a spectrum containing a quasi-particle  $\delta$ -peak and a series of satellites, representing the different plasmon peaks, each of them with a different weight factor, constituting the probability that a final state with  $n$  plasmons is contained in the initial state with no plasmons at all. This spectrum is depicted in Fig. 2.6a. Note that plasmon dispersion has been neglected (by setting  $\omega_q = \omega_p = \text{const.}$ ) at the end of Langreth's derivation. In the very same work the absorption spectral function was also calculated starting from a core hole  $G$  evaluated approximately through the first order of perturbation theory in  $W$  for the self-energy, which is to say in the  $G_0W_0$  approximation. The results, in particular compared to the exact solution for the model Hamiltonian, exhibit an important shortcoming in the description of the incoherent part of the spectrum: instead of a series of plasmon peaks one finds only one broad peak, which was a sort of average of the true satellite spectrum and was labeled *plasmaron peak* following the nomenclature of earlier works.

We report these latter findings in In Fig. 2.6b.

Following the ideas explored in the above works, Hedin decided to employ a more sophisticated and general plasmaron Hamiltonian [67] to investigate deeper the capabilities of this electron-boson model for core and also valence spectroscopies. Hedin's Hamiltonian reads:

$$H = \sum_k \epsilon_k c_k^\dagger c_k + \sum_s \omega_s a_s^\dagger a_s + \sum_{s k k'} V_{k k'}^s (a_s + a_s^\dagger) c_k^\dagger c_{k'} \quad (2.107)$$

where rather than having a single fermion level labeled by  $c$ , as in Lundqvist work, we have the two indices  $k$  and  $k'$ , where the boson of the system is labeled by  $s$  (previously the plasmon momenta  $q$ ) and where the coupling constants are *fluctuation potentials*<sup>n</sup>. Within this model, after calculating  $\Sigma_c$  (where  $c$  refers to core) with a simple plasmon dispersion relation  $\omega_q = \omega_p + \frac{q^2}{2}$  the  $GW$  spectral function for the system, the QP-energy and the strength of the QP-peak we obtained.

Hedin [67] also obtained the core spectral function for its model system in an *exact way*.  $G_c$  turns out to be, in frequency space:

$$G_c(\omega) = i \int_{-\infty}^0 dt e^{(\omega - \epsilon_c - \Delta E)t} e^{\sum_q \frac{g_q^2}{\omega_q^2} (e^{i\omega_q t} - 1)} \quad (2.108)$$

where one can define  $Z = e^{-\sum_q \frac{g_q^2}{\omega_q^2}}$  and  $E_c = \epsilon_c + \Delta E$ . A Taylor expansion of the exponent in 2.108 yields<sup>o</sup>:

$$G_c(\omega) = Z \left\{ \frac{1}{\omega - E_c} + \sum_q \frac{g_q^2}{\omega_q^2} \frac{1}{\omega - E_c - \omega_q} + \sum_q \frac{g_q^4}{\omega_q^4} \frac{1}{\omega - E_c - 2\omega_q} \dots \right\} \quad (2.109)$$

from which the spectral function can be calculated (remember the general relation  $A(\omega) = \frac{1}{\pi} \mathcal{I}m |G(\omega)|$ ) and compared with the  $GWA$  results. Eq. (2.108) show that  $G$  can be written as an exponential, the exponent is identified with the so-called cumulant. Once the latter is approximatively determined, Taylor expansion of the exponential (like in Eq. (2.109)) yields the cumulant expansion.

Looking at the poles of the above  $G_c$  one can already see how the core spectral function will exhibit one peak with strength equal to  $Z$  at  $\omega = E_c$  and then a whole series of peaks with decreasing intensity and centered at  $E_c - \omega_q$ ,  $E_c - 2\omega_q$  and so on. These values are all multiples of the plasmon frequency  $\omega_p$ : this means that the series above is actually the regularly spaced series of plasmon peaks observed already by Langreth.

On this basis Hedin drew similar conclusions to Langreth regarding the failures of the  $G_0W_0$  approximation, specifically: **i**) the  $G_0W_0$  scheme is designed to deliver a spectrum with one single plasmon peak<sup>p</sup>, **ii**) the QP position is the same in both calculations and its strength is

<sup>n</sup>Lundqvist Hamiltonian can be obtained from Hedin's one simplifying the fluctuation potential as follows  $V_{k k'}^s = g_q \delta_{k,c} \delta_{k',c} \delta_{s,q}$

<sup>o</sup>We report here only the zeroth, first and second order terms

<sup>p</sup>We will come back to this issue in Chap. 5 where, thanks to Feynman diagrams we will get to this very same conclusion without even writing down explicitly a  $GW$  spectral function.

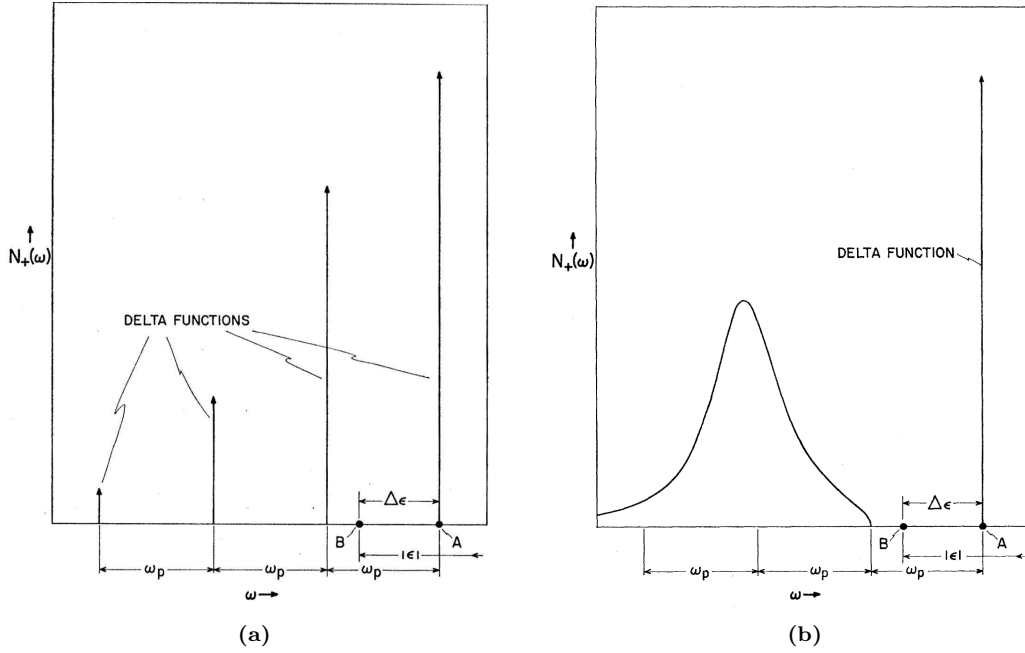


**Figure 2.6:** From Ref. [81]. Fig. 2.6a: spectral function obtained with an exact expression for the core hole Green's function as calculated from Langreth, using Lundqvist's polaron Hamiltonian. Note that in the original figure the absorption spectral function is labeled with  $N_+(\omega)$ , rather than with  $A(\omega)$ . All the satellite peaks are equispaced from the QP peak by a value equal to multiples of  $\omega_p$ . Fig. 2.6b: spectral function obtained within a  $G_0W_0$  approximation for  $\Sigma$ . Besides the QP peak only one very broad plasmon peak appears. It is a sort of broad average of the true spectrum.

very reasonable in the *GWA*, **iii**) the *GW* plasmon peak is a sort of average of the true multi-satellite spectrum.

In the final part of the same work, an even more general model Hamiltonian, where also the coupling of the deep core to particle-hole excitations is included (as in earlier work by Mahan Nozières and De Dominicis), is solved exactly<sup>9</sup>. Once more the exact core Green's function has the shape of a cumulant and the spectral function exhibits the quasi-particle peak followed by a series of plasmon satellites, where, however, the line-shape of the QP peak becomes asymmetric due to the shake-up<sup>†</sup> of electron hole pairs.

Therefore the picture seems fairly complete as far as core levels are examined; however when considering, for example, real materials (rather than model systems) also probing valence energy levels (or conduction bands for metals) becomes interesting.

The questions I will now address, following Hedin's work on the effect of recoil in the shake up spectra of metals [35] are: what are the signatures of a photoemitted *conduction electron* in the

<sup>9</sup>Exactly in the sense that a decoupling approximation of the two types of excitations -core and hole-electron and core and plasmons- is made.

<sup>†</sup>Shake up refers to any type of excitation in a spectrum which is produced by a sudden change in a quantum mechanical system

spectral function? How do they relate to the signatures of a core electron?

Rather than coming up with an entirely new treatment of the phenomena, Hedin decided to follow as close as possible the description of the core electron photoemission. We will mainly conduct our reasoning with diagrams. The set of diagrams involved in the exact expansion for  $G_c$  includes only non-interacting  $G_0$  and the electron-electron interaction (screened), see Fig. 4.5a, where contribution up to the second order in  $\Sigma$  are shown. There is no reason to think that a different set of diagrams should describe photo emission from conduction states, however, in that case, each diagram will contain *extra* physics, given by the *recoil* (change in momentum) of the photoemitted electron at each collision (see diagram in Fig. 4.5b). Hence by completely

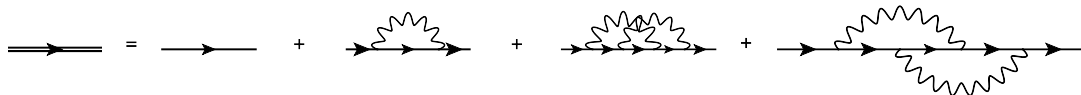


**Figure 2.7:** Set of diagrams describing the full core Green's function ( $G_c$ ). It's just a series in the non-interacting core propagator  $G_c^0$  and the screened interaction  $W$ . We will analyze this expansion in greater detail in Chapter (5), comparing this set of diagrams to the one obtained for the  $G_0W_0$  approximation to the self-energy.

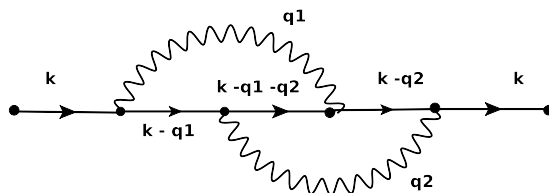


**Figure 2.8:** Second order (in  $W$ ) diagram (the last from the above series). In case of recoil at each process there is the probability of the change in momentum ( $k$ ) of the photoemitted electron.

neglecting recoil the set of diagrams describing both core and conduction photoelectrons will be identical. Instead, in order to account for recoil processes, some algebra is needed. Details of the assumptions needed to take the change in momentum into account, without however changing the set of diagrams describing the admission process can be found in [35]. These assumptions had been tested against two limiting cases, namely the high density limit and the vicinity of the QP to the Fermi surface: in both circumstances the obtained results were satisfactory and justified, *a-posteriori* all the assumptions. Some numerical calculations were also performed and indicated that the QP-peak shape and strength from photoemitted electrons extracted from the core or from the conduction levels and the shape of the plasmon satellite peaks was very similar. However their width is quite different, in particular it turns out to be reduced in presence of recoil effects.

Thanks to this pioneering work, the cumulant expansion approximation made its way into the pool of approximations used for the one-particle propagator for real materials. Examples of successful use of the cumulant expansions are, for instance, the work by Aryasetiawan *et al.* [74] who calculated the valence admission spectra of alkali metals, specifically  $Al$  and  $Na$ : despite

the strong recoil effects, due to the wide dispersion of the conduction bands in both compounds, they recover the sequence of the plasmon satellites observed in experiments, missing out a better agreement only because of the width and intensity of the peaks. Also Vos *et al.*[82] carried out calculation of spectral functions for *Al* and *Li* and compared with high energy electron momentum spectroscopy (EMS) data, obtaining a good agreement.

A further example of the accuracy of this approximation will be given in Chap. (5) with the work of Guzzo *et al.* [83].

## 2.5 Green's function from the solution of a functional differential equation

In the present work we will pursue an alternative route for the calculation of the one-body Green's function, which, as the cumulant expansion, is in principle non perturbative <sup>s</sup>. In the present work we will turn back to Eq. (2.71) and first obtain new insights about standard approximations (e.g. different *GW* flavors) by relating them directly to the aforementioned set of differential equations. Secondly we will employ Eq. (2.71) to explore and devise *alternative* approximations. Both issues will be described and dealt with in Chap. 3 and 4 of the present work. Finally, we will focus directly on the set of coupled, non linear, first order functional differential equations for  $G$ , Eq (2.71), although it has been acknowledged that no "practical technique for solving such functional differential equation exactly" [40] is available. To reach the aforementioned goals we will resort to two approximations. The first one consists in linearizing the set of equations by expanding  $V_H$  in terms of  $\varphi$  and we will provide a number of arguments to show that a great deal of many-body physics is still contained in the approximated equations.

Later we will discretize Eqs. (2.71) and consider in a first instance only one point for each space, spin, and time variable: we will call this approximation the "*1-point model*", as opposed to the full functional problem. Within the 1-point model one deals with a single algebraic ordinary differential equation (DE), thus we will derive its exact explicit solution. An attentive study of the family of solution will provide insights on the mathematical nature of the problem and a simple physical argument will lead us to solve the initial value problem for the DE, which yields the particular solution (so to say the physical one) to the problem. The full particular solution will be then employed as a precious tool: approximations for it will be explored, yielding valuable insights in the performance of current approaches, such as the  $G_0W_0$  approximation, the effects of self-consistency in  $G$  and even vertex corrections to  $\Sigma$ . In a second instance we will also devise alternative approximations reverse-engineering them, which is to say approximating the exact solution and then relating the results to direct manipulations of the initial DE, pretending nothing is known about its solution (which is in fact be the case in the full functional case). The most promising 1-point approximations for the DE will of course also be translated to the full functional framework and their actual feasibility (in some case in terms on computational implementation) will be discussed.

---

<sup>s</sup>To be more specific this alternative approach is completely non perturbative as long as the electron-electron interaction is concerned. In our development one particular approximation will lead to a perturbative (linearization) treatment of the Hartree potential with respect to the external potential.

We finally devote the last chapter of this thesis to the *generalization* of the approach. After discussing how to restore the time-dependence in the equations (see Chap. 5) we will formulate an *ansatz* for  $G$  in this more general framework, checking that it does solve the N-times DE. We will wrap up discussing strategies to solve the -now much more complicated- initial value problem, so as to also pick the particular solution from the family of solutions obtained through the ansatz and to transpose most of these latest findings to the truly full functional case. Our strategy is depicted as in the Fig. 2.5. We will work separately in the 1-point framework

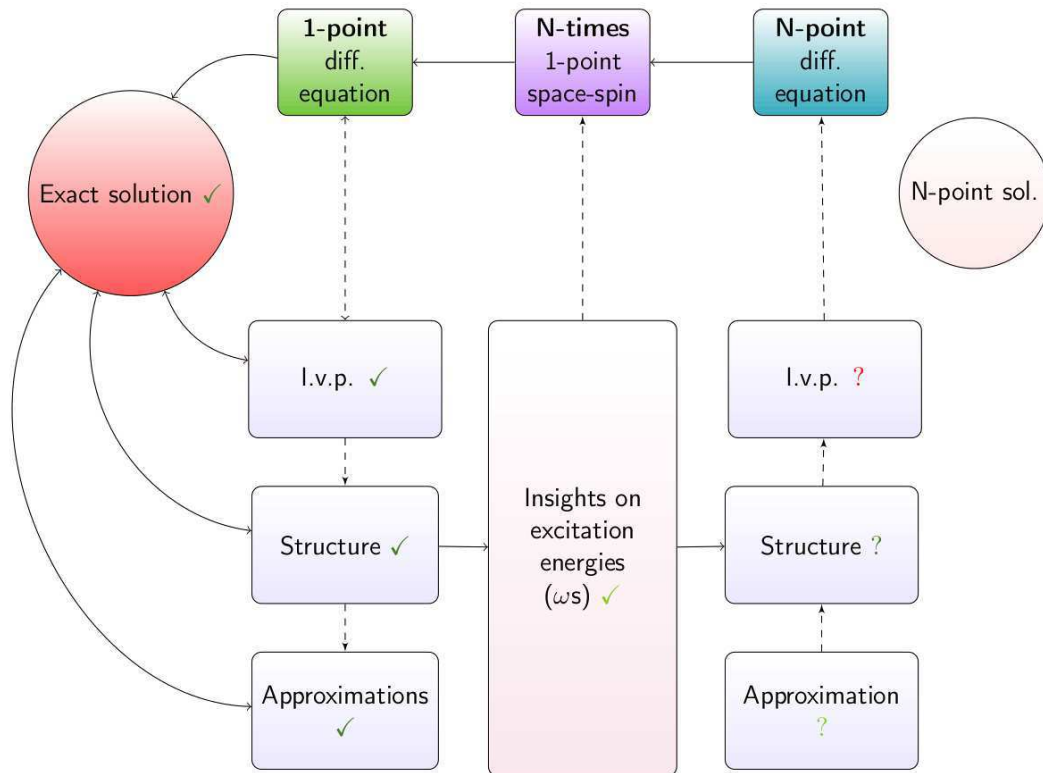


**Figure 2.9:** This diagram illustrates our strategy to tackle the set of functional differential equations for  $G$ . The problem is so complicated that we began by solving it in the simplest possible formulation.

(left), in the N-times one (center) and finally on the full functional one (right, labeled as N-points). On the left hand side we are showing that, starting from the algebraic DE we obtained its exact solution. This provided us with insights on how to solve the initial value problem (i.v.p.), on how the family of solution for the propagator looks like and last but not least which approximation to the exact solution are more or less accurate. If one knew these insight a-priori, there would no need to solve the equation exactly: an ansatz, formulated with all those information, would be enough to obtain  $G$ . A similar procedure can be adopted for the N-times framework (central part of the figure). The equations are more complicated, but a decoupling

approximation and an ansatz with an exponential form, will again lead us to the exact solution of the DE. Many more insights will also be obtained from this case. Finally on the right hand side we have the full functional (N-points) framework, where solving the equations directly is prohibitive. Using the knowledge acquired from the two previous simpler frameworks, we will formulate an ansatz and verify that it satisfies the initial DE.

# CHAPTER 3

## Exact Green's function in a simplified framework

*In the very end of the previous chapter (see Section 2.5) a fairly unexplored route to calculate the one-body Green's function has been introduced. In this chapter we hence wish to attempt a direct solution of the functional differential problem presented in Eq. (2.71). As it has been anticipated it is a tremendously complicated task and tackling the problem step by step, starting with a certain degree of simplification, to move only later on to the full problem, is advisable. Our strategy consists in dealing with the simplest possible set of equations, which can be obtained under certain approximations (detailed in the following), so that their manipulation becomes more straightforward. The first approximation we employ is a linearization of Eq. (2.71) with respect to the external perturbing potential: we will however show how most of the important physics is retained. Then a discretization of all spin, space and time variables is performed and only one-point for each type of variable is retained. In this one-point framework the set of functional differential equations reduces to a single first order differential algebraic equation (DE) which can be solved exactly, giving access to its family of solutions and, by solving the initial value problem, to the particular solution of our physical problem. Some considerations on the nature of the DE and other possible approximate ways to solve it will be also presented.*

### 3.1 Tackling the functional equation I: linearization

The *non-linearity* of Eq. (2.71) is due to the Hartree potential  $V_H$ , which contains itself a one-body Green's function, more precisely a diagonal of a *diagonal* Green's function. Note, in fact, that the diagonal of  $G$  is nothing else than the density operator  $\rho$ . This can be readily seen from the definition of the GF: if we assume locality in space and quasi-locality in time, we have that  $-iG(1, 1^+) = -i\langle\Psi_0|T[\hat{\psi}^\dagger(1)\hat{\psi}(1^+)]|\Psi_0\rangle = \langle\hat{n}(1)\rangle$ .

A Taylor expansion of the Hartree potential, where only the terms up to the 1<sup>st</sup> order in the

external potential are kept, reduces the problem to a linear one. Here we only assume linear the *response* of the system to the external perturbation, while the electron-electron interaction is fully accounted for and not treated perturbatively.  $V_H$  is hence expanded and truncated as follows:

$$\begin{aligned} V_H(3; [\varphi]) \approx & -i \int d4v(3^+, 4)G(4, 4^+; [\varphi]) \Big|_{\varphi=0} \\ & -i \int d4d5v(3^+, 4) \frac{\delta G(4, 4^+; [\varphi])}{\delta \varphi(5)} \Big|_{\varphi=0} \varphi(5) + o(\varphi^2). \end{aligned} \quad (3.1)$$

and upon the introduction of an *auxiliary Dyson equation* for  $G_H^0$ :

$$G_H^0(1, 2) = G_0(1, 2) + \int d3G_0(1, 3)V_H^0(3)G_H(3, 2), \quad (3.2)$$

where  $V_H^0(3) := -i \int d4v(3^+, 4)G(4, 4^+; [\varphi]) \Big|_{\varphi=0}$ , Eq. (2.71) can be recast as:

$$\begin{aligned} G(1, 2; [\varphi]) &= G_H^0(1, 2) \\ &- i \int d3d5G_H^0(1, 3) \left[ \int d4d5v(3^+, 4) \frac{\delta G(4, 4^+; [\varphi])}{\delta \varphi(5)} \Big|_{\varphi=0} + \delta(3, 5) \right] \varphi(5)G(3, 2; [\varphi]) \\ &+ i \int d3d4G_H^0(1, 3)v(3^+, 4) \frac{\delta G(3, 2; [\varphi])}{\delta \varphi(4)} \end{aligned} \quad (3.3)$$

Since  $\frac{\delta G}{\delta \varphi}$  (in the second term on the right-hand side of Eq. (3.3)) is a contraction of the two-particle correlation function, it yields the inverse dielectric function:

$$-i \int d4v(3^+, 4) \frac{\delta G(4, 4^+; [\varphi])}{\delta \varphi(5)} \Big|_{\varphi=0} + \delta(3, 5) = \epsilon^{-1}(3, 5), \quad (3.4)$$

and one can reformulate Eq. (3.3) as:

$$\begin{aligned} G(1, 2; [\varphi]) &= G_H^0(1, 2) + \int d3d5G_H^0(1, 3)\epsilon^{-1}(3, 5)\varphi(5)G(3, 2; [\varphi]) \\ &+ i \int d3d4G_H^0(1, 3)v(3^+, 4) \frac{\delta G(3, 2; [\varphi])}{\delta \varphi(4)}. \end{aligned} \quad (3.5)$$

A *rescaled* perturbing potential can be now introduced:

$$\bar{\varphi}(3) := \int d5\epsilon^{-1}(3, 5)\varphi(5), \quad (3.6)$$

and, using the chain rule  $\frac{\delta G}{\delta \varphi} = \frac{\delta G}{\delta \bar{\varphi}} \frac{\delta \bar{\varphi}}{\delta \varphi}$  in the last term of the right-hand side of Eq. (3.5), we get:

$$\begin{aligned} G(1, 2; [\bar{\varphi}]) &= G_H^0(1, 2) + \int d3d5G_H^0(1, 3)\bar{\varphi}(3)G(3, 2; [\bar{\varphi}]) \\ &+ i \int d3d5G_H^0(1, 3)W(3^+, 5) \frac{\delta G(3, 2; [\bar{\varphi}])}{\delta \bar{\varphi}(5)}, \end{aligned} \quad (3.7)$$

Here  $W = \epsilon^{-1}v$  is the screened Coulomb potential at vanishing  $\varphi$ . Hence, for this *linearized differential equation* we have that:  $G_H^0$  is a Hartree Green's function containing the Hartree potential at vanishing  $\varphi$ ,  $\bar{\varphi} = \epsilon^{-1}\varphi$  is the renormalized external potential, and  $W = \epsilon^{-1}v$  is the screened Coulomb potential with  $\epsilon$  the dielectric function at  $\varphi = 0$ <sup>a</sup>.

Three remarks can be made on Eq. (3.7).

First of all, through the linearization, the screened interaction  $W$  becomes the central quantity of the equation: this can be justified by the physics of extended systems, where screening and plasmons are dominant mechanisms.

Second,  $W$  can in principle be the *exact* screened interaction, which of course is not known. One could however adopt two strategies: either consider  $W$  as an *externally* given quantity, obtained within a good approximation, e.g. from a time-dependent density functional theory calculation; or one could recalculate  $W$  from  $G[\bar{\varphi}]$  (see the next Chapter for more details on this). Here we chose for the former approach. The procedure is schematically described in Fig. 3.1.

Such a philosophy is rigorously justified: for instance, in the framework of functional theory, one can move from a *Luttinger-Ward functional* (which is a functional of  $G$ , but indeed also of the bare Coulomb interaction  $v$ ) to the so-called  $\Psi$ -*functional*, where  $v$  is replaced by  $W$  [84].

In this type of functional, when an appropriate model  $W$  is chosen, conserving properties of the  $GW$  approach are not lost. Finally a weaker but more "traditional" argument supporting our choice: the route described above is by far the most "well-trodden path" of the many-body perturbation theory community. It exemplifies a  $GW$  calculation to the "best  $G$ , best  $W$ " approach (see e.g. in Ref. [50] but not only): where the non-interacting  $G$  is taken e.g. to be the Kohn-Sham Green's function, and  $W$  is calculated as well as possible, e.g. in time-dependent local density approximation (TDLDA). The last remark on the linearization procedure concerns the degree of approximation present in Eq (3.7).

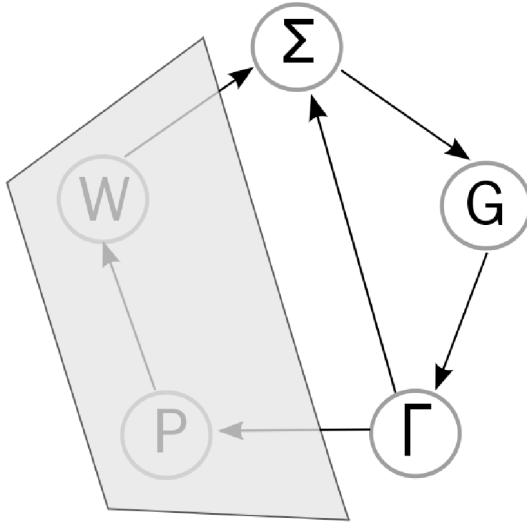


**Figure 3.1:** Hedin's pentagon where  $P$  and  $W$  have been "cut out" from the full loop. This means that when performing self consistent calculations, only  $G$ ,  $\Sigma$  and  $\Gamma$  are updated, while  $P$  and  $W$  are evaluated once for all at the beginning. We will hence talk about  $W_0$  rather than  $W$  to indicate that the screened interaction has been kept fix to some "accurate enough" value.

the *inverse* of  $G$  with respect to the potential.

*How does it compare to well-known approximations for the Green's function?*

Recasting the functional derivative  $\frac{\delta G(3, 2; [\bar{\varphi}])}{\delta \bar{\varphi}(5)}$

according to Eq. (A.6), yields an expression for

<sup>a</sup>For simplicity we use the same symbol for  $G[\bar{\varphi}]$  and  $G[\varphi]$ ; of course it is understood that the corresponding functional is taken

Substituting in Eq. (3.7) the  $G^{-1}$  obtained from inverting a Dyson-like equation, one obtains:

$$\begin{aligned}
G(1, 2; [\bar{\varphi}]) &= G_H^0(1, 2) + i \int d3 G_H^0(1, 3) \bar{\varphi}(3) G(3, 2; [\bar{\varphi}]) \\
&- i \int d3546 G_H^0(1, 3) W(3^+, 5) G(3, 4; [\bar{\varphi}]) \\
&\times \frac{\delta}{\bar{\varphi}(5)} \left[ G_H^{0^{-1}}(4, 6) - \Sigma(4, 6) - \bar{\varphi}(4) \delta(4, 6) \right] G(6, 2; [\bar{\varphi}]) \quad (3.8)
\end{aligned}$$

And assuming the self-energy independent of  $\bar{\varphi}$ , one gets:

$$\begin{aligned}
G(1, 2; [\bar{\varphi}]) &= G_H^0(1, 2) + \int d3 G_H^0(1, 3) \bar{\varphi}(3) G(3, 2; [\bar{\varphi}]) \\
&+ i \int d35 G_H^0(1, 3) W(3^+, 5) G(3, 5; [\bar{\varphi}]) G(5, 2; [\bar{\varphi}]) \quad (3.9)
\end{aligned}$$

where we can define  $\Sigma_{GW}(3, 5) = iW(3^+, 5)G(3, 5; [\bar{\varphi}])$ : this effective potential is nothing else than the  $GW$  approximation to the self-energy.

Note that this alternative derivation of the  $GW$  approximation suggests that the screened interaction  $W$  should be the full measurable test-charge test-charge one (Eq. (3.6) is hinting at this) and  $G$  should be calculated in a self-consistent way. Finally, the above result shows that, even though the linearization procedure is an approximation, Eq. (3.7) is still a promising starting point to analyze the different flavors of the  $GW$  approximations and to go beyond, since  $GW$  appears to be the simplest approximation to this equation.

## 3.2 Tackling the functional equation II: 1-point model

The second step is to perform a *basis transformation* of Eq. (3.7), which gives:

$$\begin{aligned}
G_{nm}(t_1, t_2; [\bar{\varphi}]) &= G_{H_{nm}}^0(t_1, t_2) \\
&+ \sum_{s,k} \int dt_3 G_{H_{ns}}^0(t_1, t_3) \bar{\varphi}_{sk}(t_3) G_{km}(t_3, t_2; [\bar{\varphi}]) \\
&+ i \sum_{skil} \int dt_3 dt_5 G_{H_{ns}}^0(t_1, t_3) W_{sil}(t_3, t_5) \\
&\times \frac{\delta G_{km}(t_3, t_2; [\bar{\varphi}])}{\delta \bar{\varphi}_{il}(t_5)}, \quad (3.10)
\end{aligned}$$

where

$$G_{ij}(t_1, t_2) = \int dx_1 dx_2 \phi_i^*(x_1) G(1, 2) \phi_j(x_2), \quad \bar{\varphi}_i(t_1) = \int dx_1 \phi_i^*(x_1) \bar{\varphi}(1) \phi_j(x_1) \quad (3.11)$$

and

$$W_{ijkl}(t_1, t_2) = \int dx_1 dx_2 \phi_i^*(x_1) \phi_j^*(x_2) W(1, 2) \phi_k(x_2) \phi_l(x_1). \quad (3.12)$$

In this way the space variables (from now on the spin variables will be consolidated with them) are discretized. Furthermore, assuming that the basis we have employed *diagonalizes both* the

Hartree Green's function at zero perturbing potential  $G_H^0$  and the full Green's function  $G$ , that is  $G_{mn}(t_1, t_2; [\bar{\varphi}]) = G_{mn}(t_1, t_2; [\bar{\varphi}]) \cdot \delta_{mn}$ , we can recast the above expression as:

$$\begin{aligned} G(t_1, t_2; [\bar{\varphi}]) &= G_H^0(t_1, t_2) + \int dt_3 G_H^0(t_1, t_3) \bar{\varphi}(t_3) G(t_3, t_2; [\bar{\varphi}]) \\ &+ i \int dt_3 dt_5 G_H^0(t_1, t_3) W(t_3, t_5) \frac{\delta G(t_3, t_2; [\bar{\varphi}])}{\delta \bar{\varphi}(t_5)}. \end{aligned} \quad (3.13)$$

This is a separate differential equation for each element of  $G$ . The projection of the equation over this diagonal basis simplifies the problem significantly, however a number of difficulties remains. Hence, on a first instance, we will also introduce the discretization of the time variable obtaining the so called *1-point model*.

Within this approximation (which implications we will discuss later in the chapter) we will obtain an exact solution for the -now algebraic- linearized differential equation. We will come back to Eq. (3.13) in Chapter (6).

### 3.2.1 Limits and validity of the model

We will here briefly discuss the limits of our model and to what extent the findings presented in this framework are applicable to more complicated (and eventually realistic) physical systems. Considering only 1-point in spin (or no spin dependence in our case) is currently being done in a number of approaches: for example calculations of the paramagnetic phase of certain solids are currently carried out *without* spin, rather than with random spin configurations. The 1-point in space is obtained projecting the DE onto single-orbital basis set, which is then assumed to *diagonalize* both the fully interacting Green's function and the zero-potential Hartree  $G$ ; it basically acts as a *decoupling* approximation. This simplification, which at first sight may look a bit rough, still retains a lot of physics in the system's description. We will provide greater details about it in Chap. (5). The really crude approximation employed throughout this and the following chapter, is to retain only 1-point in time: the model cannot exhibit any *frequency* dependence, and regrettably many of the interesting information contained in the  $GF$  are provided by its poles. Therefore we will always stress out when particular care has to be taken in extending our result to realistic systems.

On the other hand we will show that, especially when certain features of the calculated GF mainly depend on the mathematical structure of Eq. (3.7), the obtained results are capable of providing at least qualitative insights in established approximations and are definitely a good benchmark tool to devise alternative ones.

Further support to the argument above comes from the literature on the 1-point model: a number of authors have employed it different contexts. In Refs. [85, 86] Hedin's equations are combined into one single algebraic differential equation which is solved as a series expansion: this allows the authors to enumerate the diagrams for a certain expansion order. Several expansion parameters are analyzed, such as  $vg^2$ , with  $v$  the bare Coulomb potential and  $g$  the Hartree Green's function,  $vG^2$ , with  $G$  the exact Green's function,  $WG^2$ , with  $W$  the screened Coulomb potential, etc., which shows how at various orders of expansion the number of diagrams decreases by increasing the degree of renormalization. This is also the spirit behind the linearized equation (3.7), in which the natural expansion parameter would be  $Wg^2$ , where  $W$  is treated as an externally

given interaction. The advantage of using the 1-point framework is that the equations become algebraic and thus the enumeration of diagrams is facilitated. In Ref. [87] a similar strategy as in Refs. [85, 86] is used to enumerate diagrams, focusing in particular on the asymptotic behavior of the counting numbers. Moreover Hedin's equations are transformed into a single first order differential equation for the GF as a function of an interaction parameter, and an implicit solution is obtained. In order to fix the particular solution of this differential equation the initial condition  $G_{(v=0)} = G_0$  is used.

Instead here we concentrate on (2.71), or better its linearized form (3.7), which is *another* differential equation for  $G$ , as a functional of an external potential. This choice allows us to **(i)** emphasize the essential physics contained in the screened Coulomb interaction  $W$ , **(ii)** discuss various aspects of the many-body problem in a clear and simple way, **(iii)** obtain an exact explicit solution of the approximate equation that can be used as a benchmark. Moreover we believe that the 1-point version of Eq. (3.7) can be a natural starting point for a generalization to the full functional problem.

After having justified our choice for a simple framework, which is however capable of providing us with a great deal of insights, let's examine the form for the the 1-point differential equation and its general and particular solutions.

### 3.2.2 Exact general solution

In the 1-point model Eq. (2.71) reduces to an algebraic, non-linear, first order differential equation

$$y_u(x) = y_0 + vy_0y_u^2(x) + y_0xy_u(x) - vy_0\frac{dy_u(x)}{dx} \quad (3.14)$$

where  $\bar{\varphi} \rightarrow x$ ,  $G(1, 2; [\bar{\varphi}]) \rightarrow y_u(x)$ , and  $G_0(1, 2) \rightarrow y_0$ . Moreover  $iv(3^+, 4) \rightarrow -v$ : this change of prefactor compensates for the time- or frequency integrations that have been dropped in the 1-point model and corresponds to a standard procedure [85, 87] in this context<sup>b</sup>. We can now linearize Eq. (3.14) in the same way as we did starting with Eq. (2.71) and obtaining Eq. (3.7). This yields

$$y_u(x) = y_H^0 + y_H^0xy_u(x) - uy_H^0\frac{dy_u(x)}{dx}. \quad (3.15)$$

and with respect to Eq. (3.7),  $G_H^0(1, 2) \rightarrow y_H^0$ , and  $iW(3^+, 5) \rightarrow -u$ . In the following, for simplicity of notation, we denote  $y_H^0$  by  $y_0$  unless stated differently. In Appendix B we sketch the main steps to solve Eq. (3.15), based on the general ansatz  $y_u(x) = A(x) \cdot I(x)$ . With the choice

$$A(x) = e^{\left[\frac{x^2}{2u} - \frac{x}{uy_0}\right]} \quad (3.16)$$

one obtains the equation

$$\frac{dI(x)}{dx} = \frac{1}{u}e^{-\left[\frac{x^2}{2u} - \frac{x}{uy_0}\right]} \quad (3.17)$$

---

<sup>b</sup>Moreover very simple examples, e.g.  $V_H(1) = \int d2\rho(2)v(1, 2) = -i \int d2G(2, 2^+)v(1, 2)$  show that it is a reasonable procedure.

and the general solution  $y_u(x)$  reads

$$y_u(x) = \sqrt{\frac{\pi}{2u}} e^{\left[\frac{x^2}{2u} - \frac{x}{uy_0} + \frac{1}{2uy_0^2}\right]} \times \left\{ \operatorname{erf} \left[ \left(x - \frac{1}{y_0}\right) \sqrt{\frac{1}{2u}} \right] - C(y_0, u) \right\}, \quad (3.18)$$

where  $C(y_0, u)$  is to be set by an initial condition. In the limit  $x \rightarrow 0$ , which is the equilibrium solution we are looking for, Eq. (3.18) becomes

$$y_u = -\sqrt{\frac{\pi}{2u}} e^{\frac{1}{2uy_0^2}} \times \left\{ \operatorname{erf} \left[ \sqrt{\frac{1}{2uy_0^2}} \right] + C(y_0, u) \right\}. \quad (3.19)$$

Note the choice of employing the *ansatz* in (3.15) to solve the algebraic differential equation: one could have easily used a wrapped solution from classical textbooks such as [88]. However, with the ultimate goal of *generalizing* our result, such strategy would not be effective, while employing a method which better capture the mathematical structure of the DE (3.15) will prove (in Chapter 6) to better suite the scope.

We are now left with the non trivial issue of solving the initial value problem for the general solution in order to set  $C(u, y_0)$ .

### 3.2.3 Exact particular solution: alternative solution of the initial value problem

In general in order to set  $C(y_0, u)$ ,  $y_u(x)$  has to be known for a given potential  $x_\beta$  (i.e.  $y_u(x_\beta) = y_u^\beta$ ). However it is far from obvious to formulate such a condition in the realistic full functional case; this would indeed require the knowledge of the full interacting  $G$  for some given potential  $\varphi$ . Therefore the question is whether one can reformulate the condition in a simpler way in order to set  $C$ : in particular one hopes to be able to use the same strategy to set the initial condition for the 1-point problem and the full general one.

To answer this question we expand the exact solution for small values of  $u$  (in analogy to what is done in standard perturbation theory), obtaining:

$$y_u \approx -\sqrt{\frac{\pi}{2u}} e^{\frac{1}{2uy_0^2}} \left( 1 + C(u, y_0) \right) + \left\{ y_0 - uy_0^3 + 3u^2y_0^5 - 15u^3y_0^7 + o(u^4) \right\}. \quad (3.20)$$

Knowing that for  $u \rightarrow 0$  the one-body Green's function  $G$  has to reduce to the non interacting  $G_0$ , in our framework this translates into:  $y_u \Big|_{u \rightarrow 0} \equiv y_0$ .

Imposing this condition in Eq. (3.20) gives

$$\sqrt{\frac{\pi}{2u}} e^{\left[\frac{1}{2y_0^2 u}\right]} \left( 1 + C(u, y_0) \right) = 0, \quad u \rightarrow 0, \quad (3.21)$$

which is satisfied if

$$C(u, y_0) = -1, \quad u \rightarrow 0. \quad (3.22)$$

Hence the DE's *particular solution* reads:

$$y_u = -\sqrt{\frac{\pi}{2u}} e^{\frac{1}{2uy_0^2}} \left\{ \operatorname{erf} \left[ \sqrt{\frac{1}{2uy_0^2}} \right] - 1 \right\}. \quad (3.23)$$

This result for  $C$  holds also for  $u \neq 0$ : it guarantees a non-divergent result for any non-vanishing potential  $x$  in (3.18) and it also reproduces the perturbative result which is obtained by iterating Eq. (3.15). For instance the sixth iterative step (starting with  $y^{(0)} = y_0$ ) reads:

$$y_u^{(6)} = y_0 - uy_0^3 + 3u^2y_0^5 - 15u^3y_0^7. \quad (3.24)$$

This is precisely the same series as the one appearing in Eq. (3.20) when  $C(u, y_0)$  is set to  $-1$ . This very same result, can also be obtained, as we will see later on, in an alternative way: also in that case, however, one will have to require the Green's function to be *non-divergent*.

### 3.2.4 Exact particular solution: traditional solution of the initial value problem

The initial value problem for Eq. (3.15) could be also solved within the more "classical" approach, that is, knowing  $y_u(x)$  for a given potential  $x_\beta$  (i.e.  $y_u(x_\beta) = y_u^\beta$ ). However, to be realistic we have to suppose that we can only guess solutions that do not depend on  $u$ : this holds for a quite pathological case, namely  $x_\beta \rightarrow -\infty$ . We will now show how with this choice  $C$  can be set and we will also show, *a-posteriori* the validity of the above statement, that is  $C(u, y_0) = -1, \forall u$  (since the constant does not depend on  $u$ , its value at  $u = 0$  can be employed also for any value of the interaction).

For an infinitely large potential  $x$ , one may calculate  $y_u(x \rightarrow -\infty)$  by means of its expansion and the linearized DE.  $y_u(x)$  can be expressed as:

$$y_u(x) = \Delta_0 + \Delta_1 \frac{1}{x} + \Delta_2 \frac{1}{x^2} + \mathcal{O}\left(\frac{1}{x^3}\right) \quad (3.25)$$

inserting Eq. (3.25) into Eq. (3.15) yields:

$$\begin{aligned} \Delta_0 + \Delta_1 \frac{1}{x} + \Delta_2 \frac{1}{x^2} + \mathcal{O}\left(\frac{1}{x^3}\right) &= y_0 + y_0 \left[ \Delta_0 + \Delta_1 \frac{1}{x} + \Delta_2 \frac{1}{x^2} + \mathcal{O}\left(\frac{1}{x^3}\right) \right] x \\ &- uy_0 \frac{d}{dx} \underbrace{\left[ \Delta_0 + \Delta_1 \frac{1}{x} + \Delta_2 \frac{1}{x^2} + \mathcal{O}\left(\frac{1}{x^3}\right) \right]}_{-\frac{\Delta_1}{x^2} - \frac{\Delta_2}{x^3} + \mathcal{O}\left(\frac{1}{x^4}\right)} \end{aligned} \quad (3.26)$$

and for the different orders in  $x$  one has:

$$\mathcal{O}(x) \quad \Delta_0 = 0 \quad (3.27)$$

$$\mathcal{O}(0) \quad \Delta_0 = y_0 + y_0 \Delta_1 \rightarrow \Delta_1 = -1 \quad (3.28)$$

$$\mathcal{O}\left(\frac{1}{x}\right) \quad \Delta_1 = y_0 \Delta_2 \rightarrow \Delta_2 = -\frac{1}{y_0} \quad (3.29)$$

substituting the coefficients in (3.25) gives:

$$y_u(x) = -\frac{1}{x} - \frac{1}{y_0 x^2} + \mathcal{O}\left(\frac{1}{x^3}\right) \quad (3.30)$$

where the leading term (the first on the right hand side) simply shows that  $y(x \rightarrow -\infty) = 0$ , *no matter the value taken by  $u$* <sup>c</sup>.

Now, using our ansatz  $y(x) = A(x) \cdot \mathcal{I}(x)$  we can extrapolate the large  $x$  behavior for  $\mathcal{I}(x)$ , in fact:

$$\lim_{x \rightarrow -\infty} \mathcal{I}(x) = \lim_{x \rightarrow -\infty} \left( y_u(x) \cdot \frac{1}{A(x)} \right) = 0. \quad (3.31)$$

Also in this case the result does not depend in any way from  $u$ . Hence any other finding relying on (3.31) will be valid for any range of screened interaction considered.

To find  $\mathcal{I}(x)$  one has to integrate (3.17) and for a given lower limit of integration, a particular constant for the solution of the initial value problem will be obtained since  $\mathcal{I}(x) = \int_a^x dt \frac{d\mathcal{I}(t)}{dt} + \mathcal{I}(a)$ . Assuming  $a = -\infty$  we have:

$$\mathcal{I}(x) = \frac{1}{u} \int_{-\infty}^x dt \frac{1}{A(t)} + \mathcal{I}(-\infty) \quad (3.32)$$

we have just shown that  $\mathcal{I}(-\infty) = 0$ , hence the above expression reduces to:

$$\begin{aligned} \mathcal{I}(x) &= \frac{1}{u} \int_{-\infty}^x dt \frac{1}{A(t)} \stackrel{\text{see Eq. B.7}}{=} \sqrt{\frac{2}{u}} e^{\frac{1}{2uy_0^2}} \int_{-\infty}^{\tilde{x}} d\tilde{t} e^{-\tilde{t}^2} \\ &= \sqrt{\frac{2}{u}} e^{\frac{1}{2uy_0^2}} \int_{-\infty}^0 d\tilde{t} e^{-\tilde{t}^2} + \sqrt{\frac{2}{u}} e^{\frac{1}{2uy_0^2}} \int_0^{\tilde{x}} d\tilde{t} e^{-\tilde{t}^2}. \end{aligned} \quad (3.33)$$

where  $x \rightarrow \tilde{x} = \frac{x}{\sqrt{2u}} - \frac{1}{\sqrt{2uy_0^2}}$  as in Eq. (B.7) The second term has been already treated before. Regarding the first term we have:

$$\int_{-\infty}^0 d\tilde{t} e^{-\tilde{t}^2} = \int_0^{\infty} e^{-\tilde{t}^2} d\tilde{t} = \frac{\sqrt{\pi}}{2} \quad (3.34)$$

which gives the prefactor obtained in (B.8).  $\mathcal{I}(x)$  can finally be expressed as:

$$\mathcal{I}(x) = \sqrt{\frac{\pi}{2u}} e^{\frac{1}{2uy_0^2}} \cdot \text{erf} \left[ \left( x - \frac{1}{y_0} \right) \frac{1}{\sqrt{2u}} \right] + \underbrace{\sqrt{\frac{\pi}{2u}} e^{\frac{1}{2uy_0^2}}}_{\bar{C}(u, y_0)} \quad (3.35)$$

---

<sup>c</sup>This point will be also proved afterwards, starting from the exact solution for the 1-point Green's function

and the 1-point Green's function reads:

$$y_u(x) = A(x) \cdot \mathcal{I}(x) = \sqrt{\frac{\pi}{2u}} e^{\left[\frac{x^2}{2u} - \frac{x}{uy_0} + \frac{1}{2uy_0^2}\right]} \cdot \text{erf} \left[ \left(x - \frac{1}{y_0}\right) \frac{1}{\sqrt{2u}} \right] + \sqrt{\frac{\pi}{2u}} e^{\left[\frac{x^2}{2u} - \frac{x}{uy_0} + \frac{1}{2uy_0^2}\right]} \quad (3.36)$$

which in the limit of  $x = 0$  becomes:

$$y_u = \sqrt{\frac{\pi}{2u}} e^{\frac{1}{2uy_0^2}} \cdot \text{erf} \left[ -\sqrt{\frac{1}{2uy_0^2}} \right] + \sqrt{\frac{\pi}{2u}} e^{\frac{1}{2uy_0^2}} = -\sqrt{\frac{\pi}{2u}} e^{\frac{1}{2uy_0^2}} \left\{ \text{erf} \left[ \sqrt{\frac{1}{2uy_0^2}} \right] - 1 \right\} \quad (3.37)$$

where  $-1 = C(u, y_0)$ , a result which we have already obtained in (3.22) by means of a different reasoning.

Therefore the main results of this subsection can be summarized as follows: **i)** the initial value problem for the 1-point DE can be solved in different ways, namely one can **i-a)** either employ the limit  $u = 0$ , expand the exact solution and require that  $y(u = 0) = y_0$ , **i-b)** or use a more traditional argument, that is  $y_u(x)$  is known for a given potential  $x$ , specifically  $x = -\infty$ . **ii)** Both strategies yields the same result:  $C(u, y_0) = -1$  and that such constant does not depend on  $u$ .

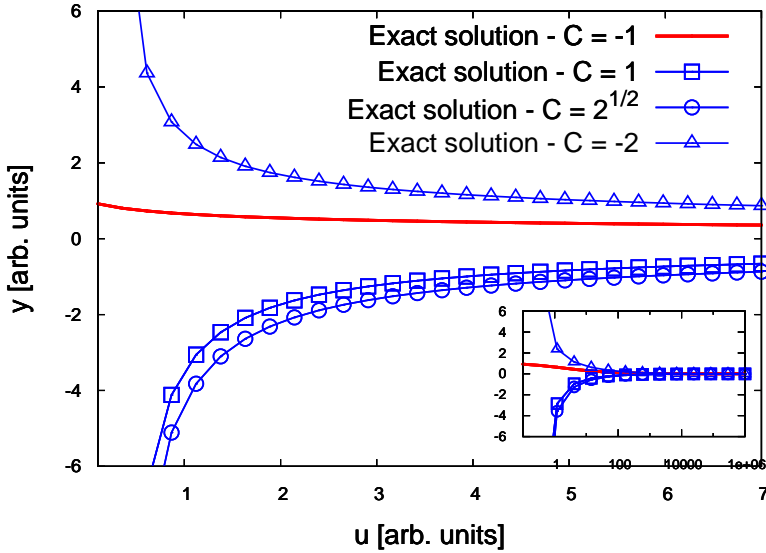


**Figure 3.2:** DE's exact solution depicted for different values of  $C$ . Specifically for  $C = -1$  (red plain curve) we obtain the "physical" particular solution for the Green's function. For the blue dotted curves various values for  $C$  are shown. In the small  $u$  limit, only the red curve is non-divergent, while for the large  $u$  limit, the choice of  $C$  does not influence the behavior of the curves at all: they all approach the exact physical solution of Eq. (3.19)

Finally, notice how, considering the (infinitely) large  $u$  limit, provides us with a family of general solutions which all collapse into the particular one obtained by setting  $C(u, y_0) = -1$ , while in the infinitely small  $u$  limit, all particular solutions have a different behavior. We will shortly come back to this with an analysis of the mathematical nature of the algebraic DE.

However, while this last statement has been shown rigorously to be true within the latter approach (**i-b)**), it was not in the former (we concluded so only by induction). However, within both strategies, one requires the Green's function to be *non-divergent*.

### 3.2.5 DE's solution by iteration

Let us analyze more carefully the iterative procedure that lead to the result of Eq. (3.24). We will begin employing a very conventional starting point, namely:  $y_u^{(0)}(x) = y_0$  (later on we will propose some other initial guesses and examine their effects on the final result).

The  $n^{\text{th}}$  iteration produces

$$y_u^{(n+1)}(x) = y_0 + y_u^{(n)} x y_0 - u y_0 \frac{dy_u^{(n)}(x)}{dx}. \quad (3.38)$$

For  $x = 0$  the first two orders in  $u$  read

$$y_u^{(2)} = y_0 - u y_0^3, \quad (3.39)$$

$$y_u^{(4)} = y_0 - u y_0^3 + 3u^2 y_0^5, \quad (3.40)$$

and Eq. (3.24) for the third order. Results as a function of  $u$  are depicted in Fig. 3.3 together with the exact solution.

Two observations can be made: **i)** very few terms are needed to obtain a good approximation to the exact solution in the small  $u$  regime; **ii)** for a given  $u = u_n$ , the expansion diverges starting from an order  $n$ . The larger is  $u_n$ , the smaller is  $n$ , which limits

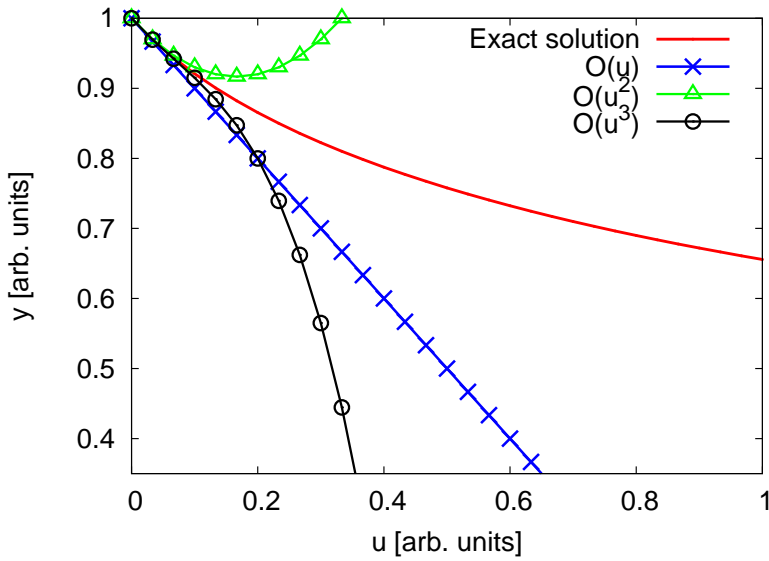


**Figure 3.3:** Comparison between the exact solution (red plain line, Eq. (3.19)) and the iterative solution for  $x = 0$  of (Eq. (3.38)). The blue stars show the 1<sup>st</sup> order expansion (Eq. (3.39)), while the green triangles and the black circles are respectively the 2<sup>nd</sup> (Eq. (3.40)) and 3<sup>rd</sup> order (Eq. (3.24)). All the three orders are close to the exact solution for small  $u$  values, whereas when a given order of the series starts to diverge, the lower orders of the expansion reproduce the exact results better. For each curve  $C(u, y_0) = -1$ , and we set  $y_0 = 1$

sue will be discussed at the next section of this chapter.

the precision that can be obtained. As previously mentioned, the iteration coincides with the expansion for small  $u$  of the exact solution. Since the small  $u$  expansion is *de facto* the asymptotic expansion of the error function times an exponential (as can be seen in (3.20)) the divergent behavior of the iteration in (3.38) is not surprising. Divergences of higher orders have also been found in perturbation expansions for realistic systems, e.g. for orders higher than 3 in the Møller-Plesset scheme [89, 90], more on this issue

### 3.3 A singular perturbation problem

Some mathematical considerations will now be provided regarding the nature of Eq. (3.15). The problem we have just solved belongs to the class of the so-called *singular perturbation problems*. It may be convenient to distinguish between the -more common- *regular* perturbation problems (RPP) and the *singular* perturbation problems (SPP). In the former, the solution that can be obtained for a small value of the perturbing parameter -let  $\epsilon$  be such parameter-, is at least *qualitatively*, the same as that of the unperturbed problem, for which  $\epsilon = 0$ . In the latter, this is not true anymore: the unperturbed solution is qualitatively different from the solution for non-null values of  $\epsilon$  (very often its approximate form will consist in one, or more than one, *asymptotic expansion* with respect to  $\epsilon$ ). Intuitively this means that the problem we deal with behaves differently depending on the *scale* (i.e. time or length, but not only) we are looking at. Furthermore SPPs can then be divided up in two broad classes: boundary layer problems and multi-scale problems, which are commonly solved by matched asymptotic expansions (MMAE) and method of multiple scales (MMS) respectively. We will now shed some more light on the divergent nature of the result in Eq. (3.24).

#### 3.3.1 An approximate solution from asymptotic expansions

As we have shown in the previous section, a physicist would probably solve (approximately) the DE by *iterating* it; a mathematician, knowing they are facing a singular perturbation problem, would probably try out an approximate solution obtained through an *asymptotic expansion*. For a regular perturbation problem, *a single* approximate solution, in terms of an expansion of the unknown in powers of the perturbing parameter, could describe well our problem on a very large scale (for all the parameters appearing in the equations).

Instead, for a singular perturbation problem, we would notice that such methodology does not really lead to a full solution of the problem, but rather to a partial one: e.g. in the case of a  $n^{th}$  order differential equation one employs only  $n - 1$  initial conditions (and is hence left with an unused one) or in case of an algebraic equation of degree  $n$  one would obtain less than the expected  $n$  solutions.

However, through a *rescaling* of the variables, it is possible to restore the nature of the equation and find *two asymptotic expansions* (or more, depending on the so called *layers*, which are nothing else than the areas where one approximate solution and not the others describe accurately the problem), one valid for  $\epsilon = 0$  (the so-called inner solution, which is often the solution we would obtain treating the problem as a regular perturbation one) and the second valid for some other small  $\epsilon$  (outer solution). The two expansions can be then appropriately matched to obtain a very good approximation to the exact solution of the equation  $\forall \epsilon$ .

Here we will first show how, treating the DE as if it were a regular perturbation problem, just provides us with an approximation which is excellent for  $\epsilon \rightarrow 0$ , but quickly diverges for larger (although still very small) values of the perturbing parameter.

First of all let's recast Eq. (3.15) in a slightly different form, dividing both sides by  $y_0$ :

$$\begin{aligned}\frac{y_u(x)}{y_0} &= 1 + xy_u(x) - u \frac{d y_u(x)}{dx} \\ y_u(x) \left[ \frac{1}{y_0} - x \right] &= 1 - u \frac{d y_u(x)}{dx}\end{aligned}\quad (3.41)$$

and then defining a rescaled potential  $\tilde{x} = \frac{1}{y_0} - x$  and employing a chain rule for the derivative, (3.41) reads:

$$\begin{aligned}y_u(\tilde{x})\tilde{x} &= 1 - u \frac{d y_u(\tilde{x})}{d\tilde{x}} \frac{d(\frac{1}{y_0} - x)}{dx} = 1 + u \frac{d y_u(\tilde{x})}{d\tilde{x}} \\ y_u(\tilde{x})\tilde{x} - 1 - u \frac{d y_u(\tilde{x})}{d\tilde{x}} &= 0\end{aligned}\quad (3.42)$$

If we tried the solution of the equation as if it was a RPP, we would assume that the following asymptotic expansion:

$$y_u(\tilde{x}) \approx y_1(\tilde{x}) + uy_2(\tilde{x}) + u^2y_3(\tilde{x}) + \mathcal{O}(u^3) \quad (3.43)$$

might possibly be a good approximation for the DE. The goal is to calculate all the coefficients  $y_1, y_2, y_3, \dots$  of the expansion. We simply substitute (3.43) into (3.42):

$$[y_1(\tilde{x}) + uy_2(\tilde{x}) + u^2y_3(\tilde{x})] \tilde{x} - 1 - u \frac{d}{d\tilde{x}} [y_1(\tilde{x}) + uy_2(\tilde{x}) + u^2y_3(\tilde{x})] = 0 \quad (3.44)$$

and solve an equation for each order of  $u$  separately:

$$y_1\tilde{x} - 1 = 0 \quad \mathcal{O}(0) \quad (3.45)$$

$$y_2\tilde{x} - \frac{dy_1(\tilde{x})}{d\tilde{x}} = 0 \quad \mathcal{O}(u) \quad (3.46)$$

$$y_3\tilde{x} - \frac{dy_2(\tilde{x})}{d\tilde{x}} = 0 \quad \mathcal{O}(u^2) \quad (3.47)$$

One obtains:

$$y_1 = \frac{1}{\tilde{x}} \quad (3.48)$$

$$y_2 = \frac{d}{d\tilde{x}} \left( \frac{1}{\tilde{x}} \right) \frac{1}{\tilde{x}} = -\frac{1}{\tilde{x}^3} \quad (3.49)$$

$$y_3 = \frac{d}{d\tilde{x}} \left( -\frac{1}{\tilde{x}^3} \right) \frac{1}{\tilde{x}} = \frac{3}{\tilde{x}^5} \quad (3.50)$$

Inserted in (3.43) they yield:

$$y_u(\tilde{x}) \approx \frac{1}{\tilde{x}} - u \frac{1}{\tilde{x}^3} + u^2 \frac{3}{\tilde{x}^5} \quad (3.51)$$

going back to the original variables  $\{y_0, x\}$

$$y_u(x) \approx \frac{1}{\left[ \frac{1}{y_0} - x \right]} - u \frac{1}{\left[ \frac{1}{y_0} - x \right]^3} + u^2 \frac{3}{\left[ \frac{1}{y_0} - x \right]^5} \quad (3.52)$$

which in the usual limit of  $x \rightarrow 0$  becomes:

$$y_u(x) \approx y_0 - uy_0^3 + 3u^2y_0^5 \quad (3.53)$$

This is precisely the *same* result as the one obtained with the *iterative* solution for the DE (see Eq. (3.39)).

Such a result fully rationalizes the divergence encountered by iterating Eq. (3.15): they correspond to solving the DE through an asymptotic expansion which is meant to be a good approximation for the exact solution only in the proximity of  $u = 0$ : elsewhere the expansion performs quite poorly, but this *has* to be expected since the DE constitutes a SPP.

Note that, for the full functional differential equation, a solution by iteration would be equivalent to the generalized version of the above asymptotic expansion. Unfortunately the time didn't allow for obtaining a second expansion (corresponding to the outer layer), which could have been joined to the inner solution, so as to reproduce accurately the exact solution of Eq. (3.23). We will only briefly sketch how this should be done.

As we have mentioned before the asymptotic expansion (3.43) is not capable to describe the DE's solution over the whole interval for  $\tilde{x}$ . This means that we have to expect, at a given value for  $x$  a so called boundary layer, for which another approximate solution for the DE has to be found. Once this critical value for  $x$  has been identified, one constructs a so-called *boundary layer coordinate*, which in our case is  $x_l = \frac{x}{u^\alpha}$ , where  $\alpha > 0$ . This procedure has the effect of *stretching the area near the boundary layer point*, in fact if  $x_l$  is kept fixed while expanding again our solution in terms of  $u$ ,  $x$  will become larger. A new equation in the rescaled variables will have to be solved through asymptotic expansions, with the only difference that the presence of the power  $\alpha$  in the perturbing parameter  $u$  will make the problem slightly more complicated than before. This second solution has now to be *matched* to the inner one. The matching is performed in two steps: first both inner and outer solutions are rescaled in terms of an intermediate variable, which satisfies certain constraints, then, assuming that the domains of validity of both the inner and outer solutions overlap, one requires that terms of the same order for both expansions are equal.<sup>d</sup> One has thus obtained a so-called *composite expansion*, which, in principle, should reproduce accurately the exact DE's solution.

In conclusion it will be certainly worthwhile to explore this route further as an alternative to traditional perturbation theory.

### 3.3.2 Other famous examples of divergences

Divergences are not unique to the iteration of the differential equation (3.15), but are also found within other perturbation techniques applied to both real and model systems, an example of this is the Møller-Plesset (MPn) scheme [91].

It has in fact been observed that, for certain atoms and molecular systems, expansions beyond the 2<sup>nd</sup> order exhibit, seldom, either an oscillatory, or erratic or even a completely divergent behavior [89]. A particularly critical system is constituted by the hydrogen fluoride (HF), where the calculation of several molecular constants within MP4 has been found to be systematically

---

<sup>d</sup>In general it is enough to match the solution for the first order of the expansions: being asymptotic expansions we know that very few terms -in the limit of a single one- are needed to reach a good accuracy.

worse than MP2 [90].

Another example is the homogeneous electron gas which exhibits a divergent series expansion in terms of the bare Coulomb potential  $v$  and resummation of the largest divergent integrals of such expansion have been discussed, for instance, in [? ].

Together with the two examples above we should number the (in)famous case of the quartic anharmonic oscillator when treated within the ordinary Rayleigh-Schrödinger perturbation theory (RS-PT).

One deals with an eigenvalue problem defined by:

$$\left( \frac{d^2}{dx^2} + \frac{1}{4}x^2 + \frac{1}{4}\lambda x^4 \right) \Phi(x) = E(\lambda)\Phi(x) \quad (3.54)$$

where  $\lambda$  is the perturbing parameter. The boundary conditions for the above differential equation are  $\lim_{x \pm \infty} \Phi(x) = 0$ .

This particular anharmonic oscillator has been extensively studied since it represents a very simple model field theory<sup>e</sup> in one dimensional space-time.

The perturbation theory for such model was studied, among the others by Bender and Wu [92], first by mean of Feynman diagrams and later on with a mixed analytical and computational approach. A greater deal of insights was obtained mainly within the latter approach and it was found that the theory provides coefficients  $c_n$  of the energy eigenvalues  $E_0(\lambda) = \sum_n c_n \lambda^n$  constituting the asymptotic series:

$$c_n \approx (-1)^{n+1} \left( \frac{3}{2} \right)^n \Gamma(n + \frac{1}{2}), \quad n \rightarrow \infty \quad (3.55)$$

yielding an energy of the type:

$$E_0(\lambda) = \sum_n \left( -\frac{3\lambda}{2} \right)^n \Gamma(n + \frac{1}{2}) \quad (3.56)$$

The expression in Eq. (3.56) is proportional to a particular hyper geometric series<sup>f</sup> of the form:

$$\begin{aligned} {}_2F_0\left(\frac{1}{2}, 1; -\frac{3}{2}\lambda\right) &= \sum_{n=0}^{\infty} \left(\frac{1}{2}\right)_n \left(-\frac{3\lambda}{2}\right)^n \\ &= \sum_{n=0}^{\infty} \frac{\Gamma(n + \frac{1}{2})}{\Gamma(\frac{1}{2})} \left(-\frac{3\lambda}{2}\right)^n \\ &= \sqrt{\pi} \sum_{n=0}^{\infty} \Gamma(n + \frac{1}{2}) \left(-\frac{3\lambda}{2}\right)^n \\ &= \sum_{n=0}^{\infty} (-1)^n \frac{(2n-1)!!}{2^n} \left(\frac{3\lambda}{2}\right)^n \end{aligned} \quad (3.57)$$

<sup>e</sup>Where the theory is defined by  $H = \frac{1}{2}\dot{\varphi}^2 + \frac{1}{2}m^2\varphi^2 + \lambda\varphi^4$  and  $[\varphi, \dot{\varphi}] = i$

<sup>f</sup>It is a *divergent* generalized hyper geometric series. Once the series is expressed as  ${}_nF_m \left( \begin{matrix} a_1 & \cdots & a_p \\ b_1 & \cdots & b_q \end{matrix} ; \mathbf{T} \right)$ , the following convergence rules apply: if  $p \leq q$  we have absolute convergence for all  $\mathbf{T}$ , if  $p = q + 1$  then it converges absolutely for  $\|T\| < 1$  and diverges for  $\|T\| > 1$  and finally if  $p > q$  -which is our case- it diverges. These properties can be found, e.g. in Ref [93]

where the Pochhammer notation for  $\left(\frac{1}{2}\right)_n$  has been transformed in an equivalent expression made up of  $\Gamma$  functions and the  $\Gamma$  functions have, in turn, been expressed through multiple factorials. <sup>g</sup> Let's now define a new variable  $z$  as a function of the perturbing parameter  $\lambda$  as:  $z = \frac{3}{2}\lambda$ , this definition will be handy later. Now let's turn for a second to another special function, the *error function* and its conjugate, the *erfc*. The asymptotic expansion for an *erfc*( $z$ ), with  $z$  large, reads:

$$\operatorname{erfc}(z) = \frac{e^{-z^2}}{z\sqrt{\pi}} \sum_{n=0}^{\infty} \frac{(2n-1)!!}{(2z^2)^n} \quad (3.58)$$

The above expression is remarkably similar to the one in Eq. (3.57), except for an exponential factor. What if we plug Eq. (3.58) into the exact solution for the DE (substituting  $\sqrt{\frac{1}{2uy_0^2}} = z$  and setting  $y_0 = 1$  <sup>h</sup>)? One obtains:

$$y_u = \sum_{n=0}^{\infty} \frac{(2n-1)!!}{(2z^2)^n} \quad (3.59)$$

which is identical to the result in (3.57)! Note that in both cases  $z$ , which we assume to be large, is the *inverse* of the perturbing parameters  $u$  (for the DE) and  $\lambda$  (for the anharmonic oscillator), which are supposedly small.

Thus both the divergence observed in the perturbation expansion of the differential equation and the one observed for the perturbation expansion of this specific model system can be formally ascribed, at least partly<sup>i</sup>, to the divergent nature of the asymptotic expansion of the error function.

---

<sup>g</sup>More specifically we used the relation  $(a)_n = \frac{\Gamma(a+n)}{\Gamma(a)}$  (being  $a = \frac{1}{2}$  and  $m = n$ ) and  $\Gamma(n + \frac{1}{2}) = \frac{(2n-1)!!}{2^n} \frac{1}{\sqrt{\pi}}$

<sup>h</sup>More detailed algebraic steps are given in App. C

<sup>i</sup>Partly here refers to the quartic anharmonic oscillator, where in [92] the divergence of the series was attributed mainly to an infinite number of branch point -with a singular point at  $\lambda = 0$ - in the energy levels obtained with the analytical continuation

# CHAPTER 4

## Insights from the 1-point model

*In this chapter we will discuss a number of insights obtained through the solution of the differential equation for the Green's function in the 1-point framework, which has been presented in the previous chapter. Firstly the DE's exact solution is compared to established approximations, such as  $G_0W_0$ , self-consistent  $GW_0$ , and to both a self-consistent and a non-self consistent scheme which includes a first order vertex correction (respectively  $G_0W_0\Gamma^{(1)}$  and  $GW_0\Gamma^{(1)}$ ). The validity and the possibility of extending our insights to real calculations is also discussed. In the second part of the chapter we will instead devise alternative approximations to the  $GW$ -based ones. We will discuss their advantages and caveats and, where possible, we will present their extension to the full  $N$ -points framework.*

### 4.1 Established approximations

In this section the introduction of a self-energy  $\Sigma$  in order to calculate the GF, will be discussed, along with its most common approximations.

The Dyson-like form for Eq. (3.15), which is the equivalent of Eq. (2.89), reads:

$$y_u(x) = y_0 + y_0 x y_u(x) + y_0 \Sigma_u [y_u(x)] y_u(x) \quad (4.1)$$

where a self-energy kernel

$$\Sigma_u [y_u(x)] = -u \frac{dy_u(x)}{dx} \frac{1}{y_u(x)}, \quad (4.2)$$

has been introduced. Using  $\frac{dy_u(x)}{dx} = -y_u(x)^2 \frac{dy_u^{-1}(x)}{dx}$  and the definition  $\Gamma_u [y_u(x)] = -\frac{dy_u^{-1}(x)}{dx}$  for the vertex function, the self-energy reads

$$\Sigma_u [y_u(x)] = -u y_u(x) \Gamma_u [y_u(x)], \quad (4.3)$$

which is the equivalent of Eq. (2.100). Note that in Eq. (4.3) the reducible vertex is used. However since here the Hartree potential is independent of the external potential, then  $\Gamma = -\frac{dy^{-1}}{dx} = -\frac{dy^{-1}}{dV} \frac{dV}{dx} = -\frac{dy^{-1}}{dV} = \tilde{\Gamma}$  and Eq. (4.3) is equivalent to (2.100). Here  $V = V_H^0 + x$ . Starting from from (4.1) one can then derive the Bethe-Salpeter equation for the vertex function  $\Gamma$

$$\begin{aligned} \frac{dy_u^{-1}(x)}{dx} &= -1 - \frac{d\Sigma_u[y_u(x)]}{dx} \\ &= -1 - \frac{d\Sigma_u[y_u(x)]}{dy_u(x)} \frac{dy_u(x)}{dx}, \end{aligned} \quad (4.4)$$

from which for  $x \rightarrow 0$

$$\Gamma_u(y_u) = 1 + \frac{d\Sigma_u(y_u)}{dy_u} \Gamma_u(y_u) y_u^2 \quad (4.5)$$

where  $y_u = y_u(x \rightarrow 0)$ . For  $x = 0$  Eqs. (4.1), (4.3), and (4.5) are equivalent to Hedin's equations [14] for a fixed  $W$  (see also Fig. 3.1). In the following we will compare various type of approximations for these equations to the DE's exact solution, in order to obtain greater insight in these self-energy based techniques. From now on all the quantities we deal with are understood to be taken at vanishing external potential ( $x = 0$ ).

#### 4.1.1 $G_0W_0$ and fully self-consistent GW

Let us first analyze the different flavors of the  $GW$  approximation [14]. Setting  $\Gamma_u(y_u)$  to unity, it follows that  $\Sigma_u(y_u) = -uy_u$ . Within the initial guess  $y_u^{(0)} = y_0$ , one gets the  $G_0W_0$  self-energy:  $\Sigma_u = -uy_0$ . This is then inserted in the Dyson equation (4.1) in order to get an improved  $y_u^{(1)}$ . To go beyond this first approximation one can iterate further within the  $GW$  approximation, i.e. keeping  $\Gamma_u(y_u) = 1$ . This procedure corresponds to an iteration towards a so-called  $GW_0$  result, since  $G$  is iterated towards self-consistency while  $u$ , which represents the screened interaction, is kept fixed.

We report here the expressions obtained for  $G_0W_0$ , i.e. the first solution of the Dyson equation, and for three successive loops

$$y_u^{(1)} = y_u^{G_0W_0} = \frac{y_0}{1 + uy_0^2}, \quad (4.6)$$

$$y_u^{(2)} = y_0 \frac{1 + uy_0^2}{1 + 2uy_0^2}, \quad (4.7)$$

$$y_u^{(3)} = y_0 \frac{1 + 2uy_0^2}{1 + 3uy_0^2 + u^2y_0^4}, \quad (4.8)$$

$$y_u^{(4)} = y_0 \frac{1 + 3uy_0^2 + u^2y_0^4}{1 + 4uy_0^2 + 3u^2y_0^4}. \quad (4.9)$$

We call this procedure *iterative self-consistent* scheme, opposite to the *direct self-consistent* scheme, where one solves directly the Dyson equation (4.1), for  $x = 0$ , with  $\Sigma_u = -uy_u$ . In this latter case one gets a second-order equation with two solutions

$$y_u = \frac{\pm \sqrt{1 + 4uy_0^2} - 1}{2uy_0}. \quad (4.10)$$

One may wonder if *both these solutions are physical*, i.e. meaningful. Fortunately there are certain constraints a physical Green's function must obey to, hence one could use them as checkpoints. A *necessary* condition is that for vanishing electron-electron interaction the full Green's function has to reduce to the non-interacting one, that is  $u = 0 \mapsto y_u = y_0$ . Taylor expanding the square root around  $u = 0$

$$y_u \approx \pm \left( y_0 + \frac{1}{2uy_0} \right) - \frac{1}{2uy_0}. \quad (4.11)$$

It is immediate to verify that only one of the two solutions fullfills the above condition. The physical solution hence reads

$$y_u = \frac{\sqrt{1 + 4uy_0^2} - 1}{2uy_0}. \quad (4.12)$$

In the next paragraph we will analyze more in depth certain aspects of the above two schemes, mainly the influence of the starting point on the final result.

### Starting point in iterative schemes

A further question concerning the sc- $GW_0$  iterative scheme may be: *does the result of the procedure depend on the starting point of the iteration?*

In the previous sections we have naturally chosen  $y_u^{(0)} = y_0$ , but of course other choices are possible. Let us therefore analyze from a more general point of view the iterative scheme obtained by solving the Dyson equation (4.1) for  $x = 0$

$$y_u^{(n+1)} = \frac{1}{1 + y_0 u y_u^{(n)}}. \quad (4.13)$$

Starting with  $y_u^{(0)} = y^s$ , substituting, at each step, on the right hand side of Eq. (4.13), an improved  $y^n$ , one obtains (e.g. after three iterations)

$$y_u^{(3)} = \frac{y_0}{1 + \frac{uy_0^2}{1 + \frac{uy_0^2}{1 + y_0 u y^s}}}. \quad (4.14)$$

This contains nothing else but the continued fraction representation [93] for the square root

$$\sqrt{1+z} = 1 + \frac{z/2}{1 + \frac{z/4}{1 + \frac{z/4}{1 + \frac{z/4}{1 + \frac{z/4}{1 \dots}}}}}, \quad (4.15)$$

corresponding to the physical solution  $y_u = \frac{\sqrt{1+z} - 1}{2uy_0}$  where  $z = 4uy_0^2$ . It converges *no matter* the value of the terminator  $y^s$ . Therefore this iterative scheme will always converge to the physical solution. One might now wonder if also the *negative root* of Eq. (4.10) can be obtained

through some iterative scheme. The answer is *yes*. Recasting the Dyson equation (4.1) as:  $-uy_u = +\frac{1}{y_0} - \frac{1}{y_u}$  (in other words,  $\Sigma = G_0^{-1} - G^{-1}$ ) and iterating it by starting again with a generical  $y_u^{(0)} = y^s$ , we get

$$y_u^{(n+1)} = -\frac{y_0}{uy_0} + \frac{1}{uy_u^{(n)}}, \quad (4.16)$$

hence

$$2uy_0y = -2 - \frac{2uy_0^2}{1 + \frac{uy_0^2}{1 + \frac{uy_0^2}{1 + \frac{uy_0^2}{\dots}}}}. \quad (4.17)$$

which together with Eq. (4.15) is the continued fraction representation for the unphysical solution  $y_u = -\frac{\sqrt{1 + 4uy_0^2} + 1}{2uy_0}$ . We hence conclude that it is the *type of iterative scheme* employed, rather than the *choice of the starting point* to determine the good quality of the final result. This is, at the same time, a comforting and worrisome statement. Comforting because usually the iterative scheme adopted in the context of *GW* calculations is rather the first, safe one. Worrisome because when going beyond *GW*, higher order equations appear and more and more solutions are available. If we imagine that each solution can be obtained through a different iterative scheme, then there will be surely an increased danger to run into a non-physical solution. This should be kept in mind when trying to add vertex corrections beyond *GW*.

After this parenthesis, we can go back to the results of the iterative and the direct *sc-G<sub>0</sub>W<sub>0</sub>* schemes and get a pictorial representation of the expressions discussed so far.

When a small range of interaction is considered, both even and odd iteration seem to converge, fairly quickly, to the direct *sc-G<sub>0</sub>W<sub>0</sub>* result. When a larger *u* range is considered (see the inset of Fig. 4.1), *odd* iterations quickly converge to the *physical* solution, while *even* iterations do also converge but at a much slower pace. It can be shown that for  $u \rightarrow \infty$  their  $u \rightarrow \infty$  limit forms the sequence of rational numbers  $\left\{ \frac{1}{2}; \frac{1}{3}; \frac{1}{4}; \frac{1}{5}; \frac{1}{6} \dots \right\}$  which ultimately approaches 0. This result would suggest, for instance, routes to speed up the convergence calculations by separating odd and even orders of the iteration (by using simple procedures to separate odd and even orders of the continued fraction).

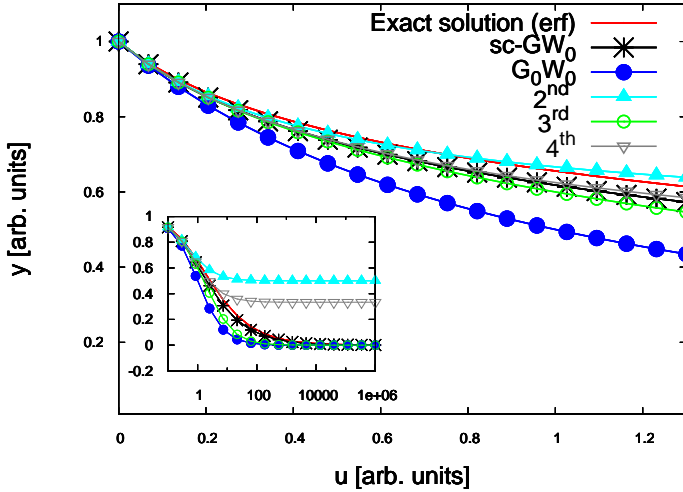


**Figure 4.1:** Comparison between the exact solution (red plain line, Eq. (3.19)) and different flavors of the *GW* approximation. In general the self-energy based approximations perform better than the iteration of the DE shown in Fig. 3.3. In the main panel the self-consistent *G<sub>0</sub>W<sub>0</sub>* (black stars, Eq. (4.10)) is the best approximation to the exact result and its iterations converge towards the self-consistent result (the 2<sup>nd</sup> iteration blue triangles, the 3<sup>rd</sup> green squares and the 4<sup>th</sup> grey triangles). However, analyzing a larger *u* range (inset), one can clearly observe that odd iterations tend to the exact  $u = \infty$  limit, while the even ones don't.

### 4.1.2 Vertex corrections

We will analyze in this section the effects of a first order vertex correction [14] which is obtained by employing the self-energy  $\Sigma_u = -uy_u$  in Eq. (4.5). The first order vertex will hence read

$$\Gamma_u^{(1)}(y_u) = \frac{1}{1 + uy_u^2}. \quad (4.18)$$

Using this  $\Gamma$  the self-energy in Eq. (4.3) becomes

$$\Sigma_u^{(1)}(y_u) = -uy_u \left[ \frac{1}{1 + uy_u^2} \right], \quad (4.19)$$

Two routes can now be taken and either a  $G_0W_0\Gamma^{(1)}(y_0)$  or a self-consistent  $GW_0\Gamma^{(1)}(y_u)$  calculation can be carried out.

Nowadays there is still much debate about how to properly insert a vertex correction in a self-energy based scheme: cancellation effects are frequent [94, 95] and it is not so obvious to improve on the simpler self-consistent results. Therefore we will test both approaches and compare their performances. Let us start with employing a vertex correction in a *one-shot* calculation: the canonical initial guess for the Green's function is  $y^{(0)} = y_0$  and consequently the vertex and the self-energy in (4.18), (4.19) read respectively  $\Gamma_u^{(G_0W_0\Gamma)}(y_0) = \frac{1}{1 + uy_0^2}$  and  $\Sigma_u^{(G_0W_0\Gamma)}(y_0) = -uy_0 \left[ \frac{1}{1 + uy_0^2} \right]$ .

Solving the Dyson equation with the above ingredients yields:

$$y_u^{G_0W_0\Gamma} = \frac{y_0 (1 + uy_0^2)}{1 + 2uy_0^2}. \quad (4.20)$$

Instead, solving the Dyson equation in a *self-consistent* fashion, with the expressions (4.18-4.19) yields:

$$\begin{aligned} y_u^{GW_0\Gamma} &= \sqrt[3]{\frac{y_0}{2u} + \sqrt{\frac{1}{27u^3} + \frac{1}{4u^2}}} \\ &\quad - \sqrt[3]{\frac{y_0}{2u} - \sqrt{\frac{1}{27u^3} + \frac{1}{4u^2}}}. \end{aligned} \quad (4.21)$$

As it can be noticed from the result a cubic equation for the unknown  $y_u$  had to be solved within this more sophisticated approach. Again the limit of vanishing interaction has been used to pick the physical solution.

In Fig. 4.2 we can directly compare the two types of vertex corrections. For small  $u$  values their performance is similar, however, in a wider  $u$  range (see inset), the  $G_0W_0\Gamma^{(1)}$  scheme diverges from the exact solution and has the wrong asymptotic limit  $u \rightarrow \infty$ : it hence behaves as the first iteration of the sc- $GW_0$  approach, which also exhibits the wrong large  $u$  limit. The same figure also shows how the  $GW_0\Gamma^{(1)}$  scheme, for small  $u$  values, slightly improves over the sc- $GW_0$ . However, given the augmented complexity already at this first order of the correction (one

could very well iterate further the equations for  $\Gamma$  and  $\Sigma$  and get higher order corrections), the benefits of employing vertex corrections are not obvious. Also note that interestingly, on the scale from  $u = 0$  to  $u \rightarrow \infty$ , the closest curve to the exact one is the sc- $GW_0$  one. In conclusion the Dyson equation is really powerful: when solved even within a simple approximation for the self-energy, it yields very good results as compared to the straightforward finite iteration. There are issues of self-consistency, but the solution seems to be determined by the kind of iterative scheme that is used,

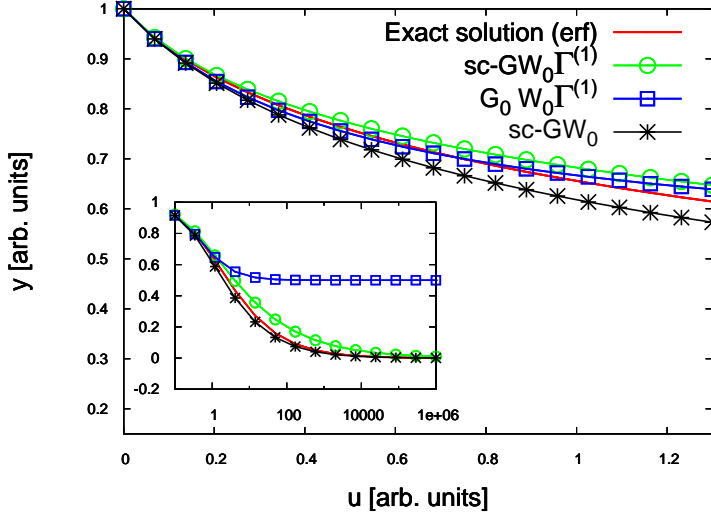


**Figure 4.2:** In the main panel a comparison between the DE's exact solution (red plain line, Eq. (3.19)),  $G_0 W_0 \Gamma^{(1)}$  (blue squares, Eq. (4.20)),  $GW_0 \Gamma^{(1)}$  (green dots, Eq. (4.21)) and sc- $GW_0$  (black stars, Eq. (4.10)) is shown. In this range of  $u$ , adding a vertex correction, no matter if within a self-consistent scheme or not, improves over the simpler self-consistent  $GW_0$ . However, analyzing a wide  $u$  range (inset, semi-logarithmic plot), gives a different perspective: the iterative  $G_0 W_0 \Gamma^{(1)}$  clearly exhibits a wrong  $u \rightarrow \infty$  limit. Moreover the sc- $GW_0$  scheme is, in this case, the closest curve to the exact result.

not by the starting point. It should however be reminded that here  $W_0$  is kept fixed: nothing can hence be said regarding the benefits of calculating  $W$  with an internal vertex.

## 4.2 Alternative approximations

### 4.2.1 An alternative vertex correction

An underlying working recipe in Green's function theory, is to often resort to the non-interacting Green's function, which one can easily calculate, in order to access the properties of the full  $GF$ . One may hence wonder if relying so much on the  $G_0$  can be a good strategy also in the scheme of vertex corrections: what about for instance having  $\Sigma$  as an *explicit* functional of  $y_0$  rather than of the full  $y_u$ ? This is the idea, which already had appeared in the literature with the work by Schindlmayr and Godby [96], that led us to the derivation and test of an alternative vertex correction in the 1-point framework.

The alternative formulation of Hedin's vertex devised in [96]<sup>a</sup> is based on a sequence of functional manipulations performed on the original irreducible  $\tilde{\Gamma}$  (see Eq. (2.94)), and yielding a vertex with a similar structure as that of Hedin:

$$\bar{\Gamma}^{(n+1)}(1, 2; 3) = \delta(1, 2)\delta(1, 3) + \int d4d5d6d7 \frac{\delta \Sigma^{(n)}(1, 2)}{\delta G^{(0)}(4, 5)} G^{(0)}(4, 6) G^{(0)}(7, 5) \bar{\Gamma}^{(1)}(6, 7; 3) \quad (4.22)$$

<sup>a</sup>We indicate this alternative vertex as  $\bar{\Gamma}$ , to distinguish it from an approximate Hedin's one.

but it contains on the right hand side operators of a lower order than the ones appearing in (2.94). In particular, having the non-interacting Green's function rather than full propagator reduced the computational cost of such vertex considerably.

Mapping Schindlmayr and Godby's vertex in the 1-point framework yields:

$$\bar{\Gamma}_u^{(n+1)}(y_u) = 1 + \frac{d\Sigma^{(n)}(y_u)}{dy_0} y_0^2 \quad (4.23)$$

( $\bar{\Gamma}^{(1)}$  on the right hand side is fixed to unity) and a first order correction reads:

$$\bar{\Gamma}_u^{(1)}(y_u) = 1 + \frac{d\Sigma^{(1)}(y_u)}{dy_0} y_0^2. \quad (4.24)$$

We have now to evaluate the term  $\frac{d\Sigma_u^{(1)}(y_u)}{dy_0}$ . Starting from the  $GW$  approximation to  $\Sigma$  (the prescription in [96] employs  $G_0$  for the self-energy evaluation) one obtains:

$$\frac{d\Sigma_u^{(1)}(y_0)}{dy_0} \stackrel{\text{From Eq.11 in ([96])}}{=} -u + y_0 (-2u^2) y_0^2 \quad (4.25)$$

which inserted in Eq. (4.24) yields:

$$\bar{\Gamma}_u^{(1)}(y_0) = 1 + y_0 (-u - 2u^2 y_0^3) y_0 \overset{\text{fixed } u}{\approx} 1 - uy_0^2 \quad (4.26)$$

where the approximation in the last term stems from the fact that we are employing a constant  $u$  value (consistently with our linearization) whereas the neglected term  $-2u^2 y_0^3$  stems from the derivative of  $W$  ( $u$  in the model).

Interestingly this vertex correction is a  $\mathcal{O}(1)$  approximation to Hedin's original vertex (see Eq. (4.18)). The first order correction to the self-energy (evaluated from  $\Sigma^{(2)} = -uy_0\Gamma^{(1)}$ ) can be now evaluated:

$$\Sigma_u^{(2)}(y_u) = -uy_0 (1 - uy_0^2) \quad (4.27)$$

and employing the Dyson equation for  $y_u$ , one obtains:

$$y_u = \frac{y_0}{1 + uy_0^2 (1 - uy_0^2)}. \quad (4.28)$$

The performance of this alternative first order vertex correction is depicted in Fig. 4.3a. We can see that is not particularly good: more of the quality of a  $G_0W_0$  calculation rather than of a first order vertex correction like the one in (4.19).

We will now test again the first order of the vertex in Eq. (4.23) but starting from a self-consistent  $GW$  calculation for  $\Sigma$  (rather than a  $G_0W$  one) namely using  $\Sigma_u^{(1)} = -uy_u$ .

Schematically: **i)** one calculates the self consistent  $GW$  Green's function, as obtained in Eq. (4.12) and **ii)** recalculates  $\Sigma$  as:

$$\Sigma^{GW} = \frac{1 - \sqrt{1 + 4uy_0^2}}{2y_0}. \quad (4.29)$$

iii) Performing the derivative  $\frac{d\Sigma^{GW}}{dy_0}$  yields:

$$\begin{aligned}\frac{d\Sigma^{GW}}{dy_0} &= \frac{1}{2y_0^2} \left[ \sqrt{1+4uy_0^2} - 1 - \frac{8uy_0^2}{2\sqrt{1+4uy_0^2}} \right] \\ &= -\frac{1}{2} + \frac{1}{2\sqrt{1+4uy_0^2}}\end{aligned}\quad (4.30)$$

and the first order vertex correction reads:

$$\bar{\Gamma}_u^{(1)}(y_0) = \frac{1}{2} + \frac{1}{2\sqrt{1+4uy_0^2}}. \quad (4.31)$$

The above result is inserted in the self-consistent  $\Sigma^{GW}$ , giving:

$$\bar{\Sigma}_u^{(2)}(y_0) = \frac{1}{2y_0} \left[ 1 + \sqrt{1+2uy_0^2 - \frac{2uy_0^2}{\sqrt{1+4uy_0^2}}} \right]. \quad (4.32)$$

and finally, inserting  $\bar{\Sigma}_u^{(2)}$  into the Dyson equation and solving for  $y_u$  yields

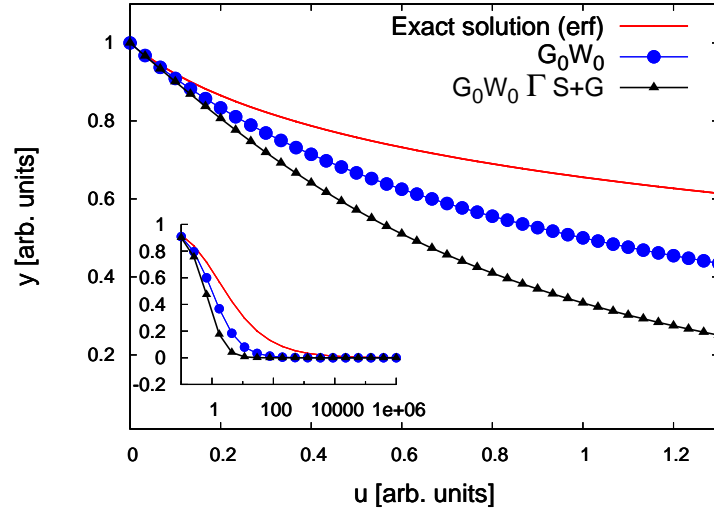
$$y_u = \frac{2y_0}{1 + \sqrt{1+2uy_0^2 + \frac{2uy_0^2}{\sqrt{1+4uy_0^2}}}} \quad (4.33)$$

In Fig. 4.3b we benchmark the performances of  $\bar{\Gamma}_u^{(1)}$  when employed within a self-consistent scheme, against Hedin's  $\Gamma$  and the exact DE's solution. On a small  $u$  range it is slightly poorer than the traditional (first order)  $\Gamma$ , whereas on a larger  $u$  scale (see inset) it improves on it.

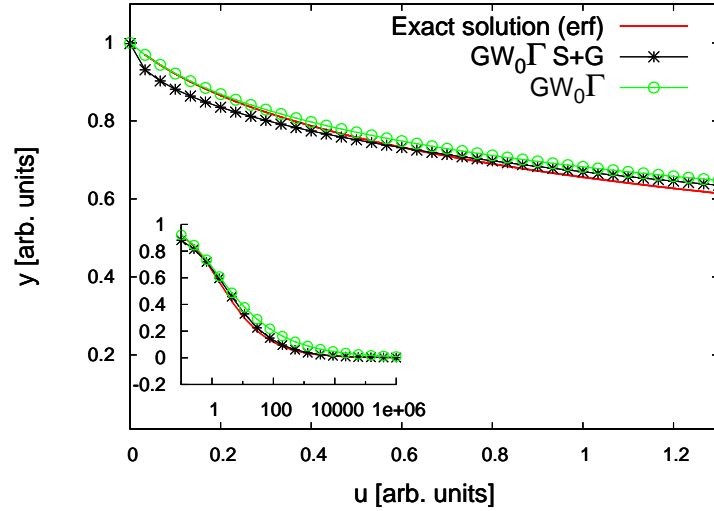
There is quite a bit of discrepancy between the performance of  $\bar{\Gamma}$  when used in a non self-consistent scheme rather than in a self-consistent one and in our model the latter is better than the former. Schindlmayr and Godby, on the other side, employed the non self-consistent scheme obtaining satisfactory results on a Hubbard cluster for the calculation of  $W$ .

Why do we seem to disagree from their conclusions? Firstly we haven't used the correction as it was originally meant to be: in fact, in Eq. (4.26) we had to neglect the quantity  $\frac{du}{dy_0}$  since our screened interaction has been kept fixed. This is one of the cases where it would be interesting to recalculate both  $y_H^0$  and  $u$  in a self-consistent way<sup>b</sup> although we are comparing to the "exact" solution when  $u$  and  $y_H^0$  are also fixed. Secondly, conclusions concerning the effect of vertex corrections on  $G$  (in our case) and on  $W$  (in [96]) might be different. In any case the generalization of the self-consistent Schindlmayr-Godby  $\bar{\Gamma}$  would definitely be interesting. It is, of course, highly non trivial because there is no way, in the full functional framework of obtaining directly the self-consistent Green's function. One could, however, use different Green's functions from the different orders of an iterative self-consistent scheme (see Eqs. 4.6-4.9) and see how the correction performs in each case.

<sup>b</sup>Self-consistent calculations of  $u$  and  $y_H^0$  will be discussed in greater detail at the end of this chapter.



(a)



(b)

**Figure 4.3:** Fig. 4.3a: in the main panel a comparison between the DE's exact solution (red plain line, Eq. (3.19)), a  $G_0W_0\bar{\Gamma}$  (4.23) (black triangles) and a  $G_0W_0$  (blue dots) calculations is shown. Both in the small  $u$  range and in the larger one (see inset)  $\bar{\Gamma}^{(1)}$  is an unsatisfactory approximation to the exact curve. Note that, due to Schindlmayr and Godby's prescription, the vertex has been used in a non-self consistent way. The large  $u$  limit for the alternative  $\bar{\Gamma}_u^{(1)}$  is however the correct one. Fig. 4.3b: we compare here the exact solution (red plain line, Eq. (3.19)) to the  $GW_0\bar{\Gamma}_u^{(1)}$  (black stars) result -calculated within a self-consistent scheme- and Hedin's vertex (green dots). Thanks to the self-consistent scheme the performance of  $\bar{\Gamma}_u^{(1)}$  has considerably improved. On a large  $u$  range it is even slightly better than Hedin's first order  $\Gamma$ . For a very small  $u$  value the traditional vertex is instead slightly more accurate.

### 4.2.2 Continued fraction approximations

One well-known approximation for the error function is its *continued fraction* representation [97]. Within this approximation, the exact expression for  $y_u$  (Eq. (3.19)) can be transformed into

$$y_u = \frac{1}{\sqrt{2u}} \frac{1}{\frac{1}{\sqrt{2uy_0^2}} + \frac{1/2}{\frac{1}{\sqrt{2uy_0^2}} + \frac{1}{\frac{1}{\sqrt{2uy_0^2}} + \frac{3/2}{\frac{1}{\sqrt{2uy_0^2}} + \dots}}}} \quad (4.34)$$

$$= \frac{y_0}{1 + \frac{uy_0^2}{1 + \frac{2uy_0^2}{1 + \frac{3uy_0^2}{1 + \dots}}}}. \quad (4.35)$$

We will now show how it is possible to obtain the expression in Eq. (4.35) starting simply from the initial DE in Eq. (3.15), without any information about its exact solution: this is actually the idea behind *any* of the alternative approximations we will devise in this chapter. Beginning with Eq. (3.15) and taking successively higher order derivatives of the equation one obtains :

$$\frac{dy_u(x)}{dx} = y_0 y_u(x) + y_0 x \frac{dy_u(x)}{dx} - uy_0 \frac{d^2 y_u(x)}{dx^2} \quad (4.36)$$

$$\frac{d^2 y_u(x)}{dx^2} = 2y_0 \frac{dy_u(x)}{dx} + y_0 x \frac{d^2 y_u(x)}{dx^2} - uy_0 \frac{d^3 y_u(x)}{dx^3} \quad (4.37)$$

$$\frac{d^3 y_u(x)}{dx^3} = 3y_0 \frac{d^2 y_u(x)}{dx^2} + y_0 x \frac{d^3 y_u(x)}{dx^3} - uy_0 \frac{d^4 y_u(x)}{dx^4} \quad (4.38)$$

and so on. If we neglect derivatives e.g. from the 4<sup>th</sup> order on and then set  $x = 0$ , this *truncation* allows us to solve all the above equations, beginning with Eq. (4.38) (now an algebraic equation in the unknown  $\frac{d^3 y_u(x)}{dx^3}$  by keeping  $\frac{d^2 y_u(x)}{dx^2}$  as parameter); subsequently we insert the result in (4.37) and solve for  $\frac{d^2 y_u(x)}{dx^2}$ , (4.36) for  $\frac{dy_u(x)}{dx}$  and ultimately Eq. (3.15) obtaining

$$y_u = \frac{y_0}{1 + \frac{uy_0^2}{1 + \frac{2uy_0^2}{1 + 3uy_0^2}}}, \quad (4.39)$$

which is precisely the result yielded from the approximation of the exact solution with a continued fraction formula for the error function ( Eq. (4.35) ). We will name this manipulation *limited order differential equation* (LODE).

In Fig. 4.4 we compare the different orders of this approximation to the exact expres-

sion for  $y_u$ : we can see that it gets rapidly closer to the exact solution by including higher derivatives. Specifically, at the very first order ( $G_0W_0$  level), the two schemes give an

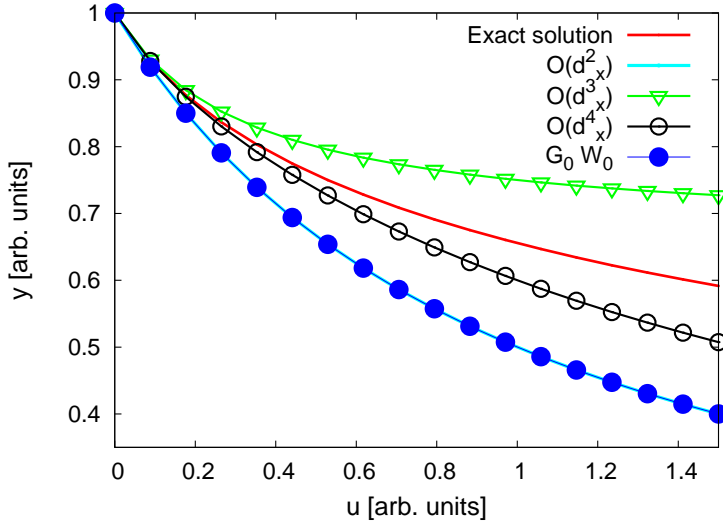


**Figure 4.4:** Comparison between the exact solution (red plain line, Eq. (3.19)) of the DE and the results obtained through the first three orders of the *limited order differential equation* (refer to Eq. (4.39)). The notation  $O(d_x^n)$  indicates that derivatives of order  $\geq n$  have been neglected. As expected the result improves when more terms are included: the curve  $O(d_x^2)$  (light blue line, Eq. (4.36)) is superimposed to the  $G_0W_0$  one (dark blue dots, Eq. (4.6)) and the curve  $O(d_x^4)$  (black circles, Eq. (4.38)) is close to the exact result in a small  $u$  range.

exact solution, whereas the latter only to the self-consistent  $GW_0$  solution.

identical result, while later on, order by order, display a self-energy with an identical structure, which differs only by the coefficients. Also in this continued fraction odd and even orders converge towards the exact result with a different speed. In analogy with the continued fraction of Eq. (4.15) even iterations have the correct large  $u$  limit, while the odd ones don't, although they do eventually tend to it for a very large number of steps. Furthermore we notice that the above continued fraction converges slower than the one arising from the sc- $GW_0$ ; however, the former will eventually converge towards the exact

A direct analytical comparison between the two types of continued fraction (iterative sc-GW and limited order continued fraction) is presented in Tables (4.2.2-4.2.2). Analyzing the  $u \rightarrow \infty$  limit for the limited order continued fraction it is straightforward to observe the different behavior of even and odd orders. One may now wonder at which order of the iteration the

Order	Iterative sc-scheme		$u \rightarrow \infty$
$y_u^{(1)} = y_u^{G_0W_0}$	$y_u = \frac{y_0}{1+uy_0^2}$	$\Sigma_u = -uy_0$	$y_u = 0$
$y_u^{(2)}$	$y_u = y_0 \frac{1+uy_0^2}{1+2uy_0^2}$	$\Sigma_u = -\frac{uy_0}{1+uy_0^2}$	$y_u = \frac{1}{2}$
$y_u^{(3)}$	$y_u = y_0 \frac{1+2uy_0^2}{1+3uy_0^2+u^2y_0^4}$	$\Sigma_u = -\frac{uy_0(1+uy_0^2)}{1+2uy_0^2}$	$y_u = 0$

**Table 4.1:** We report here different the expressions for  $y_u$ , for  $\Sigma_u$  and the Green's function in the large  $u$  limit when an iterative self-consistent scheme (Eqs. 4.6- 4.9) is employed.

limited order DE will outdo the iterative sc-GW scheme. In can be observed in Fig. 4.5a that

Order	Limited order DE		$u \rightarrow \infty$
$O(d_x^1)$	$y_u = \frac{y_0}{1+uy_0^2}$	$\Sigma_u = -uy_0$	$y_u = 0$
$O(d_x^2)$	$y_u = \frac{y_0}{1 + \frac{uy_0^2}{1+2uy_0^2}}$	$\Sigma_u = -\frac{uy_0}{1+2uy_0^2}$	$y_u = \frac{1}{2}$
$O(d_x^3)$	$y_u = \frac{y_0}{1 + \frac{uy_0^2}{1 + \frac{2uy_0^2}{1+3uy_0^2}}}$	$\Sigma_u = -\frac{uy_0(1+3uy_0^2)}{1+5uy_0^2}$	$y_u = 0$

**Table 4.2:** We show again different expressions for  $y_u$ , for  $\Sigma_u$  and the Green's function in the large  $u$  limit when the limited order differential equation (LODE) scheme (Eqs. 4.36- 4.38) is used. These values should be compared with the ones from Tab. 4.2.2.

this happens around the  $O(d_x^5)$  of the novel scheme. The LODE approach is hence definitely worth being analysed further, in particular it would be interesting to explore the possibility of a generalization to the full functional framework. Below we will sketch the generalization of the approach (while all the details can be found in Appendix (D)).

Differentiating Eq. (3.7) with respect to the external potential  $\bar{\varphi}$  one gets

$$\begin{aligned}
\frac{\delta G(1, 2; [\bar{\varphi}])}{\delta \bar{\varphi}(6)} &= \int d3 G_H^0(1, 3) \frac{\delta \bar{\varphi}(3)}{\delta \bar{\varphi}(6)} G(3, 2; [\bar{\varphi}]) \\
&+ \int d3 G_H^0(1, 3) \bar{\varphi}(3) \frac{\delta G(3, 2; [\bar{\varphi}])}{\delta \bar{\varphi}(6)} \\
&+ i \int d3 d5 W(3^+, 5) G_H^0(1, 3) \frac{\delta^2 G(3, 2; [\varphi])}{\delta \bar{\varphi}(6) \delta \bar{\varphi}(5)}. \tag{4.40}
\end{aligned}$$

Truncating the highest order derivative  $\frac{\delta^2 G}{\delta \bar{\varphi}^2}$  and solving for  $\varphi = 0$  (which means also  $\bar{\varphi} = 0$ ) one obtains:

$$\frac{\delta G(1, 2; [\bar{\varphi}])}{\delta \bar{\varphi}(5)} = G_H^0(1, 5) G(5, 2; [\bar{\varphi}]) \tag{4.41}$$

which reinserted in Eq. (3.7) yields:

$$\begin{aligned}
G(1, 2; [\bar{\varphi}]) &= G_H^0(1, 2) + i \int d3 d5 G_H^0(1, 3) W(3^+, 5) \\
&\times G_H^0(3, 5) G(5, 2; [\bar{\varphi}]). \tag{4.42}
\end{aligned}$$

Note that the above expression provides the one-particle GF within the  $G_0W_0$  approximation to the self-energy: we have hence perfectly reproduced a result known from the 1-point framework. However our goal is to go beyond the  $G_0W_0$  accuracy. Differentiating Eq. (4.40) with respect to  $\bar{\varphi}$  and neglecting the third order derivative  $\frac{\delta^3 G}{\delta \bar{\varphi}^3}$  yields

$$\begin{aligned}
G(1, 2) &= G_H^0(1, 2) - i \int d5 389 G_H^0(1, 3) W(3^+, 5) \\
&\times \bar{m}^{-1}(3, 5; 9, 8) G_H^0(9, 8) G(8, 2) \tag{4.43}
\end{aligned}$$

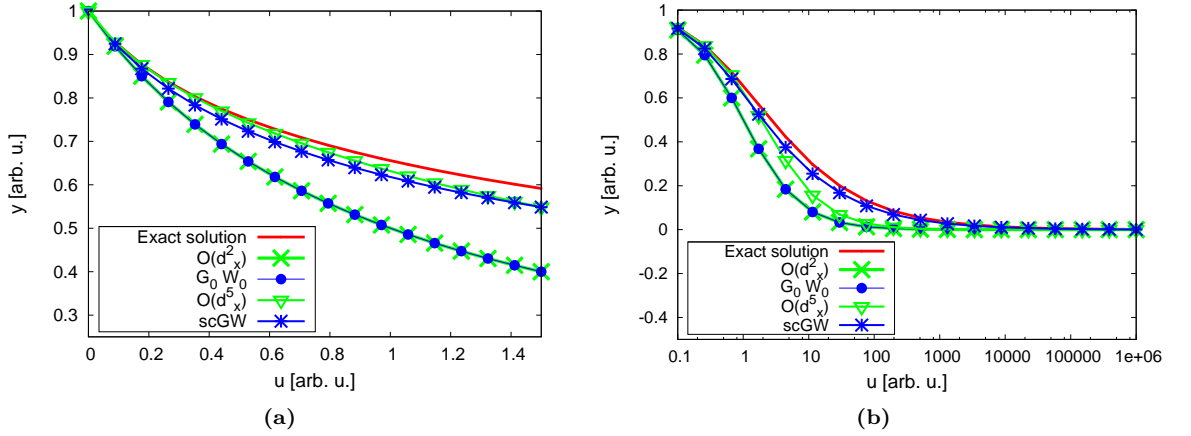


**Figure 4.5:** Fig. 4.5a: comparison between the exact solution (red plain line, Eq. (3.19)) of the DE and some specific orders of the iterative sc-GW scheme and the limited order DE. Both schemes give an identical result at the first order (see the overlap between the green stars  $O(d_x^1)$  of the LODE and the blue dotted line, representing the  $G_H^0 W_0$  result). However it is only at the iteration of order  $O(d_x^5)$  that the novel scheme performs once for all better than the conventional self-energy based one (which can provide, at its best, only the direct sc-GW curve -blue starred curve in the plot-). Fig. 4.5b: the same curves of Fig. 4.5a are depicted here, however we examine a much larger  $u$  range. It is interesting to remark that in this scale the  $O(d_x^5)$  is not constantly performing better than the sc-GW result.

with

$$\begin{aligned} \bar{m}(16; 57) : &= -\delta(15)\delta(76) + i \int d3W(3^+, 5)G_H^0(1, 3)\delta(7, 6) \\ &\times [G_H^0(3, 6) + G_H^0(3, 5)], \end{aligned} \quad (4.44)$$

which is a four-point quantity of a similar complexity as a Bethe-Salpeter kernel. Starting from the above equation one can write a Dyson equation reading:

$$G(1, 2) = G_H^0(1, 2) + \int d3d8G_H^0(1, 3)\Sigma(3, 8)G(8, 2) \quad (4.45)$$

where the self-energy has been defined as:

$$\Sigma(3, 8) = -i \int d5d9W(3^+, 5)m^{-1}(3, 5; 8, 9)G_H^0(9, 8). \quad (4.46)$$

The above self-energy resembles the  $GW$  one, with the difference of being a modified three point interaction, i.e.  $\int d5W(3^+, 5)m^{-1}(3, 5; 8, 9) := \mathcal{O}(3; 9, 8)$ .

The complexity of the above result could have been expected: complicated manipulations do not guarantee anymore to smoothly and exactly move from solving  $O(d_x^n)$  (with  $n \geq 4$ ) equations to  $O(d_x^1)$  equations. On the other hand, the LODE approach does not require at any step an iterative procedure: this might turn out to be a significant advantage, compared, e.g. to adding vertex corrections to  $\Sigma$ . All considered the LODE approach is worth being explored further. Since

its main caveat, when going to higher orders, is the appearance of larger matrices, one could, for example, use some local approximation or decoupling in order to keep all the quantities involved in the equations below the 4-points.

### 4.2.3 Large electron-electron interaction expansions

Perturbation theory usually deals with weak interactions, hence the small  $u$  limit. It is however very interesting to examine the *large*  $u$  limit for several reasons. First of all it is the regime of *strong correlation*, where the current approximations exhibit failures. Secondly, the large  $u$  expansion for the exact solution gives a convergent series (being a product of two convergent Taylor expansions, one for the exponential and the other one for the error function) and one could think of obtaining a better approximation to the exact solution by adding higher order terms, contrary to what has been observed for the small  $u$  (asymptotic) expansion of the solution. Last but not least, excellent approximations for the exact solution are *Padé approximants* [98], which have to be constructed using *both* the small and large  $u$  limit. In this subsection we will present two possible routes to approach this limit: the first is a straightforward large  $u$  expansion of the exact solution for  $y_u$ , while the second combines the latter with the large  $u$  expansion for the Dyson equation.

#### Straightforward expansion for the solution

By expanding both the exponential prefactor and the error function appearing in Eq. (3.19):

$$e^{\frac{1}{2uy_0^2}} \approx 1 + \frac{1}{2uy_0^2} + \frac{1}{8u^2y_0^4} + \dots, \quad (4.47)$$

$$\text{erf}\left[\sqrt{\frac{1}{2uy_0^2}}\right] \approx \frac{2}{\sqrt{\pi}} \left[ \sqrt{\frac{1}{2uy_0^2}} - \frac{1}{6uy_0^2} \sqrt{\frac{1}{2uy_0^2}} + \frac{1}{40u^2y_0^5} \sqrt{\frac{1}{2uy_0^2}} + \dots \right], \quad (4.48)$$

one obtains for the different orders of the full solution

$$y_u^{(1/2)} = \sqrt{\frac{\pi}{2u}} \quad (4.49)$$

$$y_u^{(1)} = -\frac{1}{uy_0} + \sqrt{\frac{\pi}{2u}} \quad (4.50)$$

$$y_u^{(3/2)} = -\frac{1}{uy_0} + \frac{1}{2uy_0^2} \sqrt{\frac{\pi}{2u}} + \sqrt{\frac{\pi}{2u}} \quad (4.51)$$

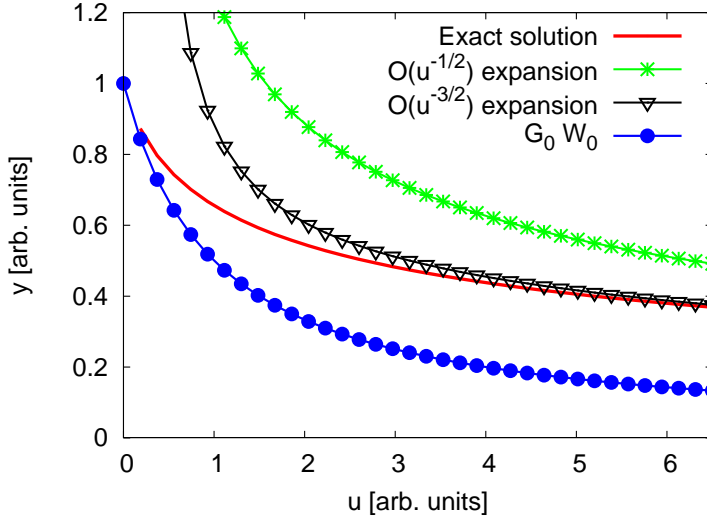
$$y_u^{(2)} = -\frac{1}{uy_0} + \frac{1}{2uy_0^2} \sqrt{\frac{\pi}{2u}} - \frac{1}{6u^2y_0^3} + \sqrt{\frac{\pi}{2u}} \quad (4.52)$$

$$y_u^{(5/2)} = -\frac{1}{uy_0} + \frac{1}{2uy_0^2} \sqrt{\frac{\pi}{2u}} - \frac{1}{6u^2y_0^3} + \frac{1}{8u^2y_0^4} \sqrt{\frac{\pi}{2u}} + \sqrt{\frac{\pi}{2u}} \quad (4.53)$$

$$y_u^{(3)} = -\frac{1}{uy_0} + \frac{1}{2uy_0^2} \sqrt{\frac{\pi}{2u}} - \frac{1}{6u^2y_0^3} + \frac{1}{8u^2y_0^4} \sqrt{\frac{\pi}{2u}} + \frac{1}{10u^3y_0^5} + \sqrt{\frac{\pi}{2u}}. \quad (4.54)$$

Fig. 4.6 shows how these different expansions perform *versus* the exact result. Overall their behaviour is very good for large  $u$  and few orders are sufficient to get a good approximation over a

wide  $u$  range (which is our ultimate goal), although for  $u = 0$  all these approximations are divergent.



This means that one could solve the set of differential equations in the large  $u$  limit and get a good approximation to the exact solution over a wide range of  $u$ . However, this approximate solution would diverge for small  $u$ .

**Figure 4.6:** Comparison between the exact solution (red plain line, Eq. (3.19)) and the large  $u$  expansion for the DE. The green dots and stars are respectively  $O(u^{3/2})$  and  $O(u)$  of the large  $u$  expansion (Eqs. (4.50-4.51)). We also report the  $G_0 W_0$  results (blue dots, Eq. (4.6)) as an example of a small  $u$  expansion. Over a wide  $u$  range the large  $u$  expansions are very satisfactory.

### Expansion combined with the Dyson equation

When  $u$  gets larger, also  $\Sigma_u$  increases. This implies that, using the Dyson equation for the one-particle Green's function  $y_u = (y_0^{-1} - \Sigma_u)^{-1}$  one could expand  $y_u$  as

$$y_u \approx -\Sigma_u^{-1} \left[ 1 + y_0^{-1} \Sigma_u^{-1} + y_0^{-1} \Sigma_u^{-1} y_0^{-1} \Sigma_u^{-1} \right]. \quad (4.55)$$

Hence to lowest order  $y_u \approx -\Sigma_u^{-1}$  or

$$\Sigma_u \approx -1/y_u. \quad (4.56)$$

This simple relation allows us to use the large  $u$  expansion of the exact solution for  $y_u$  to approximate  $\Sigma_u$  for large  $u$ ; we can then use this approximate  $\Sigma_u$  in the Dyson equation to recalculate  $y_u$ . For example, using the lowest order of the large  $u$  expansion of the exact  $y_u$  one gets the following self-energy:

$$\Sigma_u \approx - \left( \sqrt{\frac{\pi}{2u}} \right)^{-1}, \quad (4.57)$$

which, inserted in the Dyson equation  $y_u = (y_0^{-1} - \Sigma_u)^{-1}$  gives:

$$y_u \approx \frac{y_0}{1 + y_0 \sqrt{\frac{2u}{\pi}}} \quad (4.58)$$

In Fig. 4.7 the performance of this approximation for  $y_u$  is shown against two orders of the straightforward large  $u$  expansion for the Green's function, the exact solution and  $G_0W_0$ . The "large  $\Sigma$ " approach is *exact* for  $u = 0$ , mending the divergence of all the orders of straight-

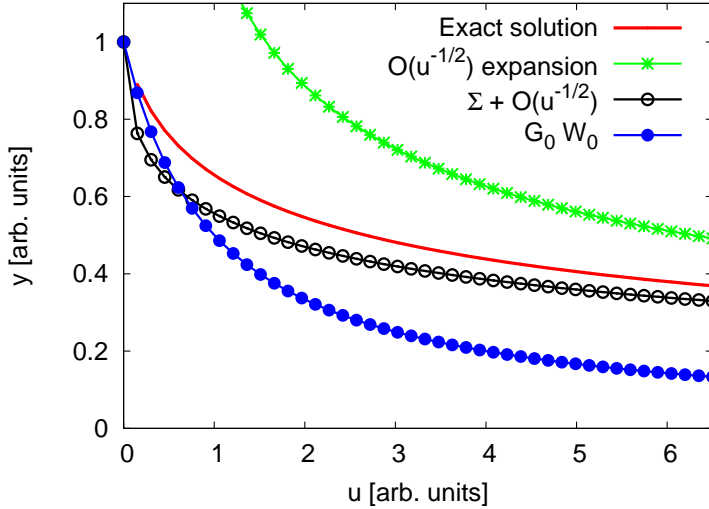


**Figure 4.7:** Comparison between the exact solution (plain red line, Eq. (3.19)), order  $O(u)$  of the large  $u$  expansion for the DE (green line, Eq. (4.50)), and the order  $O(u^{1/2})$  of the DE's large  $u$  expansion combined with the large  $\Sigma$  expansion (black dots, Eq. (4.58)); we also report the  $G_0W_0$  results as a prototype of a widely used approximation. We observe that the large  $u$  expansion of the DE combined with the large  $\Sigma$  expansion is performing extremely well over the range of  $u$  examined, being even exact both in the large and small  $u$  limits.

forward expansion for  $y_u$  in that limit. We obtained here an approximation with the desirable property of being exact in the small and large  $u$  limits, and, moreover, it shows an overall good agreement (generally better than  $G_0W_0$ , and similar to the 1st order of the straightforward large  $u$  expansion) with the exact solution. At higher orders undesired poles appear and the approach does not systematically improve on the straightforward large  $u$  expansion or the  $G_0W_0$  approach. Moreover, we have used the  $C(u, y_0) = -1$  result to solve the initial value problem, but in general, in the framework of a large  $u$  expansion, without knowing the exact solution, one would not know how to do that. Pros and cons of the methodology should definitely be explored further.

### 4.3 Self-consistent calculations of the Hartree Green's function

We elaborate here on two choices that we have made in our analysis of existing approaches, namely treating the Hartree Green's function and the screened interaction as externally given quantities. This is justified by the fact that realistic calculations are most often following such a pragmatic ansatz. In principle these quantities should be part of Hedin's self-consistent cycle. A fully self-consistent treatment, in the full functional framework, is today out of reach. In the 1-point model, however, it is possible to go beyond this limitation and indeed, the implicit solution of Hedin's equation that has been achieved in the work of [87] contains all quantities calculated on the same footing. Also in the linearized version, that is employed in the present work, one can obtain the Hartree Green's function and the screened potential consistently from

the equations, as we will discuss in the following.

Let us first turn to the Hartree Green's function  $y_H^0$ . In terms of the truly non-interacting Green's function  $y_0$  it reads

$$y_H^0 = \frac{y_0}{1 - y_0 u y_u}, \quad (4.59)$$

in other words, it depends (through the density) on the solution  $y_u$  at vanishing external potential. In a self-consistent scheme this  $y_H^0$  should then replace  $y_0$  in the solution Eq. (3.19), which leads to an implicit equation for  $y_u$ . For a self-consistent treatment of the screened interaction we can use the fact that the 1-point differential equation can be solved for  $\frac{dy_u}{dx}$ , and insert the result into the expression for the screened interaction  $u$  in terms of the bare  $v$ , which reads  $u = v + v \frac{dy_u}{dx} v$ . Two routes can be taken. The first one is based on the linearized equation (3.15) where the interaction is already screened from the very beginning. This leads to a quadratic equation for  $u$ , with two solutions

$$u = \frac{v}{2} \pm \sqrt{\frac{v^2}{4} + v^2 \left\{ 1 - \frac{y_u}{y_0} + v y_u^2 \right\}}. \quad (4.60)$$

The physical solution is the one of the positive square root, since it approaches the bare  $v$  in the limit of vanishing interaction, hence vanishing screening. The second route consists in calculating  $\frac{dy_u}{dx}$  from the initial equation (3.14), where the bare  $y_0$  and the interaction  $v$  appear. This yields

$$u = v \left( 2 - \frac{y_u}{y_0} + v y_u^2 \right). \quad (4.61)$$

In both cases, the solution for  $u$  should be used in Eq. (3.19), which again makes the expression for the GF implicit. One may argue about which of the two ways to calculate  $u$  self-consistently is more adequate.

In a realistic calculation one would probably use the former approach, in an iterative way: after calculating the GF as a functional of the external potential for a given initial interaction in the linearized DE, one would recalculate the  $W$  from the functional derivative, and so on. Whatever choice, however, does not influence the main conclusions that can be drawn from the above considerations. Specifically: **i)** a self-consistent calculation leads to an implicit solution (like in the work of [87]) which however would not be identical to theirs because of our linearization procedure; **ii)** the behaviour for the small interaction limit is unchanged by the self-consistent treatment, as one can verify from equations (4.59), (4.60) and (4.61); this means in particular that the constant  $C$  is chosen in the same way as before. **iii)** Finally also the discussion about the limit of large interaction is unchanged: by making the ansatz that to lowest order  $y_u \propto \frac{1}{\sqrt{u}}$  one finds consistency.

Altogether, this shows that the linearization of the equations does not imply necessarily that one has to treat the Hartree Green's function and the screened interaction as externally given quantities. It also shows that a more refined, self-consistent treatment does not change the overall behaviour of the solution.

In this Chapter we have presented a number of insights both on established and alternative many-body approximations for the calculation of the one-particle Green's function in a model framework, so called 1-point. In the next two Chapters we will release some of the approximations so as to move to more complicated frameworks, namely a N-times one and the full functional one, where we will attempt to generalize our approach.

# CHAPTER 5

## Beyond the 1-point model

*In this chapter we will go beyond the 1-point model results. As already discussed in the first part of the work, the main limitation of our model is the 1-point approximation for the time variable, which causes the loss of all information about the pole structure of the one-body Green's functions. In a first instance we will restore the time dependence (and consequently the frequency dependence) in the differential equation. The decoupling approximation for the space variables will however be kept. The resulting DE will be solved by resumming exactly its iterative solution. The Green's function thus obtained will have an exponential form which we will show to be analogous to the well known cumulant expansion form for  $G$ , presented extensively in Sec. (2.4.3). We will review in detail the improvements of such method over the  $G_0W_0$  approximation to  $\Sigma$ , in particular in relation to photoemission spectral functions calculations. We will briefly conclude reporting the main results obtained in the work by Guzzo [83], employing this approximation - to our knowledge rigorously derived here for the first time from fundamental equations- to valence electron spectroscopy in Silicon.*

### 5.1 Restoring the time dependence of the Green's function

In Sec. (3.2.1) we have introduced the 1-point model, discussing the approximations made on Eq. (3.7) in order to obtain it, namely **i**) projecting the equation onto a single-particle basis which is then assumed *diagonal* for all quantities, **ii**) retaining 1-point only for all the time variables. In this Chapter we will release one the second of the two approximations and propose and hint on how the first could also be partially released.

The *decoupling* approximation for the space variables may look a bit rough, because it is not possible, in general, to write both the full Green's function *and* the non-interacting one on a basis which both diagonalizes them. However if  $G$  and  $G_H^0$  are fairly similar, the above assumption can

be reasonably accurate for this purpose. In particular, since one can always choose which effective non-interacting Green's function to use, a good strategy could be to calculate the one that is closer to the full  $G$  (hence maximizing their overlap): we will see a practical implementation of this in the last section of the chapter.

The second approximation, that is retaining only 1-point for the time variables, which results in the absence of a pole structure for the 1-point Green's function, is the more dramatic limitation in our approach. In this chapter we will *fully restore* the time-dependence (and hence the frequency dependence), of the DE and of its solution.

Let's recall the expression for the time-dependent linearized DE, written on the same diagonal basis for  $G$  and  $G_H^0$ :

$$G_m(t_1, t_2; [\bar{\varphi}]) = G_{H_m}^0(t_1, t_2) + \int dt_3 G_{H_m}^0(t_1, t_3) \bar{\varphi}_m(t_3) G_m(t_3, t_2; [\bar{\varphi}]) + i \int dt_3 dt_4 G_{H_m}^0(t_1, t_3) W_{mm}(t_3^+, t_4) \frac{\delta G_m(t_3, t_2; [\bar{\varphi}])}{\delta \bar{\varphi}_m(t_4)}. \quad (5.1)$$

*What kind of Green's function solving Eq. (5.1) may yield?*

In this Chapter we will address precisely this question: our goal is, among the other things, to get greater insight on the capabilities of the linearization approximation. In the 1-point model we could not get many indications about that, while here we feel that a solution of Eq. (5.1) might address a number of questions about the "best" Green's function obtainable through the linearization procedure (we already know the "worst", non divergent, one to be the  $G_0 W_0$  Green's function, obtained by assuming  $\Sigma$  independent of  $\bar{\varphi}$ ).

### 5.1.1 Iterative solution for the N-times DE

Eq. (5.1) is still quite complicated to be solved analytically and ideally one would like to reduce the number of terms to be treated. By employing an auxiliary Dyson equation reading (for more details refer to App. (A.5)):<sup>a</sup>

$$G_{\bar{\varphi}}(t_1, t_2) = G_H^0(t_1, t_2) + \int dt_3 G_H^0(t_1, t_3) \bar{\varphi}(t_3) G_{\bar{\varphi}}(t_3, t_2) \quad (5.2)$$

one can recast Eq. (5.1) as:

$$G(t_1, t_2; [\bar{\varphi}]) = G_{\bar{\varphi}}(t_1, t_2) + i \int dt_3 dt_4 G_{\bar{\varphi}}(t_1, t_3) W(t_3^+, t_4) \frac{\delta G(t_3, t_2; [\bar{\varphi}])}{\delta \bar{\varphi}(t_4)}. \quad (5.3)$$

Hence we will first solve Eq. (5.2) and only afterwards tackle Eq. (5.3).

Note that the decoupling approximation is equivalent to a *one level* approximation: one deals only with a *single occupied (or unoccupied) level* at a time which cannot couple to any other level. Such an assumption has been, for instance, a very common one in core-electron spectroscopy. Hence all the Green's function appearing from now on will be defined either through their hole part or the electron part only. In particular we choose them to be defined by the *hole* part (since we are also interested in photoemission spectroscopy we will use strategies employed in

---

<sup>a</sup>We have dropped all the state indices  $m$ , being simply dumb indices

earlier works). Hence, considering only the hole  $GF$  the Hartree zero-potential Green's function becomes:

$$G_H^0(t_1, t_2) = i\theta(t_2 - t_1)e^{-i\epsilon(t_1 - t_2)} \quad (5.4)$$

and also  $G_{\bar{\varphi}}(t_1, t_2)$  has the same time structure:

$$G_{\bar{\varphi}}(t_1, t_2) = i\theta(t_2 - t_1)y_{\bar{\varphi}}(t_1, t_2) \quad (5.5)$$

and of course the same will apply to the full  $G$ . Inserting both (5.4) and (5.5) into (5.2) one obtains:

$$\begin{aligned} i\theta(t_2 - t_1)y_{\bar{\varphi}}(t_1, t_2) &= i\theta(t_2 - t_1)e^{-i\epsilon(t_1 - t_2)} \\ &+ i^2 \int dt_3 \theta(t_3 - t_1)e^{-i\epsilon(t_1 - t_3)} \bar{\varphi}(t_3) \theta(t_2 - t_3) y_{\bar{\varphi}}(t_3, t_2) \end{aligned} \quad (5.6)$$

dividing on both sides by  $e^{i\epsilon(t_1 - t_2)}$ :

$$\begin{aligned} i\theta(t_2 - t_1)y_{\bar{\varphi}}(t_1, t_2)e^{i\epsilon(t_1 - t_2)} &= i\theta(t_2 - t_1) + i^2 \int dt_3 \theta(t_3 - t_1)e^{-i\epsilon(t_2 - t_3)} \\ &\times \bar{\varphi}(t_3) \theta(t_2 - t_3) y_{\bar{\varphi}}(t_3, t_2). \end{aligned} \quad (5.7)$$

Considering only the time interval  $t_2 > t_1$  and including the  $\theta(t_3 - t_2)$  and  $\theta(t_3 - t_1)$  (both compatible with the initial assumption on  $t_1 > t_2$ ) in the extreme of integration on the right hand side we get:

$$\tilde{y}_{\bar{\varphi}}(t_1, t_2) = 1 + i \int_{t_1}^{t_2} dt_3 \bar{\varphi}(t_3) \tilde{y}_{\bar{\varphi}}(t_3, t_2) \quad (5.8)$$

where we have defined:

$$y_{\bar{\varphi}}(t_1, t_2)e^{i\epsilon(t_1 - t_2)} := \tilde{y}_{\bar{\varphi}}(t_1, t_2) \quad (5.9a)$$

$$y_{\bar{\varphi}}(t_3, t_2)e^{i\epsilon(t_3 - t_2)} := \tilde{y}_{\bar{\varphi}}(t_3, t_2) \quad (5.9b)$$

Eq. (5.8) can be transformed from an integral equation to a differential equation and solved exactly (see App. (F) ). One can verify that the solution of Eq. (5.8) reads:

$$\tilde{y}_{\bar{\varphi}}(t_1, t_2) = e^{i \int_{t_1}^{t_2} dt \bar{\varphi}(t)} \quad (5.10)$$

and  $G_{\bar{\varphi}}$ :

$$\begin{aligned} G_{\bar{\varphi}}(t_1, t_2) &= i\theta(t_2 - t_1)y_{\bar{\varphi}}(t_1, t_2) = i\theta(t_2 - t_1)e^{-i\epsilon(t_1 - t_2)} \tilde{y}_{\bar{\varphi}}(t_1, t_2) \\ &= i\theta(t_2 - t_1)e^{-i\epsilon(t_1 - t_2) + i \int_{t_1}^{t_2} dt \bar{\varphi}(t)}. \end{aligned} \quad (5.11)$$

The Green's function thus obtained displays, through its second exponential term, the effects of the external potential  $\bar{\varphi}$  on the propagation integrated over time.

We can now move on to solving Eq. (5.1) thanks to our latest findings. We define

$$G(t_1, t_2; [\bar{\varphi}]) = i\theta(t_2 - t_1)y(t_1, t_2; [\bar{\varphi}]) \quad (5.12)$$

which inserted into (5.1) together with (5.9a) leads to:

$$\begin{aligned} i\theta(t_2 - t_1)y(t_1, t_2; [\bar{\varphi}]) &= i\theta(t_2 - t_1)y_{\bar{\varphi}}(t_1, t_2) + i^3 \int dt_3 t_4 \theta(t_3 - t_1)y_{\bar{\varphi}}(t_1, t_3) \\ &\times W(t_3^+, t_4) \frac{\delta}{\delta\bar{\varphi}(t_4)} \left[ \theta(t_2 - t_3)y(t_3, t_2; [\bar{\varphi}]) \right] \end{aligned} \quad (5.13)$$

considering once again  $t_2 > t_1$  and multiplying both sides by  $e^{i\epsilon(t_1-t_3)}$  yields:

$$\tilde{y}(t_1, t_2; [\bar{\varphi}]) = \tilde{y}_{\bar{\varphi}}(t_1, t_2) + i^3 \int_{t_1}^{t_2} dt_3 \int dt_4 \tilde{y}_{\bar{\varphi}}(t_1, t_3) W(t_3^+, t_4) \frac{\delta \tilde{y}(t_3, t_2; [\bar{\varphi}])}{\delta\bar{\varphi}(t_4)}. \quad (5.14)$$

The above equation will be now solved through an *iterative procedure*. This choice is dictated by our finding in the 1-point framework, where a direct DE solution required also the solution of an initial value problem in order to select the physical Green's function, while the iterative scheme was providing the *GF* in a more straightforward way, and without the need of solving any i.v.p. for the equation. Starting with the zeroth-order guess  $\tilde{y}^{(0)}(t_1, t_2; [\bar{\varphi}]) = \tilde{y}_{\bar{\varphi}}(t_1, t_2)$ , the following order reads:

$$\begin{aligned} \tilde{y}^{(1)}(t_1, t_2; [\bar{\varphi}]) &= \tilde{y}_{\bar{\varphi}}(t_1, t_2) + i^2 \int dt_4 \int_{t_1}^{t_2} dt_3 \tilde{y}_{\bar{\varphi}}(t_1, t_3) W(t_3^+, t_4) \\ &\times \frac{\delta \tilde{y}_{\bar{\varphi}}(t_3, t_2)}{\delta\bar{\varphi}(t_4)} \end{aligned} \quad (5.15)$$

and using two properties of  $\tilde{y}_{\bar{\varphi}}$ :

$$\frac{\delta \tilde{y}_{\bar{\varphi}}(t_3, t_2)}{\delta\bar{\varphi}(t_4)} = \frac{\delta}{\delta\bar{\varphi}(t_4)} \left[ e^{i \int_{t_3}^{t_2} dt \bar{\varphi}(t)} \right] = i\theta(t_4 - t_3)\theta(t_2 - t_4)\tilde{y}_{\bar{\varphi}}(t_3, t_2) \quad (5.16a)$$

$$\tilde{y}_{\bar{\varphi}}(t_3, t_2)\tilde{y}_{\bar{\varphi}}(t_2, t_4) = e^{i \int_{t_2}^{t_3} dt \bar{\varphi}(t) + i \int_{t_4}^{t_2} dt \bar{\varphi}(t)} = e^{i \int_{t_4}^{t_3} dt \bar{\varphi}(t)} = \tilde{y}_{\bar{\varphi}}(t_3, t_4) \quad (5.16b)$$

one finally obtains:

$$\begin{aligned} \tilde{y}^{(1)}(t_1, t_2; [\bar{\varphi}]) &= \tilde{y}_{\bar{\varphi}}(t_1, t_2) + i^3 y_{\bar{\varphi}}(t_1, t_2) \int_{t_1}^{t_2} dt_3 \int_{t_3}^{t_2} dt_4 W(t_3^+, t_4) \\ &= \tilde{y}_{\bar{\varphi}}(t_1, t_2) \left\{ 1 + i^3 \int_{t_1}^{t_2} dt_3 \int_{t_3}^{t_2} dt_4 W(t_3^+, t_4) \right\}. \end{aligned} \quad (5.17)$$

As in the zeroth order iteration, also for this first order one, it turns out that  $y(t_1, t_2; [\bar{\varphi}]) \propto y_{\bar{\varphi}}(t_1, t_2)$ . One can then assume (eventually it can be demonstrated) this to be true for *all* orders of the iterative procedure.

We can hence make an *ansatz* for the full form of  $y(t_1, t_2; [\bar{\varphi}])$  reading:

$$\tilde{y}(t_1, t_2; [\bar{\varphi}]) = \tilde{y}_{\bar{\varphi}}(t_1, t_2) \cdot F_W(t_1, t_2) \quad (5.18)$$

where  $F_W(t_1, t_2)$  is the unknown functional we want to find and the pedix  $W$  just reminds us it has to depend on the screened interaction (see also Eq. (5.15)) and independent of  $\bar{\varphi}$  (this last assumption is then validated *a-posteriori*).

Inserting such ansatz into Eq. (5.14) one obtains an integral equation for  $F_W(t_1, t_2)$ :

$$F_W(t_1, t_2) = 1 + i^3 \int_{t_3}^{t_2} dt_4 \int_{t_1}^{t_2} dt_3 F_W(t_3, t_2) W(t_3^+, t_4). \quad (5.19)$$

If we define  $\int_{t_3}^{t_2} dt_4 W(t_{3+}, t_4) := f(t_{3+}, t_2)$ , Eq. (5.19) becomes:

$$F_W(t_1, t_2) = 1 - i \int_{t_1}^{t_2} dt_3 f(t_{3+}, t_2) \cdot F_W(t_3, t_2). \quad (5.20)$$

This equation has the same structure of (5.11) hence the solution reads

$$F_W(t_1, t_2) = e^{-i \int_{t_1}^{t_2} dt f(t, t_2)} = e^{-i \int_{t_1}^{t_2} dt \int_t^{t_2} dt_4 W(t, t_4)} \quad (5.21)$$

it follows that:

$$\tilde{y}(t_1, t_2; [\bar{\varphi}]) = e^{i \int_{t_1}^{t_2} dt \bar{\varphi}(t) - i \int_{t_1}^{t_2} dt \int_t^{t_2} dt_4 W(t, t_4)} \quad (5.22)$$

and finally:

$$G(t_1, t_2; [\bar{\varphi}]) = i\theta(t_2 - t_1) e^{-i\epsilon(t_1 - t_2) + i \int_{t_1}^{t_2} dt \bar{\varphi}(t) - i \int_{t_1}^{t_2} dt \int_t^{t_2} dt_4 W(t, t_4)} \quad (5.23)$$

$$= G_H^0(t_1, t_2) e^{i \int_{t_1}^{t_2} dt \bar{\varphi}(t) - i \int_{t_1}^{t_2} dt \int_t^{t_2} dt_4 W(t, t_4)} \quad (5.24)$$

and its equilibrium version -for zero external potential- reads:

$$G(t_1, t_2) | \bar{\varphi} = 0 = G_H^0(t_1, t_2) e^{-i \int_{t_1}^{t_2} dt \int_t^{t_2} dt_4 W(t, t_4)} \quad (5.25)$$

Note that the above Green's function is the *exact analytical solution* for Eq. (5.1).

What is the physical content of the such expression?

Eq. (5.23) contains a first term  $i\theta(t_2 - t_1) e^{-i\epsilon(t_1 - t_2)}$  describing the free propagation of a particle, a second one  $e^{+i \int_{t_1}^{t_2} dt \bar{\varphi}(t)}$  which accounts for the "story" of the perturbation and the way the system responds to it is contained in the third term  $e^{-i \int_{t_1}^{t_2} dt \int_t^{t_2} dt_4 W(t, t_4)}$ .

Is Eq. (5.38) a completely new result? The answer is no. While the derivation *is*, the expression of the Green's function thus obtained can be shown to be equivalent to the one obtained in [81] and [67] for the photoemission core  $G_c$ . In the next section we will show how the exponential in  $W$  in Eq. (5.38) can be approximated within a simple model and then expanded, yielding the same results for the core Green's function obtained in earlier works [81, 99] (where such expression for  $G$  would take the name of cumulant expansion).

### 5.1.2 Connection with the cumulant expansion formula for the Green's function

We now examine in depth the  $W$  contained in (5.38): so far no assumption has been made on its structure, in principle it can even be an "exact  $W$ " obtained as an external ingredient for the calculation of  $G$  (see the discussion in Sec. (3.1).

However, we prefer to begin with a much simpler (and well-known) structure, that is anyway plausible when the electronic loss function of a material clearly exhibits only a single peak: the *plasmon pole model*.  $W$  can hence be recast as [100]:

$$W(t_1, t_2) = -iW \left\{ \theta(t_1 - t_2) e^{-i\omega_p(t_1 - t_2)} + \theta(t_2 - t_1) e^{i\omega_p(t_1 - t_2)} \right\} \quad (5.26)$$

where  $\omega_p$  is the plasmon frequency for a given material and  $W$  the amplitude. The function  $f$  becomes:

$$\begin{aligned} f(t_{3+}, t_2) &= \int_{t_3}^{t_2} dt_4 W(t_{3+}, t_4) = -iW \int_{t_3}^{t_2} dt_4 \theta(t_3 - t_4) e^{-i\omega_p(t_3 - t_4)} \\ &\quad - iW \int_{t_3}^{t_2} dt_4 \theta(t_4 - t_3) e^{i\omega_p(t_3 - t_4)} \end{aligned} \quad (5.27)$$

$$= -iW \int_{t_2}^{t_3} dt_4 \left\{ \theta(t_4 - t_3) e^{i\omega_p(t_3 - t_4)} \right\} \quad (5.28)$$

$$= -iW \left\{ -\frac{1}{i\omega_p} e^{i\omega_p(t_3 - t_4)} \right\}_{t_3}^{t_2} \quad (5.29)$$

$$= \frac{W}{\omega_p} \left\{ e^{i\omega_p(t_3 - t_2)} - 1 \right\}. \quad (5.30)$$

Now one can calculate  $F_W$  as:

$$F_w(t_1, t_2) = e^{-i \int_{t_1}^{t_2} dt f(t, t_2)} = \exp \left[ -i \int_{t_1}^{t_2} dt \frac{W}{\omega_p} \left\{ e^{i\omega_p(t_1 - t_2)} - 1 \right\} \right] \quad (5.31)$$

$$= \exp \left[ -i \frac{W}{i\omega_p} \left[ \left[ \frac{1}{\omega_p} e^{-i\omega_p(t_2 - t)} \right]_{t_1}^{t_2} - (t_2 - t_1) \right] \right] \quad (5.32)$$

$$= \exp \left[ -\frac{W}{\omega_p^2} \left[ 1 - e^{-i\omega_p(t_2 - t_1)} \right] + i \frac{W}{\omega_p} (t_2 - t_1) \right] \quad (5.33)$$

and finally the full interacting  $G$  becomes:

$$G(t_1, t_2; [\varphi]) = i\theta(t_2 - t_1) e^{-i\epsilon(t_1 - t_2) + i \int_{t_1}^{t_2} dt \bar{\varphi}(t) - \frac{W}{\omega_p^2} [1 - e^{-i\omega_p(t_2 - t)}] + i \frac{W}{\omega_p} (t_2 - t_1)} \quad (5.34)$$

from which the equilibrium  $G|_{\bar{\varphi}=0}$  is readily obtained:

$$G(t_1, t_2)|_{\bar{\varphi}=0} = i\theta(t_2 - t_1) e^{-i\epsilon(t_1 - t_2) - i \int_{t_1}^{t_2} dt \frac{W}{\omega_p^2} [1 - e^{-i\omega_p(t_2 - t)}] + i \frac{W}{\omega_p} (t_2 - t_1)} \quad (5.35)$$

$$= G_H^0(t_1, t_2) e^{-i \int_{t_1}^{t_2} dt \frac{W}{\omega_p^2} [1 - e^{-i\omega_p(t_2 - t)}] + i \frac{W}{\omega_p} (t_2 - t_1)} \quad (5.36)$$

Now the above expression for  $G$ , if Fourier transformed, would closely resemble the expression for the core Green's function  $G_c$  in Eq. (2.109), by setting our  $\frac{W}{\omega_p^2} = Z$ .

This shows explicitly that we have retrieved the same expression for  $G$  as found in the works of Langreth and Hedin, without starting with a model Hamiltonian, but rather with a more general set of equations. Moreover, a second difference between the work presented here and the one by Almladh and Hedin in [99] or by Aryasetiawan in [74], is that at no stage a self-energy appears. On the contrary, in previous works, a  $\Sigma$  would systematically appear and would be approximated within the  $GW$  method.

As discussed in Sec. 2.4.3, one can straightforwardly obtain from the cumulant  $G$ , the core spectral function and then Taylor-expand it. Doing this for (5.35) also yields a sequence of  $W$ 's (corresponding to the bosons of the model Hamiltonian of Refs.[67, 81]), with different weights (again given by the coefficient of the expansion), sitting at energies multiple of  $\omega_p$ . In the end of

the Chapter we will briefly discuss the main results obtained in the work by Guzzo *et. al* [83], where it is shown and analysed how the exponential form for the Green's function improves over the spectral function of semiconductors where a  $G_0W_0$  approximation for  $\Sigma$  had been used.

Now let's elaborate a bit more on the physics contained in the cumulant expansion Green's function. We will do so following a good rule of thumb in many-body perturbation theory which suggests to employ Feynman diagrams for this purpose.

### 5.1.3 The cumulant expansion $W$ explained through Feynman diagrams

In this section we will compare the series of Feynman diagrams obtained *iterating* the linearized DE for  $G^b$  with the well-known diagrams one would obtain by iterating the Dyson equation for  $G$  within a  $G_0W_0$  approximation for the self-energy.

Let's recapitulate below the results obtained so far through an iterative scheme for Eq. (5.14). The zeroth and first order respectively read:

$$\tilde{y}^{(0)}(t_1, t_2; [\bar{\varphi}]) = \tilde{y}_{\bar{\varphi}}(t_1, t_2) \quad (5.37)$$

$$\tilde{y}^{(1)}(t_1, t_2; [\bar{\varphi}]) = \tilde{y}_{\bar{\varphi}}(t_1, t_2) \left\{ 1 + i^3 \int_{t_1}^{t_2} dt_3 \int_{t_3}^{t_2} dt_4 W(t_{3+}, t_4) \right\} \quad (5.38)$$

inserting (5.38) into the DE, one obtains for the second order iteration:

$$\begin{aligned} \tilde{y}^{(2)}(t_1, t_2; [\bar{\varphi}]) &= \tilde{y}_{\bar{\varphi}}(t_1, t_2) + i^2 \int_{t_1}^{t_2} dt_3 \int dt_4 \tilde{y}_{\bar{\varphi}}(t_1, t_3) W(t_3^+, t_4) \\ &\times \frac{\delta}{\delta \bar{\varphi}(t_4)} \left\{ \tilde{y}_{\bar{\varphi}}(t_3, t_2) \left[ 1 + i^3 \int_{t_5}^{t_2} dt_6 \int_{t_3}^{t_2} dt_5 W(t_{5+}, t_6) \right] \right\} \end{aligned} \quad (5.39)$$

$$\begin{aligned} &= \tilde{y}_{\bar{\varphi}}(t_1, t_2) + i^3 \int_{t_1}^{t_2} dt_3 \int dt_4 y_{\bar{\varphi}}(t_1, t_3) W(t_3^+, t_4) \tilde{y}_{\bar{\varphi}}(t_3, t_2) \\ &\times \theta(t_4 - t_3) \theta(t_2 - t_4) \left[ 1 + i^3 \int_{t_5}^{t_2} dt_6 \int_{t_3}^{t_2} dt_5 W(t_{5+}, t_6) \right] \end{aligned} \quad (5.40)$$

And finally, writing out all terms:

$$\begin{aligned} \tilde{y}^{(2)}(t_1, t_2; [\bar{\varphi}]) &= \tilde{y}_{\bar{\varphi}}(t_1, t_2) + i^3 \int_{t_1}^{t_2} dt_3 \int_{t_3}^{t_2} dt_4 \tilde{y}_{\bar{\varphi}}(t_1, t_3) W(t_3^+, t_4) y_{\bar{\varphi}}(t_3, t_2) \\ &+ i^6 \int_{t_1}^{t_2} dt_3 \int_{t_3}^{t_2} dt_4 \tilde{y}_{\bar{\varphi}}(t_1, t_3) W(t_3^+, t_4) \tilde{y}_{\bar{\varphi}}(t_3, t_2) \\ &\times \int_{t_5}^{t_2} dt_6 \int_{t_3}^{t_2} dt_5 W(t_5^+, t_6) \end{aligned} \quad (5.41)$$

Let's now express the above second order terms with Feynman diagrams. Depending on the time ordering one can get different scenarios. If  $t_1 < t_3 < t_4 < t_5 < t_6 < t_2$  one obtains the diagram of Fig. (5.1). Here, the excitation of the plasmons can occur only in a sequential way and *not*

---

<sup>b</sup>We pretend, for the moment, to ignore the exact result in Eq. (5.37), where the series for  $G$  has been already completely resummed.

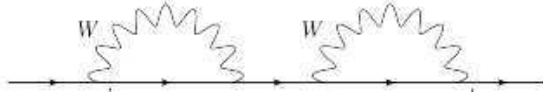


**Figure 5.1:** These diagrams appear in the second order expansion for  $G$ , however it can be considered a simple repetition of a first order one, namely a  $GW$  one.

simultaneously. Diagrams of this type occur all the time when iterating the Dyson equation for  $G$  within the  $G_0W_0$  approximation. This means that no matter to which order one iterates, no multiple plasmons can be ever observed.

The second scenario can exhibit two types of ordering, be  $t_1 < t_3 < t_5 < t_6 < t_4 < t_2$  the occurrence **b1**) and  $t_1 < t_3 < t_5 < t_4 < t_6 < t_2$  the occurrence **b2**). Their representation in terms of Feynman diagrams reads: We observe that in **b1**) nested diagrams appear: it means

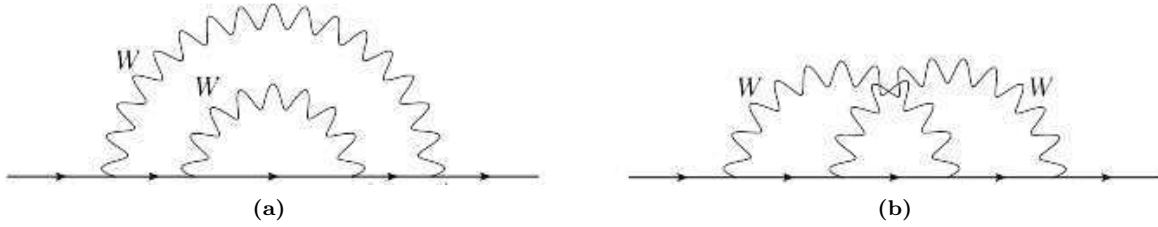


**Figure 5.2:** Fig. 5.2a: nested self-energy diagram (scenario **b1**). Also this diagram belongs to the second order terms of the expansion for  $G$ , however, contrary to the term in Fig. 5.1 it does not appear in the lower order expansion. Fig. 5.2b: intersecting self-energy diagram (scenario **b2**). As the term **b1**) it belongs only to the second order set of diagrams of the expansion. A  $G_0W_0$  expansion for the self-energy would not be able to generate this contribution, no matter the order of the expansion.

that two plasmons are being excited at the same time. Note that these diagrams would also appear in an iterative solution of the DE within a  $GW_0$  approximation to  $\Sigma$ : this clearly shows how the impossibility of describing multiple satellite excitation is inherent only to the  $G_0W_0$  approximation to the self-energy, rather than the  $GW$  method in itself.<sup>c</sup>

The third scenario, labeled **b2**) offers a new perspective: the wiggly  $W$  diagrams are intersecting: when  $t_5 > t > t_4$  one observes a simultaneous excitation of two plasmons: this is the type of physics that the cumulant expansion approximation for the GF can provide beyond  $GW$ .

<sup>c</sup>However, the spectral function would exhibit a too small amplitude for the satellite peaks according, for example, to the calculations by Holm and Aryasetiawan in [101]

## 5.2 The decoupling approximation for real materials calculations

In [83] we try to give a theoretical description of the valence photoemission spectra of bulk Silicon beyond the state-of-the-art<sup>d</sup> ab-initio calculations carried out so far. In this work several questions are addressed, namely if in the case of valence photoelectrons a series of plasmon satellites can be observed due to intrinsic effects or not, if the series is observed within the exponential framework and not employing the  $G_0W_0$  scheme, which are the failures of the latter and finally how can they be cured in a  $GW\Gamma$  framework (i.e. is it possible to devise a promising vertex correction from our approximation?). To begin with, new photoemission data are used as a comparison. Angular resolved (ARPES) photoemission experiments were carried out at the TEMPO beamline of the Soleil Synchrotron radiation facility. The spectrum thus obtained (at around 800eV for the impinging beam) is then compared with the one obtained from a Green's function calculated in the form (5.35) where a plasmon-pole approximation is used to calculate the screened interaction  $W$  and a self-energy corrected  $G_\Delta$  is employed in place of the truly non-interacting  $G_H^0$  appearing in (5.35). The agreement found with experiments is unprecedented and is shown in Fig. 5.3. Moreover, analyzing carefully both the real and imaginary part of a self-energy calculated in the  $G_0W_0$  approximation, the failure of it are attributed, in particular regarding the poor results for the bottom valence band satellite, to a zero in the denominator of  $A(\omega)$ , rather than a peak in the imaginary part of  $\Sigma$  (as instead should be). This satellite is hence an artifact of the  $G_0W_0$  method rather than a true feature of the spectrum. One can then conclude that the exponential result agrees very well with experimental data and it suggest that a *direct* treatment of the differential equation for  $G$  can be very promising.

Besides the spectral function, one may wish to employ the decoupling approximation in order to calculate other quantities by means of the Green's function, for example the total energy from the Galitskii and Migdal formula [26]. On the other hand, the simple form for the decoupled  $G$ , does not allow us to access  $\frac{\delta G([\bar{\varphi}])}{\delta \bar{\varphi}}$  (which could yield, for example, the response of the system). As it is often observed, it is very challenging to find an approximation capable of yielding improvement over all the possible observables and one should always be ready to pay a price somewhere in order to gain somewhere else. Certainly, there is still room for improvements over this first decoupling approximation. One could for instance restore part of the coupling between levels or investigate the effect of a second order term in the expansion for the Hartree potential<sup>e</sup>.

The most tempting possibility of calculating a Green's function which is beyond the one obtained by solving exactly Eq. (5.1), is to release *all* of the approximations made to obtain the N-times

<sup>d</sup>Is is understood that the start-of-the-art calculation are in the  $G_0W_0$  approximation to the self-energy

<sup>e</sup>However these developments and the formulation of new vertex corrections are not a core part of this thesis work, rather M. Guzzo's one. My contribution to [83] was limited to the initial derivation of the iterative solution for Eq. 5.3. By illustrating here these results, I intended to show how useful our linearization procedure can be in the derivation of new approximations -namely for a different derivation of the  $GW$  approximation in Chap. 3 and for an exponential  $G$  in this Chapter. Moreover we show that searching for a direct solution of Eq. 2.71 in a framework beyond the 1-point one can be successful and can be a precious as a guideline for the full functional problem.

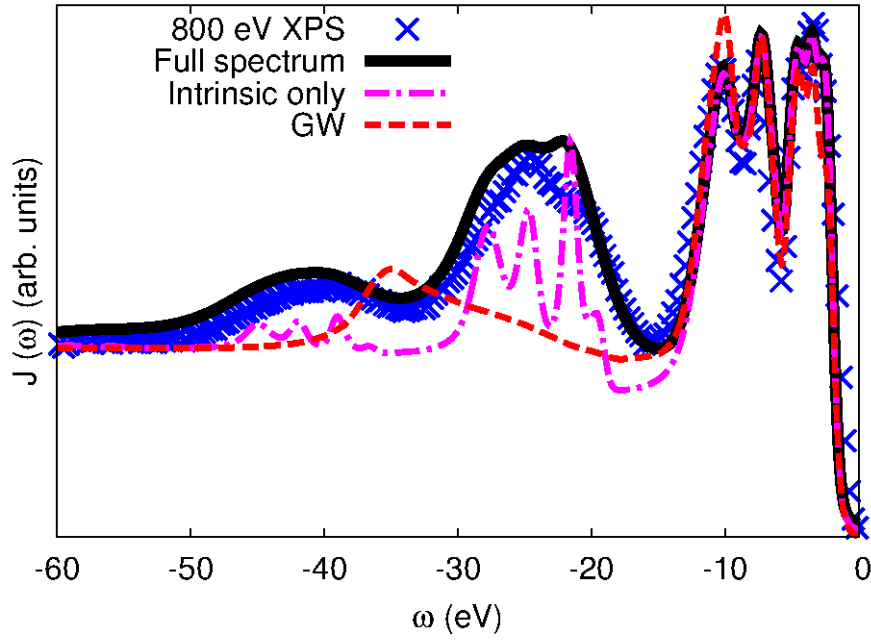


**Figure 5.3:** We show here a comparison of the experimental XPS spectrum of Si (blue crosses), at 800 eV photon energy and the calculated intrinsic spectral function  $A(\omega)$  (containing however cross sections and the secondary electron background) from the  $G_0W_0$  approximation (red dashed line) and from Eq. (5.39) (green dotted-dashed line). The black line is the spectrum as calculated from Eq. (5.39) when extrinsic and interference effects are also included. This latter spectrum is in excellent agreement with experiments.

DE: this means to go back to the full functional linearized differential equation (3.7) and attempt its direct solution, using what we have learned so far. This will be the object of the next (and last) chapter of this thesis.

# CHAPTER 6

## The full functional differential equation

*In this chapter we go back to the problem of solving the set of (linearized) functional differential equations for the one-body Green's function (see Eq. (3.7)).*

*We begin presenting in detail several hurdles that we encountered on the way to the solution, which we tried to devise through an ansatz, mostly based on insights that we obtained from the solution of the equation in the 1-point framework. In particular we will discuss how, towards the final stages of the derivation within the chosen ansatz, made up of three terms, multiple options for choosing one of them show up, making very challenging even to obtain the general solution for the full DE (note instead how within our model, this step had been a considerably easy one). To obtain greater insight on this issue we will move from the full functional framework back to the  $N$ -times (aka decoupling approximation) one, presented in the previous chapter. We will encounter also here the problem of the multiplicity of the solutions, however we will get precious indications on, at least, one way to overcome it. We will finally discuss how the insights obtained from the  $N$ -times framework might be employed for formulating an explicit general solution for the full functional differential equations. The work is however still ongoing.*

### 6.1 An ansatz for the one-body Green's function

As we have shown in Chap. (3)<sup>a</sup> a way to solve the 1-point version of the linearized differential equation (3.15) is through a general ansatz, namely  $y_u(x) = A(x) \cdot \mathcal{I}(x)$ . Within such strategy we had to solve two simpler DE for  $A(x)$  and  $\mathcal{I}(x)$  separately and then inserting the results into the initial ansatz,  $y_u(x)$  was obtained.

In that very same spirit we will formulate a *general ansatz* to solve the full functional linearized DE (3.7). Upon obtaining an explicit solution one would check only *a-posteriori* if it actually

---

<sup>a</sup>And more in detail in App. (B)

satisfies the equation: if yes, it could be considered a valid Green's function obtained *directly* solving the set of linearized differential equations.

While the previous ansatz was made up of two terms, in this more complicated framework we find that a better choice is composed of *three* pieces<sup>b</sup>, namely:

$$\boxed{G(1, 2; [\bar{\varphi}]) = \int d5f([\bar{\varphi}])a(1, 5; [\bar{\varphi}])\mathcal{J}(5, 2; [\bar{\varphi}])} \quad (6.1)$$

where  $f([\bar{\varphi}])$  is a function of the external (screened) potential  $\bar{\varphi}$  only and  $a([\bar{\varphi}])$  and  $\mathcal{J}([\bar{\varphi}])$  matrices (however they still depend on  $\bar{\varphi}$ )<sup>c</sup>; furthermore  $a([\varphi])$  has to be *invertible* and  $f([\varphi])$  non-zero. Inserting the ansatz into the linearized DE (3.7) yields:

$$\begin{aligned} \int d5f([\varphi])a(1, 5; [\varphi])\mathcal{J}(5, 2; [\varphi]) &= G_0(1, 2) \\ &+ \int d3d5G_0(1, 3)\varphi(3)f([\varphi])a(3, 5; [\varphi])\mathcal{J}(5, 2; [\varphi]) \\ &+ i \int d3d4d5G_0(1, 3)W(3, 4)\frac{\delta f([\varphi])}{\delta\varphi(4)}a(3, 5; [\varphi])\mathcal{J}(5, 2; [\varphi]) \\ &+ i \int d3d4d5G_0(1, 3)W(3, 4)f([\varphi])\frac{\delta a(3, 5; [\varphi])}{\delta\varphi(4)}\mathcal{J}(5, 2; [\varphi]) \\ &+ i \int d3d4d5G_0(1, 3)W(3, 4)f([\varphi])a(3, 5; [\varphi])\frac{\delta\mathcal{J}(5, 2; [\varphi])}{\delta\varphi(4)} \end{aligned} \quad (6.2)$$

We now *choose* three *simpler* differential equations -with respect to the original one- that need to be solved for  $f([\varphi])$ ,  $a([\varphi])$  and  $\mathcal{J}([\varphi])$  respectively. The equation for  $f$  reads:

$$\begin{aligned} \int d3d5G_0(1, 3)\varphi(3)f([\varphi])a(3, 5; [\varphi])\mathcal{J}(5, 2; [\varphi]) \\ + i \int d3d5G_0(1, 3)W(3, 4)\frac{\delta f([\varphi])}{\delta\varphi(4)}a(3, 5; [\varphi])\mathcal{J}(5, 2; [\varphi]) = 0 \end{aligned} \quad (6.3)$$

which after some algebra (see App. (G.1)) can be reduced to:

$$\varphi(6)f([\varphi]) = -i \int d4W(6, 4)\frac{\delta f([\varphi])}{\delta\varphi(4)}. \quad (6.4)$$

A  $f([\varphi])$  which satisfies it reads:

$$\boxed{f([\varphi]) = e^{\frac{i}{2} \int d5d6W^{-1}(6,5)\varphi(5)\varphi(6)}} \quad (6.5)$$

Note that we have assumed in first place, the dependence of  $f$  only on  $\varphi$  and no other index. It can be shown, *a-posteriori* that this assumption holds well in our particular case.

Let's turn to the equation for  $a$ :

$$\begin{aligned} \int d5f([\varphi])a(1, 5; [\varphi])\mathcal{J}(5, 2; [\varphi]) &= i \int d3d4d5G_0(1, 3)W(3, 4)f([\varphi])\frac{\delta a(3, 5; [\varphi])}{\delta\varphi(4)}\mathcal{J}(5, 2; [\varphi]) \\ a(1, 5; [\varphi]) &= i \int d3d4G_0(1, 3)W(3, 4)\frac{\delta a(3, 5; [\varphi])}{\delta\varphi(4)} \end{aligned} \quad (6.7)$$

<sup>b</sup>This strategy is *divide et impera* like. A box will appear around the different pieces of the ansatz, so that it will be easier for the reader to reconstruct the Green's function from our guesses.

<sup>c</sup>Disclaimer: to simplify the heavy notation of this chapter, from now on, we will indicate  $\bar{\varphi}$ , related to the initial external potential as  $\bar{\varphi} = \epsilon^{-1}\varphi$  as  $\varphi$ .

where a good ansatz for  $a([\varphi])$  is:

$$\boxed{a(3, 5; [\varphi]) = j(3, 5)e^{-i \int d6d7d8 \frac{j(8,5)}{j(7,5)} W^{-1}(6,7) G_0^{-1}(7,8) \varphi(6)} = j(3, 5) \epsilon(5, [\varphi])} \quad (6.8)$$

$j$  is arbitrary (and for the moment it won't be specified) and does not depend on the potential, while  $\epsilon([\varphi])$  constitutes the  $\varphi$ -dependent part. We are now left only with a differential equation for  $\mathcal{J}$ , or better an equation for  $\frac{\delta \mathcal{J}([\varphi])}{\delta \varphi}$ :

$$G_0(1, 2) + i \int d3d4d5 G_0(1, 3) W(3, 4) f([\varphi]) a(3, 5; [\varphi]) \frac{\delta \mathcal{J}(5, 2; [\varphi])}{\delta \varphi(4)} = 0 \quad (6.9)$$

multiplying from the left by the inverse of  $G_0$ :

$$\delta(6, 2) = -i \int d4d5 W(6, 4) f([\varphi]) a(6, 5; [\varphi]) \frac{\delta \mathcal{J}(5, 2; [\varphi])}{\delta \varphi(4)}. \quad (6.10)$$

This can be written in an even more compact way; defining  $A(6, 5; [\varphi]) := f([\varphi]) a(5, 6; [\varphi])$  and inserting it in the previous equation one gets:

$$\delta(6, 2) = -i \int d4d5 W(6, 4) A(6, 5; [\varphi]) \frac{\delta \mathcal{J}(5, 2; [\varphi])}{\delta \varphi(4)}. \quad (6.11)$$

It would be tempting to *invert* Eq. (6.11) in order to obtain  $\frac{\delta \mathcal{J}(5, 2; [\varphi])}{\delta \varphi(4)}$  and then integrate the result to get  $\mathcal{J}(5, 2; [\varphi])$  (this would be the analogous procedure to the one followed in the 1-point case to find  $I(x)$ ), but unfortunately this is not possible<sup>d</sup> The impossibility of inverting Eq. (6.11) is due to the fact that such equation has *too many solutions*. This is an additional difficulty of the N-points framework: finding the functional equivalent of the simple inversion performed in Eq. (3.17) is now a non-trivial task.

We will now show which alternative path can be taken to formally obtain the family of all possible  $\mathcal{J}([\varphi])$  and which bypasses the impossibility of inverting Eq. (6.11) directly.

Let's now define a new quantity, in general dependent on  $\varphi$ , reading:

$$q(6, 5, 2; [\varphi]) = \int d4 W(6, 4) A(6, 5; [\varphi]) \frac{\delta \mathcal{J}(5, 2; [\varphi])}{\delta \varphi(4)} \quad (6.12)$$

which inserted in (6.11) yields:

$$\delta(6, 2) = -i \int d5 q(6, 5, 2; [\varphi]) \quad (6.13)$$

By introducing  $q$  one can cleanly obtain  $\frac{\delta \mathcal{J}(5, 2; [\varphi])}{\delta \varphi(4)}$ . Beginning with Eq. (6.12) one can divide both the right and the left and side by  $A$ :

$$\frac{q(6, 5, 2; [\varphi])}{A(6, 5; [\varphi])} = \int d4 W(6, 4) \frac{\delta \mathcal{J}(5, 2; [\varphi])}{\delta \varphi(4)} \quad (6.14)$$

<sup>d</sup>Note that even beginning with a slightly different DE, where the external potential is transformed into a non-local one, so that the term  $\frac{\delta \mathcal{J}(5, 2; [\varphi])}{\delta \varphi(4)}$  becomes a 4-point quantity like  $\frac{\delta \mathcal{J}(5, 2; [\varphi])}{\delta \varphi(4, 5)}$  there is no way to invert this last DE for  $\mathcal{J}$ .

We have tried out several different versions of the ansatz for  $a$  and  $f$ : they all yielded equations for  $\mathcal{J}([\varphi])$  which were *not* invertible.

and integrating from the right by  $\int d6 W^{-1}(7, 6)$  one obtains:

$$\boxed{\frac{\delta \mathcal{J}(5, 2; [\varphi])}{\delta \varphi(7)} = \int d6 W^{-1}(7, 6) \frac{q(6, 5, 2; [\varphi])}{A(6, 5; [\varphi])}} \quad (6.15)$$

where  $A \neq 0$ .

For each  $q$  satisfying Eq. (6.13),  $\frac{\delta \mathcal{J}([\varphi])}{\delta \varphi}$  from Eq. (6.15) will satisfy Eq. (6.11), and upon its integration<sup>e</sup>, we will obtain the long yearned  $\mathcal{J}([\varphi])$ . Finally, inserting  $\mathcal{J}([\varphi])$  into (6.1) will then yield a formal full functional expression for the one-body Green's function (within the linearization approximation), equivalent to solving *directly* the generalized differential equation in (3.7).

This is the formal scheme that we will follow throughout the chapter.

The quest for  $\frac{\delta \mathcal{J}([\varphi])}{\delta \varphi}$  has now become a quest for  $q([\varphi])$ . Which kind of  $q([\varphi])$  can satisfy (6.11)? A prototypical one would be:

$$q^{ex}(6, 5, 2; [\varphi]) = i \delta(6, 2) \mathcal{F}(5, [\varphi]) \quad (6.16)$$

where  $\mathcal{F}(5, [\varphi])$  can be almost any functional provided that it satisfies:

$$\int d5 \mathcal{F}(5, [\varphi]) = 1 \quad (6.17)$$

in other words  $\mathcal{F}(5, [\varphi])$  has to be normalized to unity. As one can imagine this is not a particular stringent condition: many functionals can satisfy this requirement. Of course if  $q$  is not unique, also  $\frac{\delta \mathcal{J}([\varphi])}{\delta \varphi}$  isn't. Hence, contrary to the 1-point case, where a *unique*, well defined  $\frac{d\mathcal{I}(x)}{dx}$ <sup>f</sup> was satisfying the DE, here we have *multiple choices* for the final part of our ansatz.

Eq. (6.15), together with Eq. (6.13) are a central result of this work: it gives an *exact constraint* on the form of the full functional (linearized) Green's function.

This kind of constraints are few and very helpful. We can mention two, which we will shortly employ: **i)**  $G = G_0$  when both  $\varphi$  and  $W$  approach zero (we have already used this one to solve the initial problem for the 1-point DE) and **ii)**  $G = G_\varphi$  when  $W \rightarrow 0$ .

Let's now begin the quest for  $q([\varphi])$ .

<sup>e</sup>Which as we will see later in the Chapter is also very challenging ...

<sup>f</sup>The 1-point equivalent of Eq. (6.10) reads:  $y_0 = -u y_0 \frac{d\mathcal{I}(x)}{dx}$  and the inversion to calculate  $\frac{d\mathcal{I}(x)}{dx}$  is straightforward since no integration is involved.

## 6.2 The quest for $q([\varphi])$ and $\mathcal{J}(5, 2; [\varphi])$

### 6.2.1 $q([\varphi])$ from limiting cases

First of all let's recast Eq. (6.12) as a function of the exact  $G$ , rather than  $\frac{\delta\mathcal{J}([\varphi])}{\delta\varphi}$  and for simplicity we choose  $j = G_0^{\text{g}}$

$$\begin{aligned} q(6, 5, 2; [\varphi, W]) &= \int d1 \left[ -i\varphi(6) + i\frac{\delta(6, 5)}{G_0(5, 5)} \right] G(1, 2; [\varphi])G_0^{-1}(5, 1)G_0(6, 5) \\ &+ \int d4 \frac{\delta G(1, 2; [\varphi])}{\delta\varphi(4)} W(6, 4)G_0^{-1}(5, 1)G_0(6, 5) \end{aligned} \quad (6.18)$$

The above expression <sup>h</sup> for  $q([\varphi])$  is *formally exact*, but of scarce practical use to obtain  $q([\varphi])$  directly, since the fully interacting Green's function is our unknown.

At this stage of the problem, looking at *limiting cases* may turn out to be helpful. Let's examine first the case where  $\{W = 0, \varphi \neq 0\}$ : we know that the fully interacting  $G$  reduces to the non-interacting one in presence of an external potential (e.g.  $G \rightarrow G_\varphi$ ). Eq. (6.18) becomes:

$$q(6, 5, 2; [\varphi])\Big|_{W=0} = \int d1 \left[ -i\varphi(6) + i\frac{\delta(6, 5)}{G_0(5, 5)} \right] G_\varphi(1, 2)G_0^{-1}(5, 1)G_0(6, 5). \quad (6.19)$$

From the above result we can readily obtain also a second limit, namely  $\{W = 0, \varphi = 0\}$ , namely:

$$q(6, 5, 2)\Big|_{\varphi=0, W=0} = i\delta(5, 2)\delta(6, 5). \quad (6.20)$$

Indeed, performing the integration  $\int d5$  in both the above expressions correctly yields Eq. (6.13). Suppose now that one (or both) of the above coefficients are a good estimate for  $q([\varphi])$ . The next step would be to immediately calculate  $\frac{\delta\mathcal{J}([\varphi])}{\delta\varphi}$  using Eq. (6.15). Employing first (6.19) we get:

$$\begin{aligned} \frac{\delta\mathcal{J}(5, 2; [\varphi])}{\delta\varphi(7)} &= \int d6 W^{-1}(7, 6) \frac{i\delta(5, 2)\delta(6, 5)}{A(6, 5; [\varphi])} \\ &= i \frac{W^{-1}(7, 5)\delta(5, 2)}{G_0(5, 5)} e^{\left\{ -\frac{i}{2} \int d8 d9 W^{-1}(8, 9) \varphi(8) \varphi(9) + i \int d9 \frac{W^{-1}(9, 5) \varphi(9)}{G_0(5, 5)} \right\}} \end{aligned} \quad (6.21)$$

and substituting the more complicated  $q([\varphi])$  from (6.20) yields:

$$\begin{aligned} \frac{\delta\mathcal{J}(5, 2; [\varphi])}{\delta\varphi(7)} &= \int d6 \frac{W^{-1}(7, 6)}{A(6, 5; [\varphi])} \left\{ \int d1 \left[ -i\varphi(6) + i\frac{\delta(6, 5)}{G_0(5, 5)} \right] G_\varphi(1, 2)G_0^{-1}(5, 1)G_0(6, 5) \right\} \\ &= -i \int d6 d1 W^{-1}(7, 6) e^{\left\{ -\frac{i}{2} \int d8 d9 W^{-1}(8, 9) \varphi(8) \varphi(9) + i \int d8 \frac{W^{-1}(6, 8) \varphi(8)}{G_0(6, 6)} \right\}} \varphi(6) G_\varphi(1, 2) G_0^{-1}(5, 1) \\ &+ i \int d1 \frac{W^{-1}(7, 5)}{G_0(5, 5)} e^{\left\{ -\frac{i}{2} \int d8 d9 W^{-1}(8, 9) \varphi(8) \varphi(9) + i \int d6 \frac{W^{-1}(9, 5) \varphi(9)}{G_0(5, 5)} \right\}} G_\varphi(1, 2) G_0^{-1}(5, 1) \end{aligned} \quad (6.22)$$

<sup>g</sup> $j$  is still "free", so we are not making any approximation.

<sup>h</sup> $G_0(5, 5)$  may look quite pathological, but since we are now interested in a formal solution, we will not be too concerned about this.

### 6.2.2 Finding $\mathcal{J}(5, 2; [\varphi])$

Once  $q([\varphi])$  and hence  $\frac{\delta\mathcal{J}([\varphi])}{\delta\varphi}$  is (at least approximatively set) we have to proceed with the integration of  $\frac{\delta\mathcal{J}(5, 2; [\varphi])}{\delta\varphi(4)}$  (exactly as we have done in the algebraic DE), however in this more complicated framework the straightforward integration is not feasible: some extra manipulations are needed.

In a first instance we have tried to employ the following formula (its derivation is detailed in App. (G.2) and can also be found in [102]):

$$\frac{\partial\mathcal{J}(5, 2; [\bar{\varphi}])}{\partial\lambda} = \int d7 \frac{\delta\mathcal{J}(5, 2; [\bar{\varphi}])}{\delta\bar{\varphi}(7)} \frac{\partial\bar{\varphi}(7)}{\partial\lambda} = \int d7 \frac{\delta\mathcal{J}(5, 2; [\bar{\varphi}])}{\delta\bar{\varphi}(7)} \varphi(7) \quad (6.23)$$

where  $\bar{\varphi} = \lambda\varphi$ . Integrating both sides:

$$\int_0^1 d\lambda \frac{\partial\mathcal{J}(5, 2; [\bar{\varphi}])}{\partial\lambda} = \int_0^1 d\lambda \int d7 \frac{\delta\mathcal{J}(5, 2; [\bar{\varphi}])}{\delta\bar{\varphi}(7)} \varphi(7)$$

and finally:

$$\boxed{\mathcal{J}(5, 2; [\varphi]) = \mathcal{J}(5, 2; [\varphi = 0]) + \int_0^1 d\lambda \int d7 \frac{\delta\mathcal{J}(5, 2; [\bar{\varphi}])}{\delta\bar{\varphi}(7)} \varphi(7).} \quad (6.24)$$

With Eq. (6.24) we have an *explicit* expression for  $\mathcal{J}(5, 2; [\varphi])$  as a function of its derivative with respect to  $\varphi$  and the initial condition  $\mathcal{J}(5, 2; [\varphi = 0])$ <sup>i</sup>. This procedure seems very reasonable and we have tried it out to calculate approximate solutions for  $\mathcal{J}([\varphi])$ , starting from the simplest possible choice for  $q([\varphi])$  (see Eq. (6.22)). However, the differentiation of the obtained  $\mathcal{J}([\varphi])$  didn't return the initial (and correct)  $\frac{\delta\mathcal{J}([\varphi])}{\delta\varphi}$ .

We hence concluded that the expression in (6.24) is *not* universally valid for all possible integrands.

To better address this question one should enter into the details of the proof of the formula: the whole derivation is standing on the hypothesis that the functional has to be Taylor-expandable. Supposing that  $\frac{\delta\mathcal{J}(5, 2; [\bar{\varphi}])}{\delta\bar{\varphi}(7)}$  fulfilled the above condition, then its expansion would look like:

$$\mathcal{J}([\varphi]) = \overbrace{\mathcal{J}([\varphi = 0])}^{\mathcal{J}_0} + \int dx \overbrace{\frac{\delta\mathcal{J}([\varphi])}{\delta\varphi(x)} \Big|_{\varphi=0}}^{\mathcal{J}_1} \cdot \varphi(x) + \frac{1}{2} \int dx dy \overbrace{\frac{\delta^2\mathcal{F}([\varphi])}{\delta\varphi(x)\delta\varphi(y)} \Big|_{\varphi=0}}^{\mathcal{J}_2} \cdot \varphi(x)\varphi(y) + \dots \quad (6.25)$$

Differentiating with respect to the external potential would yield:

$$\frac{\delta\mathcal{J}([\varphi])}{\delta\varphi(z)} = \overbrace{\frac{\delta\mathcal{J}}{\delta\varphi}}^{\mathcal{J}_1} + \int dx \overbrace{\frac{\delta^2\mathcal{J}}{\delta\varphi^2}}^{\mathcal{J}_2} \varphi(x) + \int dy \overbrace{\frac{\delta^2\mathcal{J}}{\delta\varphi^2}}^{\mathcal{J}_2} \varphi(y) + \dots \quad (6.26)$$

<sup>i</sup>This is the equivalent of  $C(y_0, u)$  in the 1-point model, of course with all the added complexity of the full functional problem. Therefore, also in this case, obtain the specific solution for  $G$  from the family of general solution for the DE will have to go through solving this more complicated initial condition problem. In particular we will have to see weather  $\lambda = 0$  is the most convenient limit of the integration.

More schematically the above equation can be recast as:

$$\begin{aligned} \frac{\delta\mathcal{J}([\varphi])}{\varphi(z)} &= \\ &= C(z) + \frac{1}{2} \int dx a(x, z)\varphi(x) + \frac{1}{2} \int dx a(z, x)\varphi(x) \\ &= C(z) + \frac{1}{2} \int dx b(x, z)\varphi(x) + \dots \end{aligned} \quad (6.27)$$

If we could recast our  $\frac{\delta\mathcal{J}(5, 2; [\bar{\varphi}])}{\delta\bar{\varphi}(7)}$  into an expression like the one in (6.27), we would have the guarantee that  $\mathcal{J}(5, 2; [\bar{\varphi}])$  is Taylor expandable and hence the integration formula Eq.(6.24) could be correctly applied to our specific problem. As we can see from Eq. (6.27) this requires the coefficients of the expansion of  $\frac{\delta\mathcal{J}([\varphi])}{\delta\varphi}$  to be *symmetric*, e.g.  $b(x, z) = b(z, x)$  for the linear coefficient.

Unfortunately this is not the case.

In fact, considering the expression for  $\frac{\delta\mathcal{J}(5, 2; [\bar{\varphi}])}{\delta\bar{\varphi}(7)}$  in (6.21) one realizes that (upon rescaling to obtain a single quadratic  $\varphi$  and leaving aside the dumb indices 5 and 2) our integrand is composed of terms with the following structure:

$$\frac{\delta\mathcal{J}([\varphi])}{\delta\varphi(z)} = a(z)e^{-\int dt \varphi^2(t)} \quad (6.28)$$

and if Taylor-expanded yields:

$$\frac{\delta\mathcal{J}([\varphi])}{\delta\varphi(z)} = a(z) \left\{ 1 - \int dt \varphi^2(t) + \frac{1}{2} \left[ \int dt \varphi^2(t) \right]^2 - \dots \right\} \quad (6.29)$$

Eq. (6.29) neither has the same structure of Eq. (6.27) nor can be brought to it.

However, through these last equations, we have defined a further *constraint* for our ansatz, namely that the  $q[\varphi]$  we are looking for has to yield a  $\frac{\delta\mathcal{J}([\varphi])}{\delta\varphi}$  "compatible" with a Taylor expansion, which requires certain symmetries.

This last requirement, together with Eq. (6.13) and the conditions that  $G_{W=0} = G_\varphi$  form a set of *three constraints* for our ansatz. Note that this further constraint is very precious: it reduces considerably the number of possible solutions for the DE within the proposed approach.

Let's now go back to our approximate expression for  $\frac{\delta\mathcal{J}(5, 2; [\bar{\varphi}])}{\delta\bar{\varphi}(7)}$  in order to understand if it is particularly pathological and if, for a better choice of  $q([\varphi])$ , one could, in practice, find an integrand which respects all of the three constraints above, particularly the one about symmetries. Accessing the structure of the *full exact*  $\frac{\delta\mathcal{J}(5, 2; [\bar{\varphi}])}{\delta\bar{\varphi}(7)}$  would for example shed light on this issue. Unfortunately in the full functional framework it cannot be obtained as it depends on the fully interacting Green's function, which is our unknown.

One can think of going back to a simpler framework, namely the N-times one, to get greater insights about this problem. In App. (G.3) one can find manipulations for the N-times DE, which are completely analogous to the one we performed in Eqs. 6.1-6.17.

In particular let's draw our attention to Eq. (G.35) which is the expression for the *exact* N-times  $\frac{\delta \mathcal{J}([\varphi])}{\delta \varphi}$ , obtained thanks to the knowledge of the exact equilibrium N-times Green's function. <sup>j</sup> By expanding it with respect to  $\varphi$  one can show that the terms thus obtained are *symmetric* order by order, hence this exact  $\frac{\delta \mathcal{J}([\varphi])}{\delta \varphi}$  satisfies the symmetry constraint needed to be integrated with the formula in Eq. (6.24).

This insight is very important, as it shows that this last piece of our ansatz is not pathological in itself, rather it can become so upon a bad choice of  $q([\varphi])$ .

In this Chapter, we have paved the way to the design of new approximations to the full one-body Green's function: we have devised an ansatz (Eq. (6.1) together with Eq. (6.5) and Eq. (6.8)) that leads to the much simpler differential equation (6.11). We have shown that one can integrate this equation, provided that a functional  $q([\varphi])$  is chosen so that obeys a sum rule (6.13) and certain symmetry requirements (see the discussion following Eq. (6.27)). A further constraint (the correct  $W \rightarrow 0$  limit) will be needed to set integration (functional) constant. Both the 1-point model and the N-times solution have been crucial to obtain these results. They will be further used, in ongoing and future work, to demonstrate the potential of this approach within specific approximations.

---

<sup>j</sup>Its expression was obtained in the previous chapter as solution of Eq. (5.2) and reads:  $G(t_1, t_2)|_{\bar{\varphi}=0} = G_H^0(t_1, t_2) e^{-i \int_{t_1}^{t_2} dt \int_t^{t_2} dt_4 W(t, t_4)}$

# CHAPTER 7

## Conclusions and Outlook

An improved description of the Green's function is very desirable as it may yield improved quasi-particles band-structure calculations, more accurate ground state total energy calculations and last but not least, better spectral functions, which are capable of providing information about all the elementary and more complex many-body excitations ongoing in a solid.

The scope of this work has hence been twofold: on one hand to get greater insights into the state-of-the-art methods for one-body Green's function calculations, and on the other hand to develop alternative approaches in order to calculate *directly* and more accurately the one-body propagator.

After a brief review of the different routes for calculating the one-body propagator, we focused on a particular one, mentioned in [40] but not explored further, perhaps due to the complexity of tackling the problem numerically.<sup>a</sup> Such approach is strikingly simple at first sight, whereas very challenging in practice.

The main idea behind it is to manipulate and recast the equation of motion for the propagator into a set of nonlinear, coupled, first order functional differential equations (Eq. (2.71)) -pivotal to many-body perturbation theory- and attempt to solve them *directly*. As solving such set of equations exactly means also solving the many-body problem exactly, which we know to be unfeasible, some type of approximation is required to tackle the differential equations. We will explore different levels of approximations, starting from the simplest possible up to more elaborated ones.

The first approximation we perform (and that has been employed throughout the thesis) is a *linearization procedure*, where the Hartree potential is linearized with respect to the external one, while the electron-electron interaction is always accounted for to any order. This linearization, besides allowing us to proceed further with the DE's solution, turns out to be very transpar-

---

<sup>a</sup>Computer resources in the late '60s could not compare with nowadays supercomputer facilities.

ent in its physical content: one can for instance observe that the  $GW_0$  approximation to  $\Sigma$  is contained there as the simplest approximation to the equation. This proof indeed suggests that the linearized DE is a very good starting point to go beyond the state-of-the-art approaches. Furthermore it has been the starting point to re-derive, in a rigorous way, the so-called cumulant expansion for  $G$ : such derivation, besides having being already employed, very successfully, in valence photo-emission calculation for semiconductors, emphasizes the limits of the current approaches and opens up the way to improvements.

The most challenging part of this work is the attempt to get as far as possible towards the direct solution of the linearized set of functional differential equations. To this end, a second approximation is performed (and is then released in Chap. (5) and Chap. (6)): it consists of projecting the equations on a basis which diagonalizes all the Green's functions (both full and non interacting) and yields a decoupling (from here the name *decoupling approximation*) of the DEs set. Then only one point in space, spin *and* time is taken. In this way one obtains the so called 1-point model, where the set of equations reduces to a single algebraic DE.

Within this simplified model, the equation is solved exactly through an *ansatz*. This choice, rather than a more scholarly solution, has the aim of better exploring the structure of the solution, in view of a *generalization* of the approach. The mathematical nature of the algebraic DE is also explored in depth, as it is the issue of solving the initial value problem to pick the physical solution from the family of general solutions. Once again this accurate analysis has to be seen as an indispensable preliminary work aimed at the generalization of the method.

The exact DE solution becomes a benchmark for established many-body approaches over the *whole range of interaction strength*. Amongst our find we can list the following: **i)** iterations towards self-consistency in the  $GW$  scheme sensibly improve on the one-shot ( $G_0W_0$ ) calculation; **ii)** including first order vertex corrections improves the self-consistent  $GW_0$  results only slightly and only for small  $u$ . **iii)** In the case of self-consistent  $GW_0$  two solutions are possible, of which only one is physical and has to be picked through the vanishing electron-electron interaction limit. Moreover we show that the standard iterative  $GW_0$  scheme will always converge to the physical solution, while other iterative schemes may yield different -wrong- results. This finding serves as an additional warning regarding corrections beyond  $GW$ : since the number of possible solutions for the Green's function and the number of possible ways to iterate the equations is increased, also danger to worsen results augments.

Alternative approximations, with their advantages and caveats, are also explored. We find that Taylor-expanding the algebraic DE to an order  $\mathcal{O}(n)$ , and solving them backwards leads to a Green's function which is equivalent to that of a continued fraction approximation for the exact solution. This example illustrates very well our strategy in looking for alternative approximations: the idea is to devise them only through the knowledge of the initial DE and to establish a link between the manipulations needed to obtain them and some specific approximation for the exact solution. This strategy is designed to be employed also in the functional framework where only the full differential equation is known.

In this spirit we also explore the large interaction regime and find that coupling a straightforward large  $u$  expansion to a Dyson equation yields, at the first order, very good results. However this approach, for now, cannot be transposed to the full functional problem, since we had employed the knowledge of the initial condition in the expansions: this couldn't be done in a simple way

in the more complicated framework.

In the last two chapters of the work we overcome the main limitation of our model, which is to say the 1-point approximation in time, by fully restoring the time dependence (and hence frequency dependence) of the Green's function, while still keeping the decoupling approximation for the spin and time variables.

The resulting differential equation has been solved analytically by resumming exactly its iterative solution. The Green's function thus obtained has an exponential form which is analogous to that of the well known cumulant expansion form for  $G$ , discussed in Sec. (2.4.3). For illustration I have reported the main results obtained so far in M. Guzzo thesis work<sup>b</sup> where this approximation -rigorously derived here for the first time- yielded a theoretical valence electron photo-emission spectrum in Silicon in unprecedented agreement with experimental data.

The so-called N-times framework still has room for improvements. Examples of further investigations may consist in restore part of the coupling between the levels or investigating the effect of a second order term in the expansion for the Hartree potential. A better understanding of non-linear effects may shed lights on some shortcomings of the exponential form for  $G$ , namely its failure in describing the spectral function where the number of excitations is finite (e.g. in finite systems) and the approximation instead yields an unphysical number of them.

Finally we attempted the generalization of our approach to the full functional case. The main idea was to employ an *ansatz*, in the same spirit of the 1-point model, and solve a simpler differential equation for each piece of it. It turned out that a guess made up of three pieces was enough to solve two equations, while it lead to more hurdles for the third, and last, equation. Specifically the problem encountered regarded the multiplicity of solutions for such equation; the issue was anyway overcome and an *explicit formal solution* for the last piece of the ansatz ( $\frac{\delta\mathcal{J}([\varphi])}{\delta\varphi}$ ), in terms of another formal quantity labeled  $q([\varphi])$ , was obtained. This was only a partial success towards the calculation of the family of solution for the generalized  $G$ : the conditions for  $q([\varphi])$  to satisfy the auxiliary differential equation for  $\frac{\delta\mathcal{J}([\varphi])}{\delta\varphi}$  is not particularly stringent and hence one needs to choose a wise expression for it. To start with, through limiting cases, we obtained two possible expressions. The integration of  $\frac{\delta\mathcal{J}([\varphi])}{\delta\varphi}$ , calculated starting with the simplest  $q([\varphi])$  turned out to be very challenging and our first attempt to solve it was unsuccessful.

However, a deeper analysis of the problem led to the identification of the pathology of this (too simple) integrand and, most importantly, thanks to a number of insights from the N-times framework, we devised a further constraint that  $q([\varphi])$  has to satisfy to yield a  $\frac{\delta\mathcal{J}([\varphi])}{\delta\varphi}$  on which the integration can be correctly performed. This result, together with another constraint for  $q([\varphi])$  and one constraints for the full one-body  $G$ , allowed us to reduce considerably the space of possible solutions for the differential equation, suggesting that our approach is indeed a promising one. The road to the results outlined above has been winding, with deviations and trials, amongst the most significant ones we chose to report in App. G.4 an *alternative ansatz*,

---

<sup>b</sup>And relative publication [83], of which I am a co-author

inspired by the expression for the N-times exponential Green's function (rather than the 1-point one). The results so far obtained towards a direct general solution of the linearized full functional differential equation seem very encouraging. In the near future we hope to progress also towards the particular solution for the set of equations. Last but not least, we hope that this thesis will foster a number of other works beating alternative paths for the calculation of the one-body propagator beyond the state-of-the-art methods.

# APPENDIX **A**

---

## Useful manipulations for $G$

Here we report some useful manipulations for the Green's function, its inverse, its functional derivative with respect to the external potential  $\varphi$  and many more.

### A.1 Definition of $G_0$

$$\left[ i \frac{\partial}{\partial t_1} - h(r_1) \right] G_0(1, 2) = \delta(1, 2) \quad (\text{A.1})$$

where the partial derivative is taken with respect to the time  $t_1$  (it could be equally taken with respect to the time  $t_2$ ),  $h(r_1)$  is the one-body, time-independent part (namely the kinetic term) of any many-body Hamiltonian  $H$  and  $G_0(1, 2)$  is the Green's function for a system of non-interacting particles (note that in this case the Hamiltonian of the system is only made up by its kinetic part, i.e.  $H(r_1) = h(r_1)$ ).

Occasionally it may be useful to define a non-interacting Green's function in the presence of an external perturbing time dependent potential  $\varphi(t_1)$ . In this case we have that  $h(r_1) \rightarrow \tilde{h}(r_1, t_1) = h(r_1) + \varphi(t_1, t_1)$  and the equivalent of Eq. (A.1) is:

$$\left[ i \frac{\partial}{\partial t_1} - \tilde{h}(r_1, t_1) \right] G_\varphi(1, 2) = \delta(1, 2) \quad (\text{A.2})$$

### A.2 Definition of the inverse of $G$

The inverse of the one-body Green's function can be defined as:

$$\int d2 G(1, 2; [\varphi]) G^{-1}(2, 4; [\varphi]) = \delta(1, 4) \quad (\text{A.3})$$

### A.3 Expressing $\frac{\delta G([\varphi])}{\delta \varphi}$ through $\frac{\delta G^{-1}([\varphi])}{\delta \varphi}$

Differentiating  $\int d2G(1, 2; [\varphi])G^{-1}(2, 4; [\varphi]) = \delta(1, 4)$  with respect to  $\varphi$  one obtains:

$$\int d2 \left[ \frac{\delta G(5, 6; [\varphi])}{\delta \varphi(7)} G^{-1}(1, 2; [\varphi]) + G(1, 2; [\varphi]) \frac{\delta G^{-1}(2, 4; [\varphi])}{\delta \varphi(7)} \right] = 0 \quad (\text{A.4})$$

$$\int d2 \frac{\delta G(1, 2; [\varphi])}{\delta \varphi(7)} G^{-1}(2, 4; [\varphi]) = - \int d2 G(1, 2; [\varphi]) \frac{\delta G^{-1}(2, 4; [\varphi])}{\delta \varphi(7)}. \quad (\text{A.5})$$

Integrating from the right by  $G(4, 8; [\varphi])$  and using Eq. (A.3) one gets:

$$\begin{aligned} \int d2d4 \frac{\delta G(1, 2; [\varphi])}{\delta \varphi(7)} G^{-1}(2, 4; [\varphi]) G(4, 8; [\varphi]) &= - \int d2d4 G(1, 2; [\varphi]) \frac{\delta G^{-1}(2, 4; [\varphi])}{\delta \varphi(7)} G(4, 8; [\varphi]) \\ \int d2 \frac{\delta G(1, 2; [\varphi])}{\delta \varphi(7)} \delta(2, 8) &= - \int d2d4 G(1, 2; [\varphi]) \frac{\delta G^{-1}(2, 4; [\varphi])}{\delta \varphi(7)} G(4, 8; [\varphi]) \\ \frac{\delta G(1, 8; [\varphi])}{\delta \varphi(7)} &= - \int d2d4 G(1, 2; [\varphi]) \frac{\delta G^{-1}(2, 4; [\varphi])}{\delta \varphi(7)} G(4, 8; [\varphi]) \end{aligned} \quad (\text{A.6})$$

### A.4 Inverting the Dyson equation

We will invert here the Dyson-like equation for  $G$ , where the zero-potential Hartree Green's function  $G_H^0$  has been chosen instead of the usual non-interacting  $G_0$  and where we assume  $G_H^0$  somewhat known, to be able to actually calculate  $G$ . The equation reads:

$$G(1, 2; [\bar{\varphi}]) = G_H^0(1, 2) + \int d34 G_H^0(1, 3) \Sigma(3, 4; [\varphi]) G(4, 2; [\bar{\varphi}]) \quad (\text{A.7})$$

Integrating from the right by  $\int d2G^{-1}(2, 5; [\bar{\varphi}])$  and from the left by  $\int d1G_H^{0-1}(6, 1)$  yields:

$$\begin{aligned} \int d12 G_H^{0-1}(6, 1) G(1, 2; [\bar{\varphi}]) G^{-1}(2, 5; [\bar{\varphi}]) &= \int d12 G_H^{0-1}(6, 1) G_H^0(1, 2) G^{-1}(2, 5; [\bar{\varphi}]) \\ &+ \int d3412 G_H^{0-1}(6, 1) G_H^0(1, 3) \Sigma(3, 4; [\varphi]) \\ &\times G(4, 2; [\bar{\varphi}]) G^{-1}(2, 5; [\bar{\varphi}]) \end{aligned} \quad (\text{A.8})$$

Integrating where possible the  $\delta$  functions leads to:

$$G_H^{0-1}(6, 5) = G^{-1}(6, 5; [\bar{\varphi}]) + \Sigma(6, 5; [\varphi]) \quad (\text{A.9})$$

and ultimately to:

$$G^{-1}(6, 5; [\bar{\varphi}]) = G_H^{0-1}(6, 5) - \Sigma(6, 5; [\varphi]) \quad (\text{A.10})$$

## A.5 Splitting a Dyson-like equation in two parts

This procedure is often convenient when a kernel with a very complicated form appears: solving two equations with simpler kernel turns out to be an easier path to take. We will here illustrate the main steps to follow, for a typical Dyson equation with a challenging kernel, employing a symbolic notation. In the (realistic) case that functionals appeared, all the manipulations needed are already described in the previous bits of this appendix.

Say we start with:

$$G([\varphi]) = G_0 + G_0 v_H^0 G([\varphi]) + G_0 \varphi G([\varphi]) + v G_0 \frac{\delta G([\varphi])}{\delta \varphi}. \quad (\text{A.11})$$

We can multiply from the left and the right respectively by  $G^{-1}$  and  $G_0^{-1}$ , and rearranging the different terms one obtains:

$$\overbrace{G^{-1}([\varphi])}^1 = \overbrace{G_0^{-1}}^2 - \overbrace{[v_H^0 + \varphi]}^{\kappa_3 + \kappa_4} - v G^{-1}([\varphi]) \quad (\text{A.12})$$

We will now split the kernel in two pieces and formulate a Dyson equations only for the term 3 (using also the terms 1 and 2), namely:

$$\tilde{G}_H^{-1} = G_0^{-1} - v_H^0 \quad (\text{A.13})$$

From the above expression one can obtain the *first Dyson-like equation* for  $\tilde{G}_H^{-1}$ , upon multiplication by  $\tilde{G}_H$  and  $G_0$ :

$$\tilde{G}_H = G_0 + G_0 \overbrace{v_H^0}^{\kappa_3} \tilde{G}_H \quad (\text{A.14})$$

To obtain the second Dyson equation we will rely on the result above: inserting it into (A.12) yields:

$$G^{-1}([\varphi]) = \tilde{G}_H^{-1} - \varphi - v G^{-1}([\varphi]). \quad (\text{A.15})$$

Multiplying by  $\tilde{G}_H$  first and by  $G([\varphi])$  afterwards, rearranging all the terms, one gets:

$$G([\varphi]) = \tilde{G}_H + \tilde{G}_H \overbrace{\varphi}^{\kappa_4} G([\varphi]) + \tilde{G}_H v \frac{\delta G([\varphi])}{\delta \varphi} \quad (\text{A.16})$$

To solve the above equation one should first have access to  $\tilde{G}_H$ . Note that this procedure is completely general.



# APPENDIX B

## Solving the DE

Eq. (3.15) can be solved using standard textbook methods [88, 103]. Here we choose a route that yields precious information for our final aim of generalizing to the full functional problem. A general ansatz for the structure of  $y_u(x)$  is:

$$y_u(x) = A(x) \cdot \mathcal{I}(x), \quad (\text{B.1})$$

where the only restriction is that  $A$  and  $\mathcal{I}$  are not zero. Substituting the ansatz in the DE (3.15) gives:

$$\begin{aligned} A(x)\mathcal{I}(x) &= y_0 + y_0 x A(x)\mathcal{I}(x) - uy_0 \frac{dA(x)}{dx} \mathcal{I}(x) \\ &- uy_0 A(x) \frac{d\mathcal{I}(x)}{dx}. \end{aligned} \quad (\text{B.2})$$

The idea is now to solve two separate, simpler with respect to the initial one, DEs for  $A(x)$  and  $\mathcal{I}(x)$ . Putting together the left-hand side and the second and third terms of the right-hand side of Eq. (B.2) one obtains:

$$A(x)\mathcal{I}(x) = y_0 x A(x)\mathcal{I}(x) - uy_0 \frac{dA(x)}{dx} \mathcal{I}(x). \quad (\text{B.3})$$

We can choose the solution

$$A(x) = e^{\left[\frac{x^2}{2u} - \frac{x}{uy_0}\right]}. \quad (\text{B.4})$$

One is now left with the equation for  $\mathcal{I}(x)$  reading:

$$y_0 - uy_0 A(x) \frac{d\mathcal{I}(x)}{dx} = 0. \quad (\text{B.5})$$

Plugging in the expression for  $A(x)$  previously obtained and integrating on both sides one obtains:

$$\mathcal{I}(x) = \frac{1}{u} \int_0^x dt e^{\left[-\frac{t^2}{2u} + \frac{t}{uy_0}\right]} + \bar{C}(u, y_0). \quad (\text{B.6})$$

The integral on the right-hand side is:

$$\begin{aligned} \int^x dt e^{\left[-\frac{t^2}{2u} + \frac{t}{uy_0}\right]} &= \sqrt{2u} e^{\frac{1}{2uy_0^2}} \int^{\frac{x}{\sqrt{2u}} - \frac{1}{\sqrt{2uy_0^2}}} d\tilde{t} e^{-\tilde{t}^2} \\ &= \frac{\sqrt{2u\pi}}{2} e^{\frac{1}{2uy_0^2}} \\ &\quad \times \operatorname{erf}\left[\left(x - \frac{1}{y_0}\right) \frac{1}{\sqrt{2u}}\right] \end{aligned} \quad (\text{B.7})$$

where the change of variables  $\tilde{t} = \left(\frac{t}{\sqrt{2u}} - \frac{1}{\sqrt{2uy_0^2}}\right)$  has been made, and the lower limit of the last integral has been chosen to be zero, which requires to set a constant  $\bar{C}(u, y_0)$ . Hence

$$\begin{aligned} \mathcal{I}(x) &= \sqrt{\frac{\pi}{2u}} e^{\frac{1}{2uy_0^2}} \operatorname{erf}\left[\left(x - \frac{1}{y_0}\right) \frac{1}{\sqrt{2u}}\right] \\ &\quad + \bar{C}(u, y_0). \end{aligned} \quad (\text{B.8})$$

The exact solution  $y_u(x) = A(x) \cdot I(x)$  is given in Eq. (3.18), where  $C(u, y_0) = -\sqrt{\frac{2u}{\pi}} \bar{C}(u, y_0) e^{\frac{-1}{2uy_0^2}}$ .

# APPENDIX C

## Some relations between special functions

We will show how the *divergent hypergeometric function*  ${}_2F_0\left(\frac{1}{2}, 1; -\frac{3}{2}\lambda\right)$  can be intimately related to the *error function*.

Firstly let's list all the equalities between special functions which have been used in the manipulation:

$$\left(\frac{1}{2}\right)_n = \frac{\Gamma\left(n + \frac{1}{2}\right)}{\Gamma\left(\frac{1}{2}\right)} \quad (\text{C.1})$$

$$\Gamma\left(\frac{1}{2}\right) = \left(-\frac{1}{2}\right)! = \Pi\left(-\frac{1}{2}\right) = \sqrt{\pi} \quad (\text{C.2})$$

$$\Gamma\left(n + \frac{1}{2}\right) = \left(n - \frac{1}{2}\right)! = \Pi\left(n - \frac{1}{2}\right) = \sqrt{\pi} \frac{(2n)!}{4^n n!} = \sqrt{\pi} \frac{(2n-1)!!}{(2z^2)^n} \quad (\text{C.3})$$

$$(\text{C.4})$$

We also employ the *asymptotic expansion* for the  $erfc(z)$ , reading:

$$erfc(z) = \frac{e^{z^2}}{z\sqrt{\pi}} \sum_{n=0}^{\infty} (-1)^n \frac{(2n-1)!!}{(2z^2)^n} \quad (\text{C.5})$$

and for the  $erf(z)$  one simply has:

$$erf(z) = 1 - erfc(z) = 1 - \frac{e^{z^2}}{z\sqrt{\pi}} \sum_{n=0}^{\infty} (-1)^n \frac{(2n-1)!!}{(2z^2)^n} \quad (\text{C.6})$$

The exact DE's solution, where  $\sqrt{\frac{1}{2uy_0^2}} = z$ , reads

$$y_u \approx -\sqrt{\pi} z e^{z^2 \frac{1}{y_0}} \left\{ erf \left[ z \cdot \sqrt{\frac{1}{y_0}} \right] - 1 \right\} \quad (\text{C.7})$$

plugging (C.6) into (C.7) yields:

$$\begin{aligned}
 y_u &\approx -\sqrt{\pi}ze^{[z^2]} \left\{ 1 - \frac{e^{z^2}}{z\sqrt{\pi}} \sum_{n=0}^{\infty} (-1)^n \frac{(2n-1)!!}{(2z^2)^n} - 1 \right\} \\
 &= \sum_{n=0}^{\infty} (-1)^n \frac{(2n-1)!!}{(2z^2)^n} \approx {}_2F_0\left(\frac{1}{2}, 1; \mathbf{z}\right)
 \end{aligned} \tag{C.8}$$

where, let's remind,  $z = \sqrt{\frac{1}{2uy_0^2}}$  and  $\mathbf{z} = -\frac{\mathbf{2}}{\mathbf{3}\lambda}$

# APPENDIX D

## N-points limited order differential equation

We detail here the algebra employed to obtain the results shown in Eq. (4.42) and Eq. (4.43). The starting point is the following expression

$$\begin{aligned}
 G(1, 2; [\bar{\varphi}]) &= G_H^0(1, 2) + i \int d3 G_H^0(1, 3) \bar{\varphi}(3) G(3, 2; [\bar{\varphi}]) \\
 &+ i \int d3 d5 G_H^0(1, 3) W(3^+, 5) \frac{\delta G(3, 2; [\bar{\varphi}])}{\delta \bar{\varphi}(5)} \delta \bar{\varphi}(5),
 \end{aligned} \tag{D.1}$$

Differentiating it with respect to the potential  $\bar{\varphi}(6)$ , yields

$$\begin{aligned}
 \frac{\delta G(1, 2; [\bar{\varphi}])}{\delta \bar{\varphi}(6)} &= \int d3 G_H^0(1, 3) \frac{\delta \bar{\varphi}(3)}{\delta \bar{\varphi}(6)} G(3, 2; [\bar{\varphi}]) + \int d3 G_H^0(1, 3) \bar{\varphi}(3) \frac{\delta G(3, 2; [\bar{\varphi}])}{\delta \bar{\varphi}(6)} \\
 &+ i \int d3 d5 W(3^+, 5) G_H^0(1, 3) \frac{\delta^2 G(3, 2; [\bar{\varphi}])}{\delta \bar{\varphi}(6) \delta \bar{\varphi}(5)}.
 \end{aligned} \tag{D.2}$$

We now *truncate* the highest order derivative and set the *condition* of zero  $\varphi$  for the solution:

- $\frac{\delta^2 G(3, 2; [\bar{\varphi}])}{\delta \bar{\varphi}(6) \delta \bar{\varphi}(5)} = 0$  (approx.)
- $\varphi(3) = 0 \rightarrow \bar{\varphi} = 0$

We get:

$$\frac{\delta G(1, 2; [\bar{\varphi}])}{\delta \bar{\varphi}(5)} = G_H^0(1, 5) G(5, 2; [\bar{\varphi}]) \tag{D.3}$$

plugging this result into Eq. (D.1):

$$G(1, 2; [\bar{\varphi}]) = G_H^0(1, 2) + i \int d3 d5 G_H^0(1, 3) W(3^+, 5) G_H^0(3, 5) G(5, 2; [\bar{\varphi}]). \tag{D.4}$$

If one is interested in an *explicit form* for the the one-body  $G$ , it is convenient to work with its *inverse*, obtained integrated from the right by an appropriate  $G^{-1}$ :

$$\begin{aligned} \int d2G(1, 2; [\bar{\varphi}])G^{-1}(2, 5; [\bar{\varphi}]) &= \int d2 G_H^0(1, 2)G^{-1}(2, 5; [\bar{\varphi}]) \\ &+ i \int d3d5d2W(3^+, 5)G_H^0(1, 3)G_H^0(3, 5)G(5, 2; [\bar{\varphi}]) \\ &G^{-1}(2, 5; [\bar{\varphi}]) \end{aligned} \quad (D.5)$$

$$\begin{aligned} \delta(1, 5) &= \int d2G_H^0(1, 2)G^{-1}(2, 5; [\bar{\varphi}]) + i \int d3W(3^+, 5) \\ &G_H^0(1, 3)G_H^0(3, 5) \end{aligned} \quad (D.6)$$

and integrating once more from the left by  $G_H^0{}^{-1}$  we get:

$$\begin{aligned} \int d1G_H^0{}^{-1}(6, 1)\delta(1, 5) &= \int d2d1 G_H^0{}^{-1}(6, 1)G_H^0(1, 2)G^{-1}(2, 5; [\bar{\varphi}]) \\ &+ i \int d3d1 W(3^+, 5)G_H^0{}^{-1}(6, 1)G_H^0(1, 3)G_H^0(3, 5) \end{aligned} \quad (D.7)$$

$$(D.8)$$

finally we get

$$G^{-1}(6, 5; [\bar{\varphi}]) = G_H^0{}^{-1}(6, 5) - iW(5, 6^+)G_H^0(6, 5). \quad (D.9)$$

Now we move one order further ( $O(d_x^3)$ ), retaining the second derivative of  $G$  with respect to  $\bar{\varphi}$ , while neglecting the third order one.

Differentiating Eq. (D.2) with respect to a second external potential  $\bar{\varphi}(7)$ :

$$\begin{aligned} \frac{\delta^2 G(1, 2; [\bar{\varphi}])}{\delta\varphi(6)\delta\varphi(7)} &= G_H^0(1, 6)\frac{\delta G(6, 2; [\bar{\varphi}])}{\delta\bar{\varphi}(7)} + \int d3G_H^0(1, 3)\delta(3, 7)\frac{\delta G(3, 2; [\bar{\varphi}])}{\delta\bar{\varphi}(6)} \\ &+ \int d3G_H^0(1, 3)\bar{\varphi}(3)\frac{\delta^2 G(3, 2; [\bar{\varphi}])}{\delta\bar{\varphi}(6)\delta\bar{\varphi}(7)} \\ &+ i \int d3d5W(3^+, 5)G_H^0(1, 3)\frac{\delta^3 G(3, 2; [\bar{\varphi}])}{\delta\bar{\varphi}(7)\delta\bar{\varphi}(6)\delta\bar{\varphi}(5)} \end{aligned} \quad (D.10)$$

employing the usual *truncation* and taking the limit  $\varphi = 0$  for the solution:

- $\frac{\delta^3 G(3, 2; [\bar{\varphi}])}{\delta\bar{\varphi}(7)\delta\bar{\varphi}(6)\delta\bar{\varphi}(5)} = 0$
- $\bar{\varphi}(3) = 0$

Eq. (D.10) becomes:

$$\frac{\delta^2 G(1, 2)}{\delta\varphi(7)\delta\varphi(6)} = G_H^0(1, 6)\frac{\delta G(6, 2; [\bar{\varphi}])}{\delta\bar{\varphi}(7)}\Big|_{\varphi=0} + G_H^0(1, 7)\frac{\delta G(7, 2; [\bar{\varphi}])}{\delta\varphi(6)}\Big|_{\varphi=0} \quad (D.11)$$

substituting back Eq. (D.11) in Eq. (D.2) we get:

$$\begin{aligned} \frac{\delta G(1, 2; [\bar{\varphi}])}{\delta\bar{\varphi}(6)}\Big|_{\varphi=0} &= G_H^0(1, 6)G(6, 2) + i \int d3d5G_H^0(1, 3)W(3^+, 5) \\ &\times \left\{ G_H^0(3, 6)\frac{\delta G(6, 2; [\bar{\varphi}])}{\delta\bar{\varphi}(5)}\Big|_{\varphi=0} + G_H^0(3, 5)\frac{\delta G(5, 2; [\bar{\varphi}])}{\delta\bar{\varphi}(6)}\Big|_{\varphi=0} \right\}. \end{aligned} \quad (D.12)$$

We can now try to obtain, with some manipulations a convenient matrix equation to solve, such as:

$$B_{xy} = B_{xy}^0 + \sum_{qp} \gamma_{(xy)(qp)} B_{qp} \quad (\text{D.13})$$

Note that the index 2, appearing in all the terms of the equation, is dummy, hence we proceed with the following steps:

$$\begin{aligned} \frac{\delta G(1, 2; [\bar{\varphi}])}{\delta \bar{\varphi}(6)} \Big|_{\varphi=0} &= G_H^0(1, 6)G(6, 2) \\ &+ i \int d3d5 W(3^+, 5)G_H^0(1, 3)G_H^0(3, 6) \frac{\delta G(6, 2; [\bar{\varphi}])}{\delta \bar{\varphi}(5)} \Big|_{\varphi=0} \\ &+ \int d3d5 G_H^0(1, 3)W(3^+, 5)G_H^0(3, 5) \frac{\delta G(5, 2; [\bar{\varphi}])}{\delta \bar{\varphi}(6)} \Big|_{\varphi=0} \end{aligned} \quad (\text{D.14})$$

$$\begin{aligned} &= G_H^0(1, 6)G(6, 2) \\ &+ i \int d3d5d7 G_H^0(1, 3)W(3^+, 5)G_H^0(3, 6)\delta(7, 6) \frac{\delta G(7, 2; [\bar{\varphi}])}{\delta \bar{\varphi}(5)} \Big|_{\varphi=0} \\ &+ \int d3d5d7 G_H^0(1, 3)W(3^+, 5)G_H^0(3, 5)\delta(7, 6) \frac{\delta G(5, 2; [\bar{\varphi}])}{\delta \bar{\varphi}(7)} \Big|_{\varphi=0}. \end{aligned} \quad (\text{D.15})$$

In the  $2^{nd}$  term on the r.h.s. one can exchange under the integral symbol the indices  $5 \leftrightarrow 7$  and obtain:

$$\begin{aligned} \frac{\delta G(1, 2; [\bar{\varphi}])}{\delta \bar{\varphi}(6)} \Big|_{\varphi=0} &= G_H^0(1, 6)G(6, 2) \\ &+ i \int d3d5 G_H^0(1, 3)W(3^+, 5)G_H^0(3, 6)\delta(7, 6) \frac{\delta G(5, 2; [\bar{\varphi}])}{\delta \bar{\varphi}(7)} \Big|_{\varphi=0} \\ &+ \int d3d5 G_H^0(1, 3)W(3^+, 5)G_H^0(3, 5)\delta(7, 6) \frac{\delta G(5, 2; [\bar{\varphi}])}{\delta \bar{\varphi}(7)} \Big|_{\varphi=0} \end{aligned} \quad (\text{D.16})$$

$$(\text{D.17})$$

Let's define the following quantities:

- $\frac{\delta G(1, 2; [\bar{\varphi}])}{\delta \bar{\varphi}(6)} \Big|_{\varphi=0} := g(1, 6)$
- $\frac{\delta G(5, 2; [\bar{\varphi}])}{\delta \bar{\varphi}(7)} \Big|_{\varphi=0} := g(5, 7)$
- $G_H^0(1, 6)G(6, 2) := g_0(1, 6)$
- $m(16; 57) = i \int d3W(3^+, 5)G_H^0(1, 3)\delta(7, 6) [G_H^0(3, 6) + G_H^0(3, 5)]$

we can now recast Eq. D.1 using the new variables as:

$$g(1, 6) = g^0(1, 6) + \int d5d7 m(1, 6; 5, 7)g(5, 7). \quad (\text{D.18})$$

Solving for  $g$ :

$$\left[ \int d5d7m(1, 6; 5, 7) - \delta(1, 5)\delta(7, 6) \right] g(5, 7) + g_0(1, 6) = 0. \quad (\text{D.19})$$

We define

$$[m(1, 6; 5, 7) - \delta(1, 5)\delta(7, 6)] = \bar{m}(1, 6; 5, 7) \quad (\text{D.20})$$

inserting this into Eq. (D.19):

$$\int d5d7\bar{m}(1, 6; 5, 7)g(5, 7) + g_0(1, 6) = 0 \quad (\text{D.21})$$

and introducing the inverse of  $\bar{m}$  one gets:

$$\begin{aligned} \int d1657\bar{m}^{-1}(8, 9; 1, 6)\bar{m}(1, 6; 5, 7)g(5, 7) &= - \int d16\bar{m}^{-1}(8, 9; 1, 6)g_0(1, 6) \\ g(9, 8) &= - \int d16\bar{m}^{-1}(8, 9; 1, 6)g_0(1, 6). \end{aligned} \quad (\text{D.22})$$

Transforming back to the *original* variables:

$$\begin{aligned} g(9, 8) &:= \left. \frac{\delta G(9, 2; [\bar{\varphi}])}{\delta \bar{\varphi}(8)} \right|_{\varphi=0} \rightarrow \left. \frac{\delta G(1, 2; [\bar{\varphi}])}{\delta \bar{\varphi}(6)} \right|_{\varphi=0} \\ &= - \int d98\bar{m}^{-1}(1, 6; 9, 8)G_H^0(9, 8)G(8, 2) \end{aligned} \quad (\text{D.23})$$

we obtain a Green's function reading:

$$G(1, 2) = G_H^0(1, 2) - \int d53G_H^0(1, 3)W(3^+, 5) \int d98\bar{m}^{-1}(3, 5; 9, 8)G_H^0(9, 8)G(8, 2). \quad (\text{D.24})$$

The above expression can be written in form of a Dyson equation too: this allows for an identification of some  $\Sigma$ , so as to try to identify the result with some other well-known approximation for  $G$ , (as it was done for the  $O(d_x^1)$  of the LODE)

$$G(1, 2) = G_H^0(1, 2) - \int d3d8G_H^0(1, 3)\Sigma(3, 8)G(8, 2) \quad (\text{D.25})$$

where the self-energy has the form:

$$\Sigma(3, 8) = \int d5d9W(3^+, 5)\bar{m}^{-1}(3, 5; 9, 8)G_H^0(9, 8). \quad (\text{D.26})$$

# APPENDIX E

## Self-consistent calculations of $y_H^0$ and $u$

We will detail here how the result in Eq. (4.60) has been obtained. Three equations are needed, namely Eq. (3.15), the Dyson equation for  $y_H^0$  as a function of the truly non-interacting  $y_0$ , reading:

$$y_H^0 = y_0 + y_0 v y_u y_H^0 \quad (\text{E.1})$$

it follows that:

$$y_H^0 = \frac{y_0}{1 - y_0 v y_u} \quad (\text{E.2})$$

and an equation for the screened Coulomb potential  $u$  as a function of the bare one  $v$ , namely:

$$u = v + v^2 \frac{dy_u(x)}{dx}. \quad (\text{E.3})$$

The linearized 1-point differential equation can be recast in order to isolate the derivative of the Green's function with respect to the external potential:

$$\frac{dy_u(x)}{dx} = \frac{y_H^0 - y_u(x)}{u y_H^0}. \quad (\text{E.4})$$

Inserting this expression into Eq. (E.3) yields:

$$u = v + v^2 \left\{ \frac{y_H^0 - y_u(x)}{u y_H^0} \right\} \quad (\text{E.5})$$

which is the equation we want to solve *self-consistently* to obtain the screened potential  $u$ . Of course, if one aims at a fully-self consistent approach, also the zero-potential Hartree  $G$  has to be evaluated at each step starting from  $y_0$ . To account for this we also substitute (E.2) into (E.5), obtaining:

$$u = v + v^2 \left\{ \frac{\frac{y_0}{1 - v y_0 y_u} - y_u(x)}{u \frac{y_0}{1 - v y_0 y_u}} \right\} \quad (\text{E.6})$$

and after some algebra<sup>a</sup> one can write down a second order equation for  $u$ :

$$u^2 - uv - v^2 \left\{ 1 - \frac{y_u(x)}{y_0} + v y_u^2(x) \right\} = 0 \quad (\text{E.7})$$

which yields precisely the two solutions of (4.60).

To obtaining the result of Eq. (4.61) one has to follow an identical procedure, however the linearized 1-point DE has to be substituted by its non-linearized version, namely Eq. (3.14).

---

<sup>a</sup>Note that now that all the expressions following from now are taken at vanishing  $x$

# APPENDIX F

## Solving the integral equation for the auxiliary $G_{\bar{\varphi}}$

We have to solve the following *integral* equation:<sup>a</sup>

$$y(t_1, t_2; [\varphi]) = \theta(t_1 - t_2) - i \int_{-\infty}^{t_1} dt_3 \varphi(t_3) y(t_3, t_2; [\varphi]). \quad (\text{F.1})$$

The first step is to transform it into a *differential* equation, reading:

$$\frac{\partial}{\partial t_1} y(t_1, t_2; [\varphi]) = \delta(t_1 - t_2) - i\varphi(t_1) y(t_1, t_2; [\varphi]) \quad (\text{F.2})$$

A possible ansatz for the solution reads:

$$y(t_1, t_2; [\varphi]) = A(t_1, t_2) B(t_1, t_2). \quad (\text{F.3})$$

where  $A$  and  $B$  can be any non-zero function of both  $t_1$  and  $t_2$ . Inserting the ansatz into Eq. (F.2) yields:

$$\left[ \frac{\partial}{\partial t_1} A(t_1, t_2) \right] B(t_1, t_2) + \left[ \frac{\partial}{\partial t_1} B(t_1, t_2) \right] A(t_1, t_2) = \delta(t_1 - t_2) - i\varphi(t_1) A(t_1, t_2) B(t_1, t_2) \quad (\text{F.4})$$

---

<sup>a</sup>We substitute  $\tilde{y}$  with a simpler  $y$  to simplify the notation

which can be split into two simple differential equations. We begin by solving:

$$\left[ \frac{\partial}{\partial t_1} A(t_1, t_2) \right] B(t_1, t_2) = -i\varphi(t_1)A(t_1, t_2)B(t_1, t_2), \quad (\text{F.5})$$

$$\frac{\partial}{\partial t_1} A(t_1, t_2) \cdot \frac{1}{A(t_1, t_2)} = -i\varphi(t_1) \quad (\text{F.6})$$

$$\int_a^b dt_1 \frac{\partial}{\partial t_1} \ln \{A(t_1, t_2)\} = -i \int_a^b dt_{1'} \varphi(t_{1'}) \quad (\text{F.7})$$

$$A(t_1, t_2) = e^{\ln \{A(a, t_2)\} - i \int_a^{t_1} dt_{1'} \varphi(t_{1'})} \quad (\text{F.8})$$

$$A(t_1, t_2) = C(a, t_2) e^{-i \int_a^{t_1} dt_{1'} \varphi(t_{1'})} \quad (\text{F.9})$$

where  $C(a, t_2)$  is to be set to solve the initial value problem and the value of  $b$  has been arbitrarily set equal to  $t_1$  along the calculation.

One can now solve the second equation, made up of the second and the third terms of (F.4), namely:

$$\frac{\partial}{\partial t_1} B(t_1, t_2) A(t_1, t_2) = \delta(t_1, t_2). \quad (\text{F.10})$$

The equation can immediately be recast inserting the general solution for  $A(t_1, t_2)$ “

$$\frac{\partial}{\partial t_1} B(t_1, t_2) = \delta(t_1, t_2) \frac{1}{C(a, t_2)} e^{i \int_a^{t_1} dt_{1'} \varphi(t_{1'})} \quad (\text{F.11})$$

integrating on both sides with respect to  $\int_{\tilde{a}}^{\tilde{b}} dt_1$  one obtains:

$$\int_{\tilde{a}}^{\tilde{b}} dt_1 \frac{\partial}{\partial t_1} B(t_1, t_2) = \frac{1}{C(a, t_2)} \int_{\tilde{a}}^{\tilde{b}} dt_1 \delta(t_1, t_2) e^{i \int_a^{t_1} dt_{1'} \varphi(t_{1'})} \quad (\text{F.12})$$

$$B(t_1, t_2) = B(\tilde{a}, t_2) + \frac{1}{C(a, t_2)} e^{i \int_a^{t_2} dt_{1'} \varphi(t_{1'})} \quad \text{for } \tilde{b} = t_1 \quad \text{and} \quad \tilde{a} < t_2 < t_1 \quad (\text{F.13})$$

and finally the full  $y(t_1, t_2; [\varphi])$  can be written as:

$$y(t_1, t_2; [\varphi]) = C(a, t_2) e^{-i \int_a^{t_1} dt_{1'} \varphi(t_{1'})} \left[ B(\tilde{a}, t_2) + \frac{1}{C(a, t_2)} e^{i \int_a^{t_2} dt_{1'} \varphi(t_{1'})} \right] \quad (\text{F.14})$$

$$= C(a, t_2) B(\tilde{a}, t_2) e^{-i \int_a^{t_1} dt_t \varphi(t)} + e^{+i \int_{t_1}^a dt_t \varphi(t) + i \int_a^{t_2} dt_t \varphi(t)} \quad (\text{F.15})$$

$$(\text{F.16})$$

defining a unique constant  $D(a, \tilde{a}, t_2) := C(a, t_2) B(\tilde{a}, t_2)$  one can recast (F.15) as:

$$y(t_1, t_2; [\varphi]) = D(a, \tilde{a}, t_2) e^{-i \int_a^{t_1} dt_t \varphi(t)} + e^{i \int_{t_1}^{t_2} dt_t \varphi(t)} \quad (\text{F.17})$$

choosing  $D(a, \tilde{a}, t_2) = 0$  yields:

$$y(t_1, t_2; [\varphi]) = e^{i \int_{t_1}^{t_2} dt_t \varphi(t)} \quad \text{for } \tilde{a} < t_2 < t_1 \quad (\text{F.18})$$

which is precisely the solution shown in Eq. (5.11).

# APPENDIX G

## Algebra for solving the full functional DE

### G.1 Verifying the ansatz for $f$ and $a$

First we want to solve a simpler version of Eq. (6.3), namely:

$$\varphi(6)f([\varphi]) = -i \int d4W(6,4) \frac{\delta f([\varphi])}{\delta \varphi(4)} \quad (\text{G.1})$$

First we integrate from the left with the inverse of  $G_0$ :

$$\begin{aligned} & \int d3d5d1G^{-1}(6,1)G_0(1,3)\varphi(3)f([\varphi])a(3,5;[\varphi])\mathcal{J}(5,2;[\varphi]) = \\ & -i \int d3d4d5d1G^{-1}(6,1)G_0(1,3)v(3,4) \frac{\delta f([\varphi])}{\delta \varphi(4)} a(3,5;[\varphi])\mathcal{J}(5,2;[\varphi]) \end{aligned} \quad (\text{G.2})$$

$$\int d5\varphi(6)f([\varphi])a(6,5;[\varphi])\mathcal{J}(5,2;[\varphi]) = -i \int d4d5v(6,4) \frac{\delta f([\varphi])}{\delta \varphi(4)} a(6,5;[\varphi])\mathcal{J}(5,2;[\varphi]) \quad (\text{G.3})$$

To simplify even more we integrate from the right with the inverse of  $\mathcal{J}$ , and obtain:

$$\begin{aligned} \int d5d2\varphi(6)f([\varphi])a(6,5;[\varphi])\mathcal{J}(5,2;[\varphi])\mathcal{J}^{-1}(2,7;[\varphi]) &= -i \int d4d5d2v(6,4) \frac{\delta f([\varphi])}{\delta \varphi(4)} \\ &\times a(6,5;[\varphi])\mathcal{J}(5,2;[\varphi])\mathcal{J}^{-1}(2,7;[\varphi]) \end{aligned} \quad (\text{G.4})$$

$$\varphi(6)f([\varphi])a(6,7;[\varphi]) = -i \int d4v(6,4) \frac{\delta f([\varphi])}{\delta \varphi(4)} a(6,7;[\varphi]) \quad (\text{G.5})$$

$$(\text{G.6})$$

Dropping  $a(6,7;[\varphi])$  on both sides:

$$\varphi(6)f([\varphi]) = -i \int d4v(6,4) \frac{\delta f([\varphi])}{\delta \varphi(4)}. \quad (\text{G.7})$$

This will be the equation for  $f([\varphi])$  for which we formulate an exponential ansatz (see Eq. (6.5)).

In the following we verify that the ansatz really satisfy the differential equation.

Differentiating with respect to  $\varphi$  gives:

$$\begin{aligned} \frac{\delta f([\varphi])}{\delta \varphi(4)} &= \frac{i}{2} \left\{ \int d\tilde{5} d\tilde{6} W^{-1}(\tilde{6}, \tilde{5}) \delta(\tilde{5}, 4) \varphi(\tilde{6}) + \int d\tilde{5} d\tilde{6} W^{-1}(\tilde{6}, \tilde{5}) \varphi(\tilde{5}) \delta(\tilde{6}, 4) \right\} e^{\frac{i}{2} \int d5 d6 W^{-1}(6,5) \varphi(5) \varphi(6)} \\ &= \frac{i}{2} \left\{ \int d\tilde{6} W^{-1}(\tilde{6}, 4) \varphi(\tilde{6}) + \int d\tilde{5} W^{-1}(4, \tilde{5}) \varphi(\tilde{5}) \right\} e^{\frac{i}{2} \int d5 d6 W^{-1}(6,5) \varphi(5) \varphi(6)} \end{aligned} \quad (\text{G.8})$$

inserting this result into (G.1) yields:

$$\begin{aligned} \varphi(6) f([\varphi]) &= -i \left[ \frac{i}{2} \int d4 d\tilde{5} W(4, 6) W^{-1}(4, \tilde{5}) \varphi(\tilde{5}) \right. \\ &\quad \left. + \frac{i}{2} \int d4 d\tilde{6} W(4, 6) W^{-1}(4, \tilde{6}) \varphi(\tilde{6}) \right] e^{\frac{i}{2} \int d5 d6 W^{-1}(6,5) \varphi(5) \varphi(6)} \end{aligned} \quad (\text{G.9})$$

which can be written as:

$$\varphi(6) f([\varphi]) = \left[ \frac{1}{2} \varphi(6) + \frac{1}{2} \varphi(6) \right] f([\varphi]) \quad (\text{G.10})$$

where we have assumed  $W$  symmetric in order to obtain the expression in Eq. (G.10). We can readily see that the identity in Eq. (G.10) is satisfied.

We now show how also the ansatz for  $a$  (Eq. (6.8)) satisfies the respective DE:

$$\begin{aligned} \frac{\delta a(3, 5; [\varphi])}{\delta \varphi(4)} &= j(3, 5) \left\{ -i \int d\tilde{6} d\tilde{7} d\tilde{8} \frac{j(\tilde{8}, 5)}{j(\tilde{7}, 5)} W^{-1}(\tilde{6}, \tilde{7}) G_0^{-1}(\tilde{7}, \tilde{8}) \delta(\tilde{6}, 4) \right\} e^{-i \int d6 d7 d8 \frac{j(8,5)}{j(7,5)} W^{-1}(6,7) G_0^{-1}(7,8) \varphi(6)} \\ &= j(3, 5) \left\{ -i \int d\tilde{7} d\tilde{8} \frac{j(\tilde{8}, 5)}{j(\tilde{7}, 5)} W^{-1}(4, \tilde{7}) G_0^{-1}(\tilde{7}, \tilde{8}) \right\} e^{-i \int d6 d7 d8 \frac{j(8,5)}{j(7,5)} W^{-1}(6,7) G_0^{-1}(7,8) \varphi(6)} \end{aligned} \quad (\text{G.11})$$

and inserting into (6.7):

$$\begin{aligned} a(1, 5; [\varphi]) &= \left[ \int d3 d4 d\tilde{7} d\tilde{8} j(3, 5) \frac{j(\tilde{8}, 5)}{j(\tilde{7}, 5)} G_0(1, 3) W(3, 4) W^{-1}(4, \tilde{7}) G_0^{-1}(\tilde{7}, \tilde{8}) \right] \\ &\quad \times e^{-i \int d7 d8 \frac{j(8,5)}{j(7,5)} W^{-1}(6,7) G_0^{-1}(7,8) \varphi(6)} \\ &= \int d\tilde{6} d\tilde{7} d\tilde{8} j(\tilde{7}, 5) \frac{j(\tilde{8}, 5)}{j(\tilde{7}, 5)} G_0(1, \tilde{7}) G_0^{-1}(\tilde{7}, \tilde{8}) e^{-i \int d6 d7 d8 \frac{j(8,5)}{j(7,5)} W^{-1}(6,7) G_0^{-1}(7,8) \varphi(6)} \\ &= j(1, 5) e^{-i \int d6 d7 d8 \frac{j(8,5)}{j(7,5)} W^{-1}(6,7) G_0^{-1}(7,8) \varphi(6)} \\ &= a(1, 5; [\varphi]) \end{aligned} \quad (\text{G.12})$$

## G.2 Formula for the integration of $\frac{\delta \mathcal{J}([\varphi])}{\delta \varphi}$

Here we show in a more rigorous way how the functional integration formula in Eq. (6.23) can be derived.

Suppose we have a functional  $\mathcal{F}([\varphi])$  which is Taylor expandable, let's then perform the expansion with respect to  $\varphi$  and let's center it around zero (only for simplicity, any other point belonging to the domain of  $\varphi$  would also be fine). We get:

$$\mathcal{F}([\varphi]) = \mathcal{F}([\varphi = 0]) + \int dx \frac{\delta \mathcal{F}([\varphi])}{\delta \varphi(x)} \Big|_{\varphi=0} \cdot \varphi(x) + \frac{1}{2} \int dx dy \frac{\delta^2 \mathcal{F}([\varphi])}{\delta \varphi(x) \delta \varphi(y)} \Big|_{\varphi=0} \cdot \varphi(x) \varphi(y) + \mathcal{O}(3) \quad (\text{G.13})$$

which can be expressed in a more compact way as:

$$\mathcal{F}([\varphi]) = \mathcal{F}([\varphi = 0]) + \sum_{n=2}^{\infty} \frac{1}{(n-1)!} \int dx_1 \cdots dx_{n-1} \frac{\delta^{n-1} \mathcal{F}([\varphi])}{\delta \varphi(x_1) \cdots \delta \varphi(x_{n-1})} \Big|_{\varphi=0} \cdot \varphi(x_1) \cdots \varphi(x_{n-1}) \quad (\text{G.14})$$

Let's now differentiate  $\mathcal{F}([\bar{\varphi}])$  with respect to  $\bar{\varphi}$ , where  $\bar{\varphi} = \lambda \cdot \varphi$  and  $\lambda$  is simply a parameter. We obtain:

$$\begin{aligned} \frac{\delta \mathcal{F}([\bar{\varphi}])}{\delta \bar{\varphi}(z)} = 0 &+ \sum_{n=2}^{\infty} \frac{1}{(n-1)!} \int dx_1 \cdots dx_{n-1} \frac{\delta^{n-1} \mathcal{F}([\bar{\varphi}])}{\delta \bar{\varphi}(x_1) \cdots \delta \bar{\varphi}(x_{n-1})} \Big|_{\bar{\varphi}=0} \\ &\times \{ \delta(x_1 - z) \bar{\varphi}(x_2) \cdots \bar{\varphi}(x_{n-1}) + \bar{\varphi}(x_1) \delta(x_2 - z) \cdots \bar{\varphi}(x_{n-1}) + \cdots \} \quad (\text{G.15}) \\ &= \sum_{n=2}^{\infty} \frac{1}{(n-1)!} \left[ \int dx_2 \cdots dx_{n-1} \frac{\delta^{n-1} \mathcal{F}([\bar{\varphi}])}{\delta \bar{\varphi}(z) \cdots \delta \bar{\varphi}(x_{n-1})} \Big|_{\bar{\varphi}=0} \cdot \bar{\varphi}(x_2) \cdots \bar{\varphi}(x_{n-1}) \right. \\ &+ \int dx_1 dx_3 \cdots dx_{n-1} \frac{\delta^{n-1} \mathcal{F}([\bar{\varphi}])}{\delta \bar{\varphi}(x_1) \delta \bar{\varphi}(z) \cdots \delta \bar{\varphi}(x_{n-1})} \Big|_{\bar{\varphi}=0} \cdot \bar{\varphi}(x_1) \bar{\varphi}(x_3) \cdots \bar{\varphi}(x_{n-1}) \\ &+ \cdots \left. \right] \quad (\text{G.16}) \end{aligned}$$

conveniently exchanging some indices under the integral symbol (e.g. in the second term above  $x_3 \rightarrow x_2$ ) yields:

$$\begin{aligned} \frac{\delta \mathcal{F}([\bar{\varphi}])}{\delta \bar{\varphi}(z)} = 0 &+ \sum_{n=2}^{\infty} \frac{1}{(n-1)!} \left[ \int dx_2 \cdots dx_{n-1} \frac{\delta^{n-1} \mathcal{F}([\bar{\varphi}])}{\delta \bar{\varphi}(z) \cdots \delta \bar{\varphi}(x_{n-1})} \Big|_{\bar{\varphi}=0} \cdot \bar{\varphi}(x_2) \cdots \bar{\varphi}(x_{n-1}) \right. \\ &+ \int dx_2 \cdots dx_{n-1} \frac{\delta^{n-1} \mathcal{F}([\bar{\varphi}])}{\delta \bar{\varphi}(x_2) \delta \bar{\varphi}(z) \cdots \delta \bar{\varphi}(x_{n-1})} \Big|_{\bar{\varphi}=0} \cdot \bar{\varphi}(x_2) \cdots \bar{\varphi}(x_{n-1}) \\ &+ \cdots \left. \right] \quad (\text{G.17}) \end{aligned}$$

summing up all the -now equal- integrals give a prefactor which combined with the factorial in the above equations yields  $\frac{n-1}{(n-1)!} = \frac{1}{(n-2)!}$ , hence Eq. (G.17) can be recast as<sup>a</sup>:

$$\frac{\delta \mathcal{F}([\bar{\varphi}])}{\delta \bar{\varphi}(z)} = \sum_{n=2}^{\infty} \frac{1}{(n-2)!} \left\{ \int dx_2 \cdots dx_{n-1} \frac{\delta^{n-1} \mathcal{F}([\bar{\varphi}])}{\delta \bar{\varphi}(z) \cdots \delta \bar{\varphi}(x_{n-1})} \Big|_{\bar{\varphi}=0} \cdot \bar{\varphi}(x_2) \cdots \bar{\varphi}(x_{n-1}) \right\}. \quad (\text{G.18})$$

<sup>a</sup>The term  $n = 2$  has to be understood as  $\frac{\delta \mathcal{F}([\varphi])}{\delta \delta \bar{\varphi}(z)} \Big|_{\bar{\varphi}=0}$

Inserting both Eq. (G.14) and Eq. (G.18) into the functional integration formula we want to verify (Eq. (6.23)) we obtain:

$$\begin{aligned}
\mathcal{F}([\varphi = 0]) &+ \sum_{n=2}^{\infty} \frac{1}{(n-1)!} \int dx_1 \cdots dx_{n-1} \frac{\delta^{n-1} \mathcal{F}([\varphi])}{\delta \varphi(x_1) \cdots \delta \varphi(x_{n-1})} \Big|_{\varphi=0} \cdot \varphi(x_1) \cdots \varphi(x_{n-1}) \\
&= \mathcal{F}([\varphi = 0]) + \int_0^1 d\lambda \int dz \sum_{n=2}^{\infty} \frac{1}{(n-2)!} \int dx_2 \cdots dx_{n-1} \frac{\delta^{n-1} \mathcal{F}([\bar{\varphi}])}{\delta \bar{\varphi}(z) \cdots \delta \bar{\varphi}(x_{n-1})} \Big|_{\bar{\varphi}=0} \\
&\quad \cdot \lambda \varphi(x_2) \cdots \lambda \varphi(x_{n-1}) \cdot \varphi(z) \tag{G.19}
\end{aligned}$$

and finally:

$$\begin{aligned}
&\sum_{n=2}^{\infty} \frac{1}{(n-1)!} \int dx_1 \cdots dx_{n-1} \frac{\delta^{n-1} \mathcal{F}([\varphi])}{\delta \varphi(x_1) \cdots \delta \varphi(x_{n-1})} \Big|_{\varphi=0} \cdot \varphi(x_1) \cdots \varphi(x_{n-1}) = \tag{G.20} \\
&= \int_0^1 d\lambda \int dz \sum_{n=2}^{\infty} \frac{\lambda^{n-2}}{(n-2)!} dx_2 \cdots dx_{n-1} \frac{\delta^{n-1} \mathcal{F}([\bar{\varphi}])}{\delta \bar{\varphi}(z) \cdots \delta \bar{\varphi}(x_{n-1})} \Big|_{\bar{\varphi}=0} \cdot \varphi(x_2) \cdots \varphi(x_{n-1}) \cdot \varphi(z) \\
&= \sum_{n=2}^{\infty} \int dz \frac{\lambda^{n-1}}{(n-1)(n-2)!} \left\{ dx_2 \cdots dx_{n-1} \frac{\delta^{n-1} \mathcal{F}([\bar{\varphi}])}{\delta \bar{\varphi}(z) \cdots \delta \bar{\varphi}(x_{n-1})} \Big|_{\bar{\varphi}=0} \cdot \varphi(x_2) \cdots \varphi(x_{n-1}) \right\} \varphi(z) \Big|_{\lambda=0}^{\lambda=1} \\
&= \sum_{n=2}^{\infty} \frac{1}{(n-1)!} \int dz dx_2 \cdots dx_{n-1} \frac{\delta^{n-1} \mathcal{F}([\bar{\varphi}])}{\delta \bar{\varphi}(z) \cdots \delta \bar{\varphi}(x_{n-1})} \Big|_{\bar{\varphi}=0} \cdot \varphi(x_2) \cdots \varphi(x_{n-1}) \varphi(z) \tag{G.21}
\end{aligned}$$

Setting  $z = x_1$  in the second term of Eq. (G.21) satisfies the identity. The only caveat of the functional integration formula (6.23) is, as we have already mentioned in the end of Chapter (6), that the functional derivative of  $\mathcal{F}$  has to be compatible with its Taylor expansion with respect to  $\varphi$ . Unfortunately this was not the case for  $\mathcal{J}([\varphi])$ .

### G.2.1 A simple functional to which the integration formula applies

To better elucidate the caveats of the above integration formula, let's examine a simple function for which the formula yields a correct result. First let's recall the formula:

$$\overbrace{\mathcal{F}([\varphi])}^1 = \overbrace{\mathcal{F}([\varphi = 0])}^2 + \overbrace{\int_0^1 d\lambda \int dx \frac{\delta \mathcal{F}([\bar{\varphi}])}{\delta \bar{\varphi}(x)} \varphi(x)}^3. \tag{G.22}$$

Suppose we have:

$$\mathcal{F}(\varphi) = \int dz \varphi(z) \tag{G.23}$$

inserting it in Eq. (G.22) we have:

$$\int dz \varphi(z) = 0 + \int_0^1 d\lambda \int dx \frac{d}{d\lambda \cdot \varphi(x)} \left[ \int dz \lambda \cdot \varphi(z) \right] \varphi(x) \tag{G.24}$$

$$\int dz \varphi(z) = \int_0^1 d\lambda \int dx dz \delta(z-x) \varphi(x) \tag{G.25}$$

$$\int dz \varphi(z) = \int dz \varphi(z) \cdot \lambda \Big|_{\lambda=0}^{\lambda=1} = \int dz \varphi(z) \tag{G.26}$$

the last identity proves the formula to be correct for this specific case.

## G.2.2 A simple functional to which the integration formula *does not* apply

We will here provide a counter example. Let's suppose to have an  $\mathcal{F}$  reading:

$$\frac{\delta \mathcal{F}([\varphi])}{\delta \varphi(x)} = a(x) \cdot \int dy \varphi(y) \quad (\text{G.27})$$

inserting it into Eq. (G.22) yields:

$$\begin{aligned} a(x) \cdot \int dy \varphi(y) &= 0 + \int_0^1 d\lambda \int dx a(x) \varphi(x) \int dy \varphi(y) \lambda \\ &= \frac{1}{2} \int dx a(x) \varphi(x) \int dy \varphi(y). \end{aligned} \quad (\text{G.28})$$

Differentiating Eq. (G.28) with respect to  $\varphi$  should give back the original function  $\mathcal{F}$ , but we will show here it doesn't, in fact:

$$\begin{aligned} \frac{\delta \mathcal{F}([\varphi])}{\delta \varphi(z)} &= \frac{1}{2} \int dx a(x) \delta(x-z) \int dy \varphi(y) + \frac{1}{2} \int dx a(x) \varphi(x) \int dy \delta(y-z) \\ &= \frac{1}{2} a(z) \int dy \varphi(y) + \frac{1}{2} \int dx a(x) \varphi(x). \end{aligned} \quad (\text{G.29})$$

The latter expression is obviously different from the initial given functional.

## G.3 Insights from the N-times framework

We will now write down all the N-times equations -completely equivalent to the full functional ones of Chap. 6. The idea is to get some insights on the possible "pathologies" of the integrand. The N-times differential equation reads:

$$g(t_1, t_2; [\varphi]) = i\theta(t_2 - t_1) + i \int_{t_1}^{\infty} dt_3 \varphi(t_3) g(t_3, t_2; [\varphi]) + i^2 \int_{t_1}^{\infty} dt_3 \int_{t_1}^{\infty} dt_4 W(t_3, t_4) \frac{\delta g(t_3, t_2; [\varphi])}{\delta \varphi(t_4)} \quad (\text{G.30})$$

where  $i\theta(t_2 - t_1) = g_0(t_1, t_2) = G_0(t_1, t_2)e^{i\epsilon(t_1 - t_2)}$ ,  $g(t_1, t_2; [\varphi]) = G(t_1, t_2; [\varphi])e^{i\epsilon(t_1 - t_2)}$  and  $G_0$  is a hole-only non-interacting Green's function. The ansatz for  $g$  reads:<sup>b</sup>

$$g(t_1, t_2; [\varphi]) = \int dt_6 f([\varphi]) a(t_1, t_6; [\varphi]) \mathcal{J}(t_6, t_2; [\varphi]) \quad (\text{G.31})$$

which inserted into (G.30) suggests again to write down separately three differential equations for  $f([\varphi])$ ,  $a([\varphi])$  and  $\frac{\delta \mathcal{J}([\varphi])}{\delta \varphi}$ , for which the following ansatz can be formulated:

$$f([\varphi]) = e^{\frac{i}{2} \int dt_7 dt_8 W^{-1}(t_7, t_8) \varphi(t_7) \varphi(t_8)} \quad (\text{G.32a})$$

$$a(t_3, t_6; [\varphi]) = j(t_3, t_6) \epsilon(t_6, [\varphi]) = j(t_3, t_6) e^{-\int dt_9 t_7 t_8 \frac{j(t_8, t_6)}{j(t_7, t_6)} W^{-1}(t_9, t_7) \theta^{-1}(t_8 - t_7) \varphi(t_9)} \quad (\text{G.32b})$$

<sup>b</sup>Note the perfect analogy with the ansatz for the full  $G$ .

this leads to an equation for  $\frac{\mathcal{J}(t_6, t_2; [\varphi])}{\delta\varphi(t_4)}$  reading:

$$i\theta(t_2 - t_1) + i^2 \int_{t_1}^{\infty} dt_3 \int dt_6 t_4 W(t_3, t_4) f([\varphi]) a(t_3, t_6; [\varphi]) \frac{\mathcal{J}(t_6, t_2; [\varphi])}{\delta\varphi(t_4)} = 0 \quad (\text{G.33})$$

which, again *in analogy with the full functional case, cannot be inverted, since it has several possible solutions.*

It seems that so far nothing has been gained going back to the N-times playground. However, we should not forget that we *do know* the form of the exact one-body  $G$  in this case. Hence we simply express  $\mathcal{J}([\varphi])$  as a function of  $a$ ,  $f$  and  $g$  and try to get insights on the form it should have (in other words we are do some reverse engineering process on  $\mathcal{J}([\varphi])$ ). The first step is to recast Eq. (G.31) as:

$$\mathcal{J}(t_2, t_6; [\varphi]) = f^{-1}([\varphi]) \int dt_1 a^{-1}(t_6, t_1; [\varphi]) g(t_1, t_2; [\varphi]) \quad (\text{G.34})$$

then we have to perform the derivative with respect to the external potential (since we are ultimately interested in  $\frac{\mathcal{J}(t_2, t_6; [\varphi])}{\delta\varphi(t_4)}$ ):

$$\begin{aligned} \frac{\mathcal{J}(t_2, t_6; [\varphi])}{\delta\varphi(t_4)} &= \frac{\delta}{\delta\varphi(t_4)} \left( f^{-1}([\varphi]) \int dt_1 a^{-1}(t_6, t_1; [\varphi]) g(t_1, t_2; [\varphi]) \right) \\ &= f^{-1}([\varphi]) \int dt_1 a^{-1}(t_6, t_1; [\varphi]) g(t_1, t_2; [\varphi]) \left[ -i \int dt_7 W^{-1}(t_4, t_7) \varphi(t_7) \right. \\ &\quad \left. + \frac{W^{-1}(t_4, t_6)}{j(t_6, t_6)} + i\theta(t_2 - t_4)\theta(t_4 - t_1) \right]. \end{aligned} \quad (\text{G.35})$$

The complicated form of Eq. (G.35) is a further proof that finding an ansatz (from scratch) for  $\frac{\delta\mathcal{J}(t_2, t_6; [\varphi])}{\delta\varphi(t_4)}$  is really a difficult task.

This is why, as anticipated in the previous section, we will reformulate our quest for  $\frac{\delta\mathcal{J}([\varphi])}{\delta\varphi}$  in a different way, introducing also here a new quantity:

$$q(t_1, t_2, t_6; [\varphi, W]) = \int_{t_1}^{\infty} dt_3 \int dt_4 W(t_3, t_4) f([\varphi]) a(t_3, t_6) \frac{\delta\mathcal{J}(t_6, t_2; [\varphi])}{\delta\varphi(t_4)} \quad (\text{G.36})$$

where  $q$  has to satisfy:

$$i\theta(t_2 - t_1) = g_0(t_1, t_2) = \int dt_6 q(t_1, t_2, t_6; [\varphi, W]). \quad (\text{G.37})$$

We can now express  $\frac{\delta\mathcal{J}(t_2, t_6; [\varphi])}{\delta\varphi(t_4)}$  as a function of  $q(t_1, t_2, t_6; [\varphi, W])$  (see Eq. (6.15)):

$$\frac{\delta\mathcal{J}(t_2, t_6; [\varphi])}{\delta\varphi(t_7)} = \int dt_1 dt_5 \frac{\theta^{-1}(t_1 - t_5) q(t_1, t_2, t_6; [\varphi, W]) W^{-1}(t_7, t_5)}{f([\varphi]) a(t_5, t_6; [\varphi])} \quad (\text{G.38})$$

Once again, many possible  $q([\varphi])$ s can satisfy Eq. (G.37). Substituting (G.35) into (G.36) one can obtain an *exact expression* for  $q$ , namely:

$$q(t_1, t_2, t_6; [\varphi, W]) = \int_{t_1}^{\infty} dt_3 \int dt_{\bar{1}} j(t_3, t_6) g(t_{\bar{1}}, t_2; [\varphi]) j^{-1}(t_6, t_{\bar{1}}) \left[ -i\varphi(t_3) + \frac{\delta(t_3, t_6)}{j(t_3, t_3)} + i \int W(t_3, t_8) \theta(t_2 - t_8) \theta(t_8 - t_{\bar{1}}) \right] \quad (\text{G.39})$$

where  $g(t_{\bar{1}}, t_2; [\varphi])$  is the exact expression for the core  $G$  and  $j(t_3, t_6)$  hasn't been chosen yet. The above result, together with Eq. (G.35) are very precious insight delivered directly by the N-times framework: in the full functional framework we could not access the exact  $q([\varphi])$  and the exact  $\frac{\delta\mathcal{J}([\varphi])}{\delta\varphi}$  (if not formally), while here, thanks to the knowledge of the exact N-times  $G$  we actually calculated them.

## G.4 An alternative ansatz

One can also think of modifying the ansatz for  $G$  (Eq. (6.1)). Our first ansatz was mainly based on the insights that we had obtained by solving the algebraic DE in the 1-point framework. This alternative ansatz is instead based on results obtained in the context of the decoupling approximation for the N-times Green's function. Its expression is very similar to that of Eq. (5.18), where embedding the external potential  $\varphi$  in a non-interacting Green's function, had considerably simplified the problem to solve. In the full functional framework the guess would read:

$$G(1, 2; [\varphi]) = \int d3 G_{\varphi}(1, 3) \cdot \mathcal{F}_{[\varphi, W]}(3, 2). \quad (\text{G.40})$$

The above equation is slightly more complicated than the N-times one, namely  $G_{\varphi}$  and  $\mathcal{F}_{[W, \varphi]}$  are integrated, rather than simply multiplied and we have assumed  $\mathcal{F}_{[W, \varphi]}$  to be dependent also on the external potential  $\varphi$ .<sup>c</sup> From now on a symbolic notation<sup>d</sup> will be employed. Inserting the -symbolic- ansatz (G.40) into the N-points equivalent<sup>e</sup> of Eq. (5.3) one gets:

$$G_{\varphi} \cdot \mathcal{F}_{[\varphi, W]} = G_{\varphi} + G_{\varphi} W \left\{ \frac{\delta G_{\varphi}}{\delta\varphi} \cdot \mathcal{F}_{[\varphi, W]} + G_{\varphi} \frac{\delta \mathcal{F}_{[\varphi, W]}}{\delta\varphi} \right\}. \quad (\text{G.41})$$

Both  $\frac{\delta G_{\varphi}}{\delta\varphi} \cdot \mathcal{F}_{[\varphi, W]}$  and  $G_{\varphi} \frac{\delta \mathcal{F}_{[\varphi, W]}}{\delta\varphi}$  can be further evaluated. The first of the two terms can be recast as<sup>f</sup>:

$$\frac{\delta G_{\varphi}}{\delta\varphi} \cdot \mathcal{F}_{[\varphi, W]} = -G_{\varphi} \underbrace{\frac{\delta G_{\varphi}^{-1}}{\delta\varphi}}_{-1} G_{\varphi} \mathcal{F}_{[\varphi, W]} = G_{\varphi} G_{\varphi} \mathcal{F}_{[\varphi, W]} \quad (\text{G.42})$$

<sup>c</sup> $\mathcal{F}_W$  in the decoupling approximation was a function of  $W$  only.

<sup>d</sup>Since this is only a preliminary discussion it will be enough to give the idea behind this route.

<sup>e</sup>The "compact" symbolic N-point DE reads:  $G([\varphi]) = G_{\varphi} + G_{\varphi} W \frac{\delta G([\varphi])}{\delta\varphi}$ .

<sup>f</sup>This manipulation is analogous to the one shown in App. A.3 for the full  $G$ .

having used  $\frac{\delta G_\varphi^{-1}}{\delta \varphi} = -1$ .<sup>g</sup>

For the second term we have:

$$G_\varphi \frac{\delta \mathcal{F}_{[\varphi, W]}}{\delta \varphi} = G_\varphi \frac{\delta \mathcal{F}_{[\varphi, W]}}{\delta G_\varphi} \cdot \underbrace{\frac{\delta G_\varphi}{\delta \varphi}}_{\text{Eq. (G.42)}} = G_\varphi \frac{\delta \mathcal{F}_{[\varphi, W]}}{\delta G_\varphi} G_\varphi G_\varphi \quad (\text{G.43})$$

hence Eq. (G.41) can be rewritten as:

$$G_\varphi \cdot \mathcal{F}_{[\varphi, W]} = G_\varphi + G_\varphi W \left\{ G_\varphi G_\varphi \mathcal{F}_{[\varphi, W]} + G_\varphi \frac{\delta \mathcal{F}_{[\varphi, W]}}{\delta G_\varphi} G_\varphi G_\varphi \right\} \quad (\text{G.44})$$

multiplying from the left by  $G_\varphi^{-1}$  we can readily obtain:

$$\boxed{\mathcal{F}_{[\varphi, W]} = 1 + W \left\{ G_\varphi G_\varphi \mathcal{F}_{[\varphi, W]} + G_\varphi \frac{\delta \mathcal{F}_{[\varphi, W]}}{\delta G_\varphi} G_\varphi G_\varphi \right\}.} \quad (\text{G.45})$$

We have hence obtained an equation for  $\mathcal{F}_{[\varphi, W]}$  as a functional of the screened interaction  $W$  and the non-interacting Green's function in presence of the external potential  $\varphi$ .

What about the evaluation of  $\mathcal{F}_{[\varphi, W]}$ ? One would have to solve Eq. (G.45), which is again very difficult. However, to have a feeling about the potential of such ansatz, we could begin with exploring an approximate solution for  $G$ . By *neglecting* the last term in Eq. (G.45)<sup>h</sup>:

$$\mathcal{F}_{[\varphi, W]} = 1 + W G_\varphi G_\varphi \mathcal{F}_{[\varphi, W]}. \quad (\text{G.46})$$

Inversion of the above expression gives:

$$\mathcal{F}_{[\varphi, W]} = [1 - W G_\varphi G_\varphi]^{-1}. \quad (\text{G.47})$$

The above result can be inserted in the initial ansatz, providing us with a Green's function of the type:

$$G = G_\varphi [1 - W G_\varphi G_\varphi]^{-1}. \quad (\text{G.48})$$

which is equivalent to a  $GW$  approximation for the one-body propagator.<sup>i</sup>

In conclusion on the basis of the results obtained with a similar strategy in the N-times framework and on the few symbolic equations of this last section (Eqs. G.40-G.48), this alternative ansatz looks like a promising route towards the solution of the full functional linearized equation. We will definitely explore it further.

<sup>g</sup>This manipulation is equivalent to the one employed, e.g., to derive the vertex function in Hedin's equations.

<sup>h</sup>To be precise one assumes  $\mathcal{F}$  independent of  $G_\varphi$ .

<sup>i</sup>The Dyson equation has been expressed here in terms of the non-interacting  $G_\varphi$ , rather than the non-interacting  $G_0$  at vanishing potential.

## BIBLIOGRAPHY

- [1] Hartree D. *Proc. Cambridge Philos. Soc.*, 24, 1928.
- [2] Fock V. *Z. Phys.*, 61, 1930.
- [3] Kohn W. and Sham J. L. *Phys. Rev.*, 140, 1965.
- [4] Foulkes W. M. C., Mitas L., Needs R. J., and Rajagopal G. *Rev. Mod. Phys.*, 73, 2001.
- [5] Ceperley D. M. *Rev. Mod. Phys.*, 67, 1965.
- [6] Coester F. and Kummel H. *Nuclear Physics*, 17, 1960.
- [7] Helgaker T., Jørgensen P., and Olsen J. *Molecular Electronic-Structure Theory*. Wiley, Chichester, 2000.
- [8] Szabo A. and Ostlund N. S. *Modern Quantum Chemistry: Introduction to Advanced Electronic Structure Theory*. Dover Publications, Mineola, NY, 1996.
- [9] Georges A. and Kotliar G. *Phys. Rev. B*, 45, 1992.
- [10] Kotliar G., Savrasov S. Y., Haule K., Oudovenko V. S., Parcollet O., and Marianetti C. A. *Rev. Mod. Phys.*, 78, 2006.
- [11] Gell-Mann M. and Brueckner K. A. *Phys. Rev.*, 106:364–368, 1957.
- [12] Nozierès P. and Pines D. *Nuovo Cimento*, 9:470–490, 1958.
- [13] Martin P. C. and Schwinger J. *Phys. Rev.*, 115, 1959.
- [14] Hedin L. *Phys. Rev.*, 139, 1965.
- [15] van Schilfgaarde M., Kotani T., and Faleev S. *Phys. Rev. Lett.*, 96, 2006.
- [16] Papalazarou E., Gatti M., Marsi M., Brouet V., Iori F., and Reining L. et al. *Phys. Rev. B*, 80, 2009.

- [17] Chantis A. N., van Schilfgaarde M., and Kotani T. *Phys. Rev. B*, 76, 2007.
- [18] Quinn J. J. and Ferrell R. A. *Phys. Rev.*, 112:812–827, 1958.
- [19] Bohm D. and Pines D. *Phys. Rev.*, 92:609–625, 1953.
- [20] Hubbard J. *Proc. Roy. Soc.*, A342:336–352, 1957.
- [21] Nozierès P. and Pines D. *Phys. Rev.*, 111:442–545, 1958.
- [22] Wigner E. P. *Phys. Rev.*, 46, 1934.
- [23] Carr W. J. *Phys. Rev.*, 122, 1961.
- [24] Nozières P. and Pines D. *Nuclear Physics*, 111:442–454, 1958.
- [25] Huang K. and Yang C. N. *Phys. Rev.*, 105:767, 1957.
- [26] Galitskii V. M. *Zh. Eksper. Teor. Fiz.*, 34:251, 1958.
- [27] Brueckner K. A. *The Many-Body Problem*. Dunod-Wiley, New York, 1598.
- [28] Hertz H. R. *Annalen der Physik und Chemie*, 31:983–1000, 1987.
- [29] Hallwachs W. *Annalen der Physik und Chemie*, 33:301–12, 1888.
- [30] Einstein A. *Ann. Phys.*, 17:132–48, 1905.
- [31] Reinert F. and Hüfner S. *New Journal of Physics*, 7:97, 2005.
- [32] Berglund C. N. and Spicer W. E. *Phys. Rev*, 136, 1964.
- [33] Schaich W. L. and Ashcroft N. W. *Phys. Rev. B*, 3, 1970.
- [34] Mahan G. D. *Phys. Rev. B*, 2:4334, 1970.
- [35] Hedin L. *Phys. Scripta*, 21:477–480, 1980.
- [36] Fetter A. L. and Walecka J. D. *Quantum Theory of Many-Particle Systems*. Dover publications, 2003.
- [37] Gross Eberhard K. U., Runge E., and Heinonen O. *Many-particle Theory*. A. Hilger, 1991.
- [38] Stankovski M. *Local and Non Local Vertex Corrections Beyond the GW Approximation*. PhD thesis, University of York, UK, 2008.
- [39] Damascelli A., Hussain Z., and Shen Z. X. *Rev. Mod. Phys.*, 75:473, 2003.
- [40] Kadanoff L. P. and Baym G. *Quantum Statistical Mechanics*. W.A. Benjamin Inc., New York, 1964.
- [41] Csanak G., Taylor H. S., and Yaris R. *Adv. At. Mol. Phys.*, 7:289, 1971.
- [42] Schwinger J. *Proc. Nat. Accad. Sci.*, 37:452, 1951.

- [43] Abrikosov A.A., Gorkov L. P., and Dzyaloshinski I. E. *Methods of Quantum Field Theory in Statistical Physics*. Dover publications, 1975.
- [44] Gell-Mann M. and Low F. *Phys. Rev.*, 84:350, 1951.
- [45] Messiah A. *Quantum Mechanics II*. Dover Publications, 1970.
- [46] Brouder C., Stoltz G., and Panati G. *Phys. Rev. Lett.*, 10:1285–1309, 2007.
- [47] Baym G. and Kadanoff L. P. *Phys. Rev.*, 124:287, 1951.
- [48] Strinati G., Mattausch H. J., and Hanke W. *Phys. Rev. B*, 25, 1982.
- [49] Hybertsen M. S. and Louie S. G. *Phys. Rev. Lett.*, 55:1418, 1985.
- [50] Hybertsen M. S. and Louie S. G. *Phys. Rev. B*, 55:5390, 1986.
- [51] Godby R. W., Schlüter M., and Sham L. J. *Phys. Rev. B*, 37:10159, 1988.
- [52] Strinati G. *Rivista del Nuovo Cimento*, 11:1–86, 1988.
- [53] Aulbur W. G., Jönsson L., and Wilkins J. W. *Solid State Phys.*, 54:1, 1999. and references therein.
- [54] Aryasetiawan F. and Gunnarsson O. *Reports on Progress in Physics*, 61:237–312, 1998. and references therein.
- [55] Gatti M., Bruneval F., Olevano V., and Reining L. *Phys. Rev. Lett.*, 99, 2007.
- [56] Faleev S. V., van Schilfgaarde M., and Kotani T. *Phys. Rev. Lett.*, 93, 2004.
- [57] Dahlen N. E., van Leeuwen R., and von Barth U. *Phys. Rev. A*, 73:012511, 2006.
- [58] Stan A., Dahlen N. E., and van Leeuwen R. *Europhys. Lett.*, 76:298, 2006.
- [59] Nelson W., Bokes P., Rinke P., and Godby R. W. *Phys. Rev. A*, 75:032505, 2007.
- [60] Fernandez J. J. *Phys. Rev. A*, 79, 2009.
- [61] Romaniello P., Sangalli, Berger J. A, Sottile F., Molinari L. G., Reining L., and Onida G. *J. Chem. Phys.*, 130:044108, 2009.
- [62] Dabo I., Ferretti A., Poilvert N., Li Y., Marzari N., and Cococcioni M. *Phys. Rev. B*, 82:115121, 2010.
- [63] Romaniello P., Guyot S., and Reining L. *J. Chem. Phys.*, 131:154111, 2009.
- [64] L. Shirley E and Martin R. M. *Phys. Rev. B*, 47, 1993.
- [65] Verdozzi C., Godby R.W., and Holloway S. *Phys. Rev. Lett.*, 74, 1995.
- [66] Wange X., Spataru C. D., Hybertsen M. S., and Mills A. J. *Phys. Rev. B*, 77:045119, 2008.

- [67] Hedin L. *J. Phys. Cond. Matt.*, 11:R489, 1999.
- [68] Kheifets A. S., Sashin V. A., Vos M., Weigold E., and Aryasetiawan F. *Phys. Rev. B*, 68:233205, 2003.
- [69] Puig von Friesen M., Verdozzi C., and Almbladh C.-O. *Phys. Rev. Lett.*, 103:176404, 2009.
- [70] Springer M., Aryasetiawan F. A., and Karlsson K. *Phys. Rev. Lett.*, 80:2389, 1998.
- [71] Puig von Friesen M., Verdozzi C., and Almbladh C.-O. *Phys. Rev. B*, 82:155108, 2010.
- [72] F. Bruneval, Sottile F., Olevano V., Del Sole R., and Reining L. *Phys. Rev. Lett.*, 94:186402, 2005.
- [73] Romaniello P., Bechstedt F., and Reining L. *Phys. Rev. B*, 68. submitted.
- [74] Aryasetiawan F., Hedin L., and Karlsson K. *Phys. Rev. Lett.*, 77:2268, 1996.
- [75] Holm B. and von Barth U. *Phys. Rev.*, 57:2108, 1998.
- [76] Schöne W. D. and Eguiluz A. G. *Phys. Rev. Lett.*, 81:1662, 1998.
- [77] Shirley E. L. *Phys. Rev. B*, 54:7758, 1996.
- [78] von Barth U. and Holm B. *Phys. Rev.*, 54, 1996.
- [79] Lundqvist B.I. *Phys. Kondensierten Materie*, 9:236, 1969.
- [80] Hedin L., Lundqvist B.I., and Lundqvist S. *Solid State Commun.*, 5:237, 1967.
- [81] Langreth D.C. *Phys. Rev. B*, 1(2):471, 1970.
- [82] Vos M., Kheifets A. S., Sashin V. A., and Weigold E. *Phys. Rev. B*, 66:155414, 2002.
- [83] Guzzo M., Lani G., Sottile F., Romaniello P., Gatti M., Kas J. J., Rehr J. J., Silly M., Sirotti F., and L. Reining. *Phys. Rev. Lett.*, 2011. to appear.
- [84] von Barth U., Dahlen N. E., van Leeuwen R., and Stefanucci G. *Phys. Rev. B*, 72:235109, 2005.
- [85] Molinari L. G. *Phys. Rev. B*, 71:113102, 2005.
- [86] Molinari L. G. and Manini N. *European Physics Journal B*, 51:331–336, 2006.
- [87] Pavlyukh Y. and Hübner H. *J. Math. Phys.*, 48:052109, 2007.
- [88] Kamke E. *Differentialgleichungen: Lösungsmethoden und Lösungen, I, Gewöhnliche Differentialgleichungen*. B.G. Teubner, Leipzig, 1977.
- [89] Leininger M. L., Allen W. D., and Schaefer H. F. *J. Chem. Phys.*, 112:9213, 2000.
- [90] Dunning T. H. and Peterson K. A. *J. Chem. Phys.*, 108:4761, 1998.

- [91] Møller C. and Plesset M. S. *Phys. Rev.*, 46:618–622, 1934.
- [92] Bender C. M. and Wu T. T. *Phys. Rev.*, 184:1231, 1963.
- [93] Various authors. *Digital Library of Mathematical Functions*. Release date: 2010-05-07 .  
National Institute of Standards and Technology from <http://dlmf.nist.gov/>.
- [94] Mahan G. D. and Sernelius B. E. *Phys. Rev. Lett.*, 62:2718, 1989.
- [95] Del Sole R., Reining L., and Godby R. W. *Phys. Rev. B*, 49:8024, 1994.
- [96] Schindlmayr A. and Godby R. W. *Phys. Rev. Lett.*, 80:1702–1705, 1998.
- [97] Abramowitz M. and Stegun I. *Handbook of mathematical functions with formulas, graphs and mathematical tables*. Dover publications, 1964.
- [98] Roy D. *Comp. Phys. Comm.*, 180:1315–1337, 2009.
- [99] Almladh C. O. and Hedin L. *Handbook Of Synchrotron Radiation*, volume 1. E.E. Koch, North Holland, Amsterdam, 1983.
- [100] Hedin L. and Lundqvist S. *Solid State Physics*, volume 23. Ehrenreich, H. and Seitz, F. and Turnbull, D., Academic Press, New York, 1969.
- [101] Holm B. and Aryasetiawan F. *Phys. Rev. B*, 56:12825, 1997.
- [102] Brouder C. *EPJ direct*, C3:1–33, 2003.
- [103] Bronshtein I.N., Semendyayev K. A., Musiol G., and Muehlig H. *Handbook Of Mathematics*. Springer-Verlag Berlin Heidelberg, 2005.

